

Measurement of upsilon production in 7 TeV pp collisions at ATLASG. Aad *et al.**

(ATLAS Collaboration)

(Received 30 November 2012; published 4 March 2013)

Using 1.8 fb^{-1} of pp collisions at a center-of-mass energy of 7 TeV recorded by the ATLAS detector at the Large Hadron Collider, we present measurements of the production cross sections of $Y(1S, 2S, 3S)$ mesons. Y mesons are reconstructed using the dimuon decay mode. Total production cross sections for $p_T < 70 \text{ GeV}$ and in the rapidity interval $|y^Y| < 2.25$ are measured to be, $8.01 \pm 0.02 \pm 0.36 \pm 0.31 \text{ nb}$, $2.05 \pm 0.01 \pm 0.12 \pm 0.08 \text{ nb}$, and $0.92 \pm 0.01 \pm 0.07 \pm 0.04 \text{ nb}$, respectively, with uncertainties separated into statistical, systematic, and luminosity measurement effects. In addition, differential cross section times dimuon branching fractions for $Y(1S)$, $Y(2S)$, and $Y(3S)$ as a function of Y transverse momentum p_T and rapidity are presented. These cross sections are obtained assuming unpolarized production. If the production polarization is fully transverse or longitudinal with no azimuthal dependence in the helicity frame, the cross section may vary by approximately $\pm 20\%$. If a nontrivial azimuthal dependence is considered, integrated cross sections may be significantly enhanced by a factor of 2 or more. We compare our results to several theoretical models of Y meson production, finding that none provide an accurate description of our data over the full range of Y transverse momenta accessible with this data set.

DOI: [10.1103/PhysRevD.87.052004](https://doi.org/10.1103/PhysRevD.87.052004)

PACS numbers: 12.38.-t, 13.20.Gd, 14.40.Pq

I. INTRODUCTION

Since the discovery of the J/ψ and Y mesons [1,2] the study of heavy quark-antiquark systems has provided valuable input for our understanding of quantum chromodynamics (QCD). However, despite being one of the simplest systems in QCD it has proven difficult historically to describe the production properties of these states adequately. Results on J/ψ and Y hadroproduction and polarization [3–12] exhibit inconsistencies between measurements and theoretical predictions [13].

Measurements at the Large Hadron Collider (LHC) of differential production spectra of various charmonium and bottomonium states together with measurement of their spin alignments, prompt double-quarkonia production, and production of quarkonia in association with photons, vector bosons, or open heavy-flavor final states will allow discrimination between different theoretical approaches based on color-singlet corrections [14–16], color-octet terms [17], the k_T -factorization approach [18], and other production models [19], and provide additional input toward an improved understanding of quarkonium hadroproduction.

Studies of bottomonium production complement concurrent studies of charmonium systems due to the larger mass of the bottom quark compared to the charm quark, allowing more dependable theoretical calculations than in the charmonium family, which suffer from poor perturbative convergence [17]. Extension of cross section measurements to

higher meson transverse momenta provides valuable input to improvements in the theoretical description since in this regime different processes can dominate and, experimentally, the impact of spin-alignment uncertainties are mitigated.

Taking advantage of the large increase in integrated luminosity delivered by the LHC in 2011, this paper updates a previous measurement [8] and reports the $Y(1S)$ cross section presented differentially in two intervals of absolute Y rapidity [20], $|y^Y|$, and 50 intervals of Y transverse momentum, p_T^Y , and as a p_T -integrated result in 45 bins of absolute Y rapidity. In addition, new measurements of the equivalent $Y(2S)$ and $Y(3S)$ differential spectra and their production ratios relative to the $Y(1S)$ are reported.

Y production can proceed *directly*, where the Y meson of interest is produced in the hard interaction, or via the production of an excited state which subsequently decays. This so-called “feed-down” contribution complicates the theoretical description of quarkonium production as calculation of color-singlet P -wave and higher orbital angular momentum quarkonium production suffers from the presence of infrared divergences [21]. From the experimental perspective, separation of direct and feed-down contributions is hindered by the small mass splitting between the bottomonium states, which impedes the detection of additional decay products that would indicate indirect production. Contributions from feed-down vary between the $Y(1S)$, $Y(2S)$, and $Y(3S)$ states due to the changing presence of various kinematically-allowed decays and influence the inclusive production rate. Study of the Y production ratios as a function of kinematic variables as presented here thus provides an indirect but precise measure of these feed-down contributions.

This new analysis extends the p_T range of our previous cross section result [8] to 70 GeV, at which new contributions

*Full author list given at the end of the article.

to Y production [15,16] such as from associated $Y + b\bar{b}$ production may play a more important role, and the impact of the dependence of the production cross section on the spin alignment of the Y is relatively small. Both the fiducial cross section, measured in the kinematic region with muon transverse momentum $p_T^\mu > 4$ GeV and muon pseudorapidity $|\eta^\mu| < 2.3$, and the corrected cross section, which is defined in this paper as the cross section in the p_T - η phase space of the Y corrected for the acceptance of the decay products to the full Y production phase space, are reported. In the former case, the results have no dependence on assumptions about Y spin alignment, while the latter measurements are more easily compared to model predictions and to the results of other experiments.

II. THE ATLAS DETECTOR

The ATLAS detector [22] is composed of an inner tracking system, calorimeters, and a muon spectrometer. The inner detector directly surrounds the interaction point and consists of a silicon pixel detector, a silicon microstrip detector, and a transition radiation tracker, all immersed in a 2 T axial magnetic field. It covers the pseudorapidity [20] range $|\eta| < 2.5$ and is enclosed by a calorimeter system containing electromagnetic and hadronic sections. Surrounding the calorimeters is the large muon spectrometer built with three air-core toroids. This spectrometer is equipped with precision detectors (monitored drift tubes and cathode strip chambers) that provide precise measurements in the bending plane within the pseudorapidity range $|\eta| < 2.7$. In addition, resistive plate and thin gap chambers with fast response times are used primarily to construct muon triggers in the ranges $|\eta| < 1.05$ and $1.05 < |\eta| < 2.4$ respectively but are also used to provide position measurements in the nonbending plane and to improve pattern recognition and track reconstruction. Momentum measurements in the muon spectrometer are based on track segments formed in at least two of the three precision chamber planes.

The ATLAS detector employs a three-level trigger system [23], which reduces the 20 MHz proton bunch collision rate to the several hundred Hz transfer rate to mass storage. The level-1 muon trigger searches for hit coincidences between different muon trigger detector layers inside pre-programmed geometrical windows that bound the path of triggered muons of given transverse momentum and provide a rough estimate of its position within the pseudorapidity range $|\eta| < 2.4$. At level-1, muon candidates are reported in “regions of interest” (RoIs). Only a single muon can be associated with a given RoI of spatial extent $\Delta_\phi \times \Delta_\eta \approx 0.1 \times 0.1$. This limitation has a small effect on the trigger efficiency for Y mesons, corrected for in the analysis using a data-driven method based on analysis of $J/\psi \rightarrow \mu^+ \mu^-$ and $Y \rightarrow \mu^+ \mu^-$ decays. The level-1 trigger is followed in sequence by two subsequent higher-level, software-based trigger selection stages. Muon candidates

reconstructed at these higher levels incorporate, with increasing precision, information from both the muon spectrometer and the inner detector and reach position and momentum resolution close to that provided by the offline muon reconstruction.

III. DATA SET AND EVENT SELECTION

Data for this study were collected during the 2011 LHC proton-proton running period between March and August using a trigger that requires the presence of two muon candidates with opposite charges that are subject to a fit constraining them to a common vertex while taking into account track parameter uncertainties. A very loose selection on vertex χ^2 , which is fully efficient for signal candidates, was imposed to ensure proper fit convergence, as well as the requirement of opposite charge and that $p_T^\mu > 4$ GeV and $|\eta^\mu| < 2.3$. This trigger was largely unpre-scaled and collected data at a rate of approximately 20 Hz in this period of data taking.

Events are required to contain at least one primary vertex candidate that has at least five tracks with $p_T > 0.4$ GeV, and at least two muons identified by associating candidates found in the muon spectrometer with tracks reconstructed in the inner detector [8,22]. Multiple scattering in the calorimeters and toroids of the ATLAS detector degrades the muon spectrometer resolution for low energy particles. As the majority of muons selected for this analysis have low momentum, we assign values for parameters such as p_T and η to the muons based on track fits using inner detector information only. To ensure accurate inner detector measurements, each muon track must contain at least six silicon microstrip detector hits and at least one pixel detector hit. Muon candidates passing these criteria are required to have $p_T^\mu > 4$ GeV and $|\eta^\mu| < 2.3$ and a successful fit to a common vertex.

Good spatial matching ($\Delta R \equiv \sqrt{(\Delta\phi)^2 + (\Delta\eta)^2} < 0.01$) between the muon candidate in both the offline reconstruction and the trigger used to select the event is required to facilitate data-driven estimates of the dimuon trigger efficiency. Furthermore, both muons forming an Y candidate must be associated to their trigger-level candidates in this manner. In this way, the efficiency of the trigger requirements on the dimuon candidate are incorporated into the trigger efficiency correction. All dimuon candidates passing these criteria are retained for analysis.

The distribution of the invariant mass of the $\mu^+ \mu^-$ system is shown in Fig. 1 for the selected dimuon candidates. As is apparent from the plot, the mass resolution (120 MeV) for dimuon candidates detected in the central region of the detector ($|\eta^{\mu\mu}| < 1.2$) is significantly better than the resolution (214 MeV) for those candidates falling into the forward region ($1.2 \leq |\eta^{\mu\mu}| < 2.25$). A total of 3.9×10^6 and 2.3×10^6 candidates with $8 < m_{\mu\mu} < 11.5$ GeV are reconstructed in the central and forward regions, respectively.

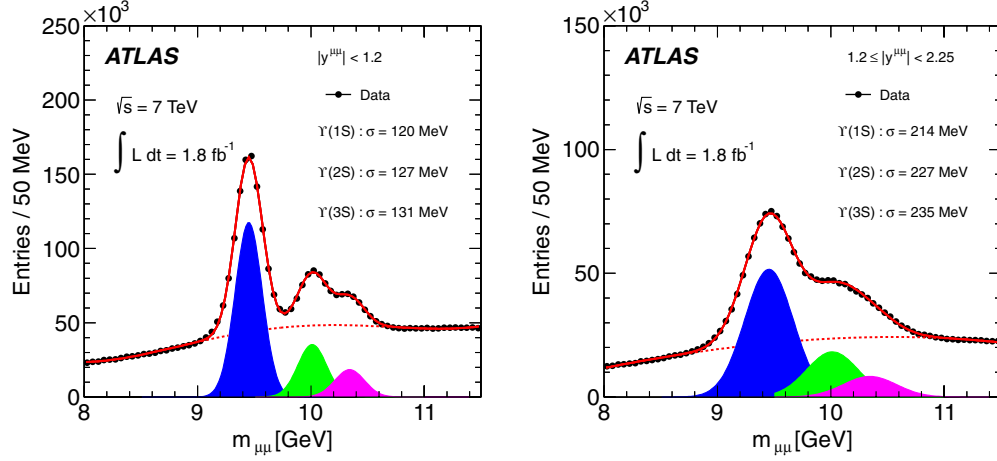


FIG. 1 (color online). The dimuon invariant mass spectrum for events used in this analysis. Separate spectra are shown for those events with the dimuon candidate (left) in the central region of the detector ($|y^{\mu\mu}| < 1.2$) and (right) in the forward region ($1.2 \leq |y^{\mu\mu}| < 2.25$). Overlaid are individual shapes of the fitted $Y(nS)$ signals (shaded regions), background-only fit (dashed curve), and the total signal plus background shape (solid curve). The background shape is modeled here by a fourth-order polynomial and the signal peaks each modeled by a single Gaussian. Also quoted are the fitted mass resolutions of each of the three signal peaks, determined from the fit with a common resolution parameter scaling with invariant mass.

IV. CROSS SECTION DETERMINATION

Differential Y cross sections are measured according to the relation

$$\frac{d^2\sigma}{dp_T dy} \times \text{Br}(Y \rightarrow \mu^+ \mu^-) = \frac{N_Y}{\int \mathcal{L} dt \times \Delta p_T \times \Delta |y|}, \quad (1)$$

where $\text{Br}(Y \rightarrow \mu^+ \mu^-)$ represents the appropriate branching fraction of the $Y(nS)$ to dimuons, $\int \mathcal{L} dt$ is the integrated luminosity, Δp_T and $\Delta |y|$ are the bin sizes in Y transverse momentum and rapidity, respectively, and N_Y is the corrected number of observed $Y(1S)$, $Y(2S)$, or $Y(3S)$ mesons in a bin. Corrections are applied to account for selection efficiencies, bin migration effects due to finite detector resolution, and, in the case of corrected cross section measurements, acceptance.

Determination of the cross sections proceeds through several steps. First, a weight is determined for each selected dimuon candidate equal to the inverse of the total efficiency for the candidate. Second, a fit is performed to the distribution of weighted events binned in dimuon invariant mass, $m_{\mu\mu}$, to determine the number of $Y(nS)$ mesons (with $n = 1, 2, 3$) produced in each $(p_T^{\mu\mu}, y^{\mu\mu})$ bin. Third, these values are corrected for $(p_T^{\mu\mu}, y^{\mu\mu})$ bin migrations. Finally, the differential cross section multiplied by the $Y \rightarrow \mu^+ \mu^-$ branching fraction is calculated for each state using the integrated luminosity and the p_T and y bin widths as in Eq. (1).

The weight, w , for each Y candidate includes the fraction of produced $Y \rightarrow \mu^+ \mu^-$ decays with both muons falling into the kinematic region $p_T^\mu > 4$ GeV and $|\eta^\mu| < 2.3$ (the acceptance, \mathcal{A} , is used only in calculating corrected cross sections), the probability that a candidate

falling within the acceptance passes the offline reconstruction requirements (the reconstruction efficiency, $\varepsilon_{\text{reco}}$), and the probability that a reconstructed event passes the trigger selection (the trigger efficiency, $\varepsilon_{\text{trig}}$). The weights assigned to a given candidate when calculating the fiducial (w_{fid}) and corrected (w_{tot}) cross sections are then given by

$$w_{\text{fid}} = (\varepsilon_{\text{reco}} \cdot \varepsilon_{\text{trig}})^{-1}, \quad w_{\text{tot}} = (\mathcal{A} \cdot \varepsilon_{\text{reco}} \cdot \varepsilon_{\text{trig}})^{-1}. \quad (2)$$

A. Acceptance

The kinematic acceptance $\mathcal{A}(p_T, y)$ is the probability that the muons from an Y with transverse momentum p_T and rapidity y fall into the fiducial volume of the detector defined by the $p_T^\mu > 4$ GeV and $|\eta^\mu| < 2.3$ selection applied to each muon in the dimuon pair. In order to calculate the acceptance as a function of the rapidity and transverse momentum of each of the Y states, taking into account possible angular dependences in their decays, we use an analytic formula describing the decay of Y states in their decay frame [24],

$$\frac{d^2N}{d \cos \theta^* d \phi^*} \propto 1 + \lambda_\theta \cos^2 \theta^* + \lambda_\phi \sin^2 \theta^* \cos 2\phi^* + \lambda_{\theta\phi} \sin 2\theta^* \cos \phi^*. \quad (3)$$

The helicity frame is used, where θ^* is the polar angle between the μ^+ momentum in the Y decay frame and the direction of the Y momentum in the laboratory frame. The corresponding azimuthal angle ϕ^* is the angle between the quarkonium production plane (defined in the quarkonium decay frame by the two momenta of the incoming protons in that frame) and the quarkonium decay plane in the lab frame.

The λ_i coefficients parametrize the spin-alignment state of the Y . In some parts of the phase space the acceptance may depend on these parameters quite strongly. We have identified five extreme cases that lead to the largest possible variations of acceptance within the phase space of this measurement and define an envelope in which the results may vary under any physically allowed spin-alignment assumption: isotropic distribution independent of θ^* and ϕ^* ($\lambda_\theta = \lambda_\phi = \lambda_{\theta\phi} = 0$, labeled FLAT); longitudinal alignment ($\lambda_\theta = -1$, $\lambda_\phi = \lambda_{\theta\phi} = 0$, labeled LONG); and three types of transverse alignment ($\lambda_\theta = +1$, $\lambda_\phi = \lambda_{\theta\phi} = 0$, labeled $T+0$; $\lambda_\theta = +1$, $\lambda_\phi = +1$, $\lambda_{\theta\phi} = 0$, labeled $T++$; $\lambda_\theta = +1$, $\lambda_\phi = -1$, $\lambda_{\theta\phi} = 0$, labeled $T+-$). The central values of our measurements are derived under the isotropic production assumption. The spread in corrected cross section results derived under all five assumptions is used to quantify the full envelope of possible variations of the result due to spin alignment. Some constraints on physically allowed λ_i combinations exist [24,25]. In particular, $\lambda_{\theta\phi}$ must be zero for $\lambda_\theta = \pm 1$ and any λ_ϕ , and $|\lambda_{\theta\phi}| \leq 0.5$ for $\lambda_\theta = \lambda_\phi = 0$. Acceptance corrections with nonzero $\lambda_{\theta\phi}$ were found to lead to corrections with smaller or equal variations from the isotropic scenario than any parameter-space scenarios on the λ_θ - λ_ϕ plane. Acceptance weights for each polarization scenario, including those with nonzero $\lambda_{\theta\phi}$, can be found in HEPDATA [26].

Figure 2 presents the two-dimensional acceptance map for $Y(1S)$, as a function of the Y transverse momentum and absolute rapidity in the unpolarized (FLAT) acceptance scenario as well as the maximum relative variation (ratio of largest to smallest acceptance correction) of the acceptance maps across all spin-alignment scenarios.

Acceptance is significantly decreased at very high rapidities due to the muon pseudorapidity requirement of $|\eta^\mu| < 2.3$. When Y are produced at rest, both muons are likely to be reconstructed in the muon spectrometer on opposite sides of the detector. When the Y has a sufficient boost, the two muons are more likely to be found in the same side of the detector and the probability that at least one muon is below the required p_T^μ threshold increases, leading to a drop in acceptance. At higher p_T the Y imparts greater momentum to the two muons, the likelihood of a muon being below threshold decreases, and the acceptance asymptotically approaches 100%. As Y transverse momentum increases the variation of the acceptance corrections between spin-alignment scenarios decreases, becoming $\lesssim 10\%$ at the largest p_T ranges studied. Similar behaviors are observed in the acceptance maps for the $Y(2S)$ and $Y(3S)$.

This spin-alignment systematic uncertainty only applies to the corrected cross section measurements. For fiducial cross sections, measured in the kinematic region $p_T^\mu > 4$ GeV and $|\eta^\mu| < 2.3$, we do not have to correct our results to the full phase space of produced Y

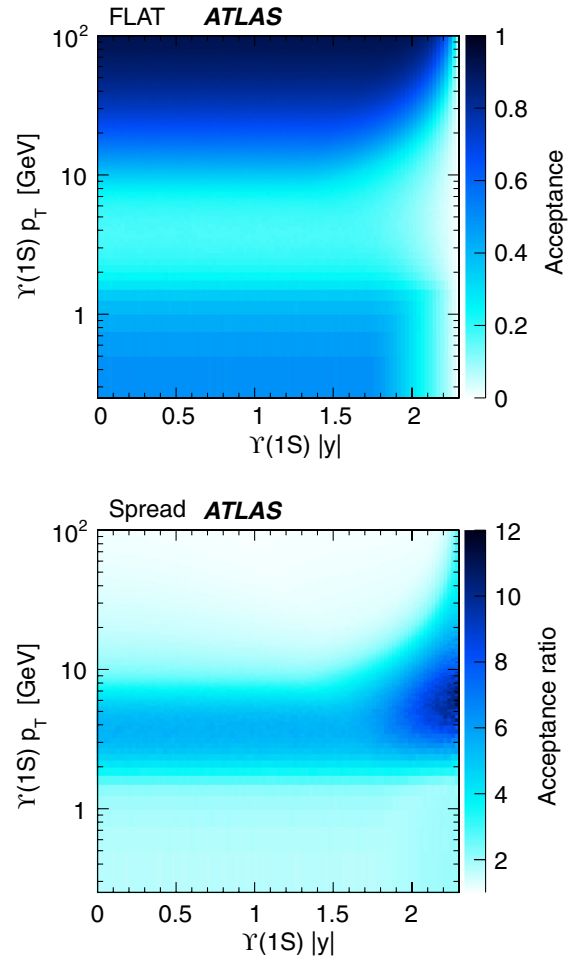


FIG. 2 (color online). Top: acceptance as a function of Y p_T and rapidity for the $Y(1S)$ in the unpolarized acceptance scenario. Bottom: the ratio of largest to smallest acceptance correction between extreme spin-alignment scenarios.

mesons. Spin alignment can thus affect only our estimates of the reconstruction and trigger efficiencies. Since we measure these in many bins of muon p_T and η , effects from differing distributions of events over individual bins due to different spin-alignment assumptions are negligible compared to other sources of systematic uncertainty.

B. Reconstruction and trigger efficiencies

The efficiency of the offline reconstruction criteria for events with muons within the fiducial region is given by

$$\begin{aligned} \varepsilon_{\text{reco}} = & \varepsilon_{\text{trk}}(p_{T1}, \eta_1) \times \varepsilon_{\text{trk}}(p_{T2}, \eta_2) \varepsilon_\mu(p_{T1}^\mu, q_1 \cdot \eta_1^\mu) \\ & \times \varepsilon_\mu(p_{T2}^\mu, q_2 \cdot \eta_2^\mu). \end{aligned} \quad (4)$$

In this equation, q represents the charge of the muon and the identities of the two muons are labeled with indices 1, 2. The efficiency of the track selection criteria, ε_{trk} , for

tracks originating from real muons is determined in Ref. [7] using data collected in 2010. Because of the presence of additional pp interactions in the same and neighboring bunch crossings in 2011 data the systematic uncertainty on the tracking efficiency has increased, with ε_{trk} assessed to be $99 \pm 1.0\%$ over the whole kinematic range.

The efficiency to reconstruct a muon, ε_μ , is derived using a tag-and-probe method on $J/\psi \rightarrow \mu^+ \mu^-$ data. The *tag* muon corresponds to a muon candidate with $p_T^\mu > 4$ GeV and $|\eta^\mu| < 2.4$ and must have fired a single-muon trigger in the event, as required by the trigger matching algorithms. The *probe* track is only required to pass the inner detector track quality, p_T , and η cuts and be consistent with having the same vertex as the identified tag muon. This technique provides a sample of muon candidates unbiased with respect to both trigger and offline reconstruction, and with favorable signal to background ratio.

The muon reconstruction efficiency is then derived in two-dimensional p_T - η bins [14 muon p_T intervals and 26 charge-signed muon pseudorapidity ($q \cdot \eta$) intervals]. The ratio of the fitted $J/\psi \rightarrow \mu^+ \mu^-$ signal yield for those probe tracks identified as muons to the fitted signal yield for all probe tracks in these double-differential intervals is identified as the single-muon reconstruction efficiency.

Because of the toroidal magnetic field, muons with positive (negative) charge are bent towards larger (smaller) pseudorapidity. This introduces a charge dependence in the muon reconstruction efficiency. We calculate efficiencies as a function of charge-signed pseudorapidity as negative muons at positive rapidities are affected in the same manner as positive muons in negative rapidities. The charge dependence is particularly noticeable at very large $|\eta|$ where the muon can be bent outside of the geometrical acceptance of the detector. In particular, at low p_T , where the muons of particular charge may be bent away from (rather than toward for the opposing charge) the middle/outer spectrometer planes, they will not be identified as muons.

The efficiency of the dimuon trigger to select events that have passed the offline selection criteria, $\varepsilon_{\text{trig}}$, is also calculated from data. This can be factorized into three terms:

$$\varepsilon_{\text{trig}} = \varepsilon_{\text{RoI}}(p_{T1}^\mu, q_1 \cdot \eta_1^\mu) \varepsilon_{\text{RoI}}(p_{T2}^\mu, q_2 \cdot \eta_2^\mu) c_{\mu\mu}(\Delta R, |y^{\mu\mu}|), \quad (5)$$

where ε_{RoI} is the efficiency of the trigger system to find an RoI for a single muon with transverse momentum, p_T^μ , and charge-signed pseudorapidity, $q \cdot |\eta^\mu|$, and $c_{\mu\mu}$ is a correction for effects related to the dimuon elements of the trigger. This correction accounts for the dimuon vertex and opposite charge requirements, and for loss of efficiency in the dimuon trigger if the two muons are close enough together to register only as a single RoI.

The dimuon correction, $c_{\mu\mu}$, itself consists of two components

$$c_{\mu\mu}(\Delta R, y^{\mu\mu}) = c_a(y^{\mu\mu}) \times c_{\Delta R}(\Delta R, y^{\mu\mu}) \quad (6)$$

each evaluated in three separate regions of dimuon rapidity: barrel ($|y^{\mu\mu}| \leq 1.0$), barrel-endcap transition ($1.0 < |y^{\mu\mu}| \leq 1.2$), and endcap ($1.2 \leq |y^{\mu\mu}| < 2.25$), to account for the different behaviors of these corrections in these regions. The correction c_a is due to the effect of vertex and opposite charge requirements on the trigger and is determined from the efficiency at large dimuon angular separations. No difference was observed from deriving the result as a function of $\Delta\eta$ and $\Delta\phi$ separately rather than versus ΔR . The asymptotic values are found using the ratio of candidate $J/\psi \rightarrow \mu^+ \mu^-$ decays selected by the standard dimuon trigger to those selected by a similar dimuon trigger that makes no charge or vertex requirements. These values are found to be $99.1 \pm 0.4\%$, $97.5 \pm 0.9\%$, $95.2 \pm 0.4\%$ in the barrel, transition, and endcap regions, respectively.

We extract this dependence on ΔR in the same three regions of dimuon rapidity as used for c_a from a sample of offline reconstructed $J/\psi \rightarrow \mu^+ \mu^-$ and $Y \rightarrow \mu^+ \mu^-$ candidates with $p_{T2}^\mu > 8$ GeV selected using a single-muon trigger with a threshold of 18 GeV. The 8 GeV requirement on the lower p_T muon is made to ensure that the efficiency for the trigger system to identify RoIs compatible with muons of $p_T > 4$ GeV reached its plateau value. The ΔR dependence of $c_{\Delta R}$ is then extracted from the fraction of fitted dimuon candidates in a ΔR interval within this control sample selected using auxiliary triggers that additionally pass the dimuon trigger used in this analysis.

The final component of the dimuon trigger efficiency, ε_{RoI} , represents the single-muon trigger efficiency with a threshold of $p_T^\mu > 4$ GeV. This is measured using well-reconstructed $J/\psi \rightarrow \mu\mu$ candidates in data that pass a single-muon trigger (with a threshold of 18 GeV). The ratio of the yield of J/ψ candidates (determined by fitting the invariant mass distributions) that pass both this single-muon trigger and the 4 GeV p_T^μ threshold dimuon trigger used in this analysis, to the yield of J/ψ candidates that pass the single-muon trigger is identified as the single-muon trigger efficiency ε_{RoI} in the p_T^μ and $q \cdot |\eta^\mu|$ interval considered. In each case, the reconstructed muon(s) are matched to the muon(s) that triggered the event for each of the single or dimuon triggers. The number of candidates passing the dimuon trigger is then further corrected by $c_{\mu\mu}$ for dimuon correlation effects [27].

The individual and overall efficiencies and weight corrections, calculated using the methods described above, are shown as functions of $p_T^{\mu\mu}$ and $|y^{\mu\mu}|$ in Fig. 3 for the $Y(1S)$.

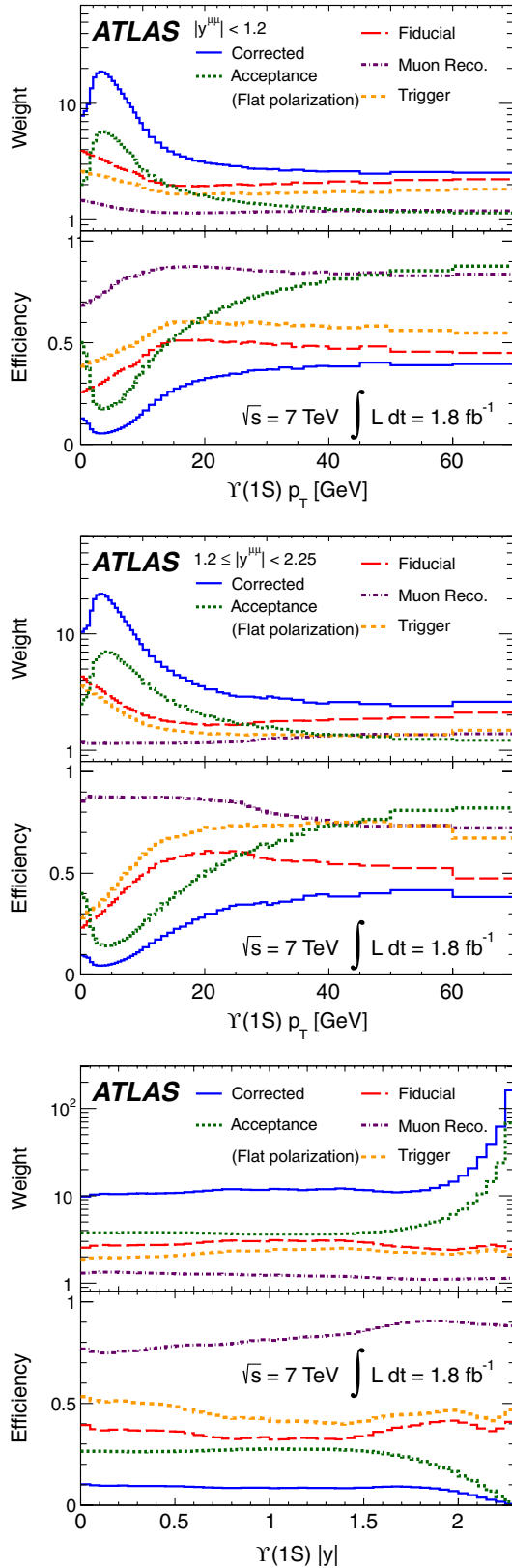


FIG. 3 (color online). Efficiency and acceptance corrections contributing to the overall fiducial and corrected efficiencies (and the inverse of the efficiency, the weight) as a function of the $Y(1S)$ $p_T^{\mu\mu}$ in the central (top) and forward (middle) regions of the detector and as a function of $|y^{\mu\mu}|$ (bottom).

C. Extracting the number of Y mesons

The number of produced $Y(nS)$ mesons used in our cross section determination is found by fitting signal and background functions to the $m_{\mu\mu}$ spectrum of weighted Y candidates. The use of per-candidate weights rather than average weights allows us to correct for acceptance and efficiency without introduction of biases associated with the use of average values for these quantities. We determine the Y differential cross sections separately for each spin-alignment scenario. We perform least squares fits to $m_{\mu\mu}$ histograms filled using the weights, w , for each candidate in bins of dimuon transverse momentum, $p_T^{\mu\mu}$, and rapidity, $y^{\mu\mu}$. The form of the χ^2 for each $(p_T^{\mu\mu}, |y^{\mu\mu}|)$ bin is

$$\chi^2 = \sum_{i=n_{\mu\mu}^{\text{bin}}} \left(\frac{n_i^{\text{data}} - n_i^{\text{pred}}}{\sigma_i} \right)^2, \quad n_i^{\text{data}} = \sum_{j=N_i} w_j; \quad \sigma_i^2 = \sum_{j=N_i} w_j^2, \quad (7)$$

where N_i represents the number of $Y(nS)$ candidates in bin i .

Predictions for each bin are constructed using four sources of dimuon candidates:

$$n^{\text{pred}}(m_{\mu\mu}) = N_{1S}F_{1S}(m_{\mu\mu}; f_{1S}) + N_{2S}F_{2S}(m_{\mu\mu}; f_{2S}) + N_{3S}F_{3S}(m_{\mu\mu}; f_{3S}) + F_{\text{bgd}}(m_{\mu\mu}; f_{\text{bgd}}), \quad (8)$$

where the f_X here represent fit function parameters and the F_X are normalized probability density functions. In order to avoid bias due to the choice of fit model, several parametrizations of signal and background, which describe the data well, are used.

Each of the three Y resonances are parametrized by single Gaussian, double Gaussian, or crystal ball functions, chosen to provide a reasonable description of the experimental mass resolution and energy loss effects that dominate the observed signal line shapes. The background parametrizations vary with dimuon p_T . At low $p_T^{\mu\mu}$, and for all rapidity bins, an error function multiplied by either a second-order polynomial, or a second-order polynomial plus an exponential, is used to model $m_{\mu\mu}$ turn-on effects accurately. At mid $p_T^{\mu\mu}$ a second-order polynomial, or second-order polynomial plus an exponential is adequate to describe the shape of the background under the Y peaks. At high $p_T^{\mu\mu}$ a first-order polynomial or a first-order polynomial plus an exponential is sufficient to describe the background contribution. Average fitted values for the numbers of $Y(nS)$ mesons (N_{1S}, N_{2S}, N_{3S}) taken over all combinations of signal and background models are used in the extraction of cross sections, while the maximum deviation of any fit result from the average is used as an estimate of the fit model systematic uncertainty.

In the fits N_{1S}, N_{2S}, N_{3S} , the peak mass of the $Y(1S)$ meson (M_{1S}), parameters describing the shape of the

$Y \rightarrow \mu^+ \mu^-$ mass distribution, and the background parameters are allowed to vary freely while M_{2S} , M_{3S} are fixed relative to M_{1S} using measured mass splittings [28]; and the line-shape width parameters σ_{2S} , σ_{3S} are related

linearly in $m_{\mu\mu}$ to σ_{1S} . The distribution of the χ^2 probabilities from the fits are uniformly distributed indicating that our signal and background parametrizations provide good descriptions of the data. Figure 4 shows the invariant

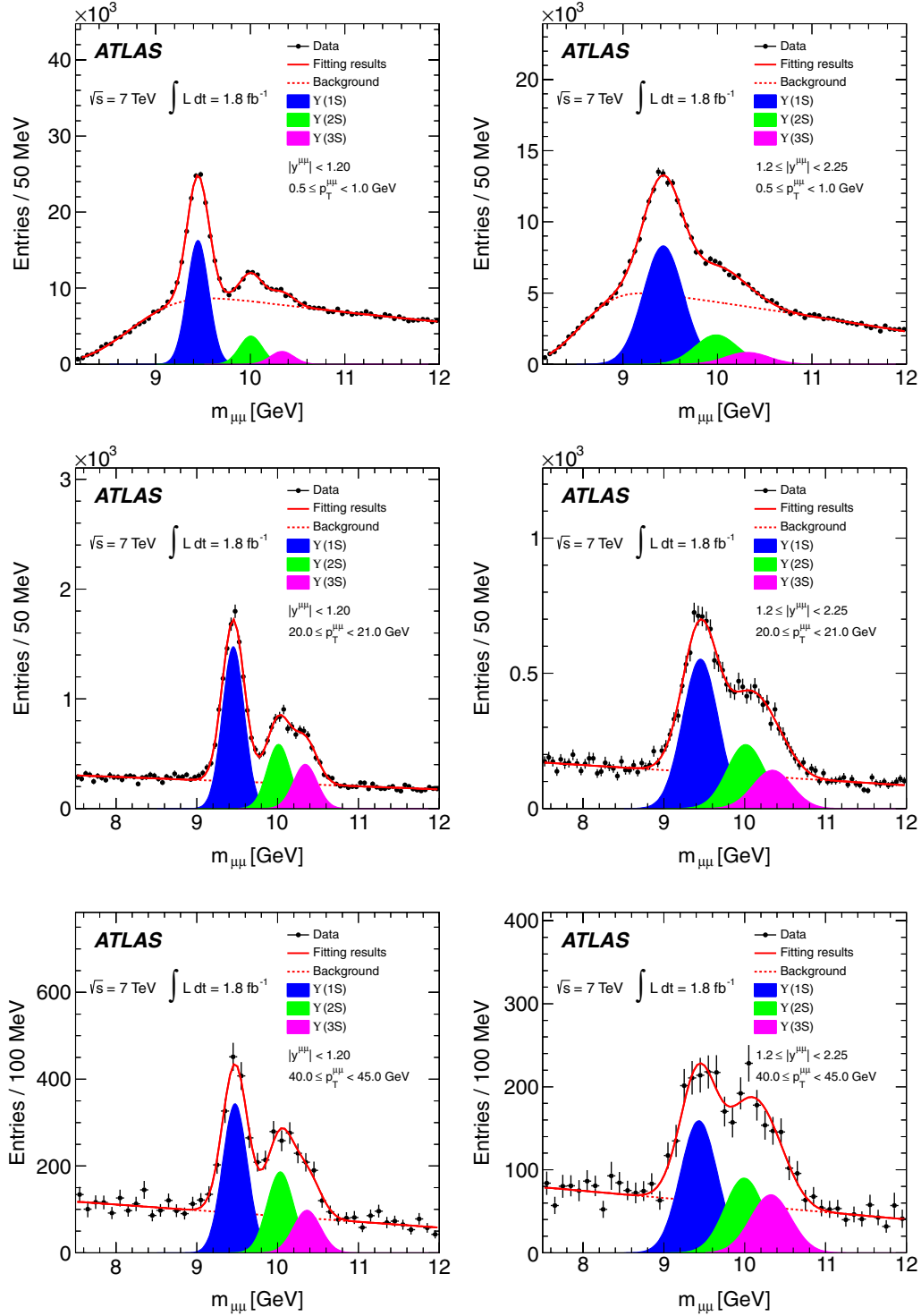


FIG. 4 (color online). Fits to the efficiency-corrected $m_{\mu\mu}$ spectra for candidates in the low (0.5–1.0 GeV; top), mid (20–21 GeV; middle), and high (40–45 GeV; bottom) $p_T^{\mu\mu}$ intervals, for central (left) and forward (right) dimuon rapidities. Fit results are shown for the simplest fit model considered: a single Gaussian signal plus either a second-order polynomial multiplied by an error function (low p_T), second-order polynomial (mid p_T), or first-order polynomial (high p_T) background parametrization.

mass distribution of the fitted signal region for representative low, mid, and high Y p_T intervals, in both the central and forward rapidity regions.

In order to account for bin migrations due to finite detector resolution, corrections in $p_T^{\mu\mu}$ are derived by first fitting a smooth analytic function to the background-subtracted $p_T^{\mu\mu}$ spectra of Y events in data. This fitted distribution is deconvolved with a Gaussian distribution using a Gauss-Hermite quadrature integration technique, with a p_T resolution derived from the fitted invariant mass and muon angular resolutions in data. From the distributions with and without convolution, migration corrections bin-by-bin are derived. These corrections are found to be within 0.5% of unity for central rapidities and within 1% of unity for forward rapidities. The number of efficiency-corrected $Y \rightarrow \mu^+ \mu^-$ decays extracted from the fits in each $(p_T^{\mu\mu}, y^{\mu\mu})$ bin are corrected for the difference between true and reconstructed values of the dimuon p_T and rapidity. Using a similar technique, bin migration corrections as functions of $y^{\mu\mu}$ are found to be negligible.

V. SYSTEMATIC UNCERTAINTIES

We consider the following sources of systematic uncertainty on the $Y(nS)$ differential cross sections: luminosity determination, reconstruction and trigger efficiencies, migration between $p_T^{\mu\mu}$ and $|y^{\mu\mu}|$ bins due to resolution, acceptance corrections, and the background and signal fit models used. The range of these uncertainties for the three Y states is summarized in Table I and their breakdown in each source is given for the corrected cross section analysis in Figs. 5–7.

The relative luminosity uncertainty of 3.9% is described in more detail in Ref. [29]. Other sources of systematic uncertainty are discussed below. As the statistical components of the uncertainties associated with the determination of $\varepsilon_{\text{reco}}$ and $\varepsilon_{\text{trig}}$ are dominant, the uncertainties on the cross sections are derived from the statistics of the control samples

used to extract them using a series of pseudoexperiments, randomly varying the weights used for each Y candidate in data, according to the uncertainties on the efficiency maps. Systematic uncertainties associated with the fit model used to extract the number of $Y(nS)$ decays from our dimuon data sample are quantified by taking the largest deviation of the fitted values of N_{ns} found in the six possible model combinations from the average value. Systematic effects, due to differences in the underlying kinematic distributions of the control sample and the data distributions, are found to be negligible due to the fine differential binning of the efficiency and acceptance corrections.

Uncertainties associated with the acceptance correction include statistical uncertainties on the determination of the correction in fine p_T and rapidity bins. This constitutes approximately a 0.5% uncertainty across the measured spectrum. A shift in the interaction point along the beam-line axis, z , influences the acceptance particularly at large rapidity. To estimate the impact of this effect, the acceptances were recalculated with shifts in z by ± 62 mm, corresponding to one Gaussian standard deviation of the vertex z position distribution in the analyzed data, and the variation in the measured cross sections was calculated as a function of Y p_T and rapidity. These variations result in uncertainties on the acceptance corrections of 0.4%–0.7% as a function of p_T , and 0.6%–1.5% as a function of rapidity, growing toward larger rapidities and lower transverse momenta. Our estimate of the correction to the number of $Y \rightarrow \mu^+ \mu^-$ decays fitted in each $(p_T^{\mu\mu}, y^{\mu\mu})$ bin for differences between reconstructed and true values of $p_T^{\mu\mu}$ due to bin migration depends on a knowledge of the dimuon p_T resolution. Allowing this resolution to vary within its uncertainty results in a negligible change in the $Y(nS)$ cross sections.

As mentioned earlier, Y spin-alignment effects have an impact on the determination of cross sections extrapolated to full phase space. As in the ATLAS measurement of J/ψ production [7], we quote an uncertainty due to Y spin

TABLE I. Summary of statistical and systematic uncertainties on the cross section measurements. The systematic uncertainty due to the acceptance determination applies only to the corrected cross section measurements and does not include possible variation of the result due to spin alignment. Values quoted refer to the range of uncertainties over $p_T^{\mu\mu}$ in each of the $y^{\mu\mu}$ regions considered.

Source	Relative uncertainty [$Y(1S)/Y(2S)/Y(3S)$] [%]	
	$ y^{\mu\mu} < 1.2$	$1.2 \leq y^{\mu\mu} < 2.25$
Statistical uncertainty	1.5–10/2–10/3–10	2–15/2.5–12/4–18
Fit model	0.3–2/0.3–10/0.3–15	0.4–10/0.3–5.0/0.2–12
Luminosity	3.9	3.9
Trigger efficiency	2.0–3.0/1.0–2.0/1.0–2.0	2.0–3.0/2.0–4.0/2.0–7.0
Muon reconstruction efficiency	0.7–2.0/0.4–1.2/0.4–1.2	0.5–5.0/0.4–3.0/0.4–3.0
Acceptance corrections	0.7–1.5	0.7–1.5
Track reconstruction efficiency	1.0	1.0

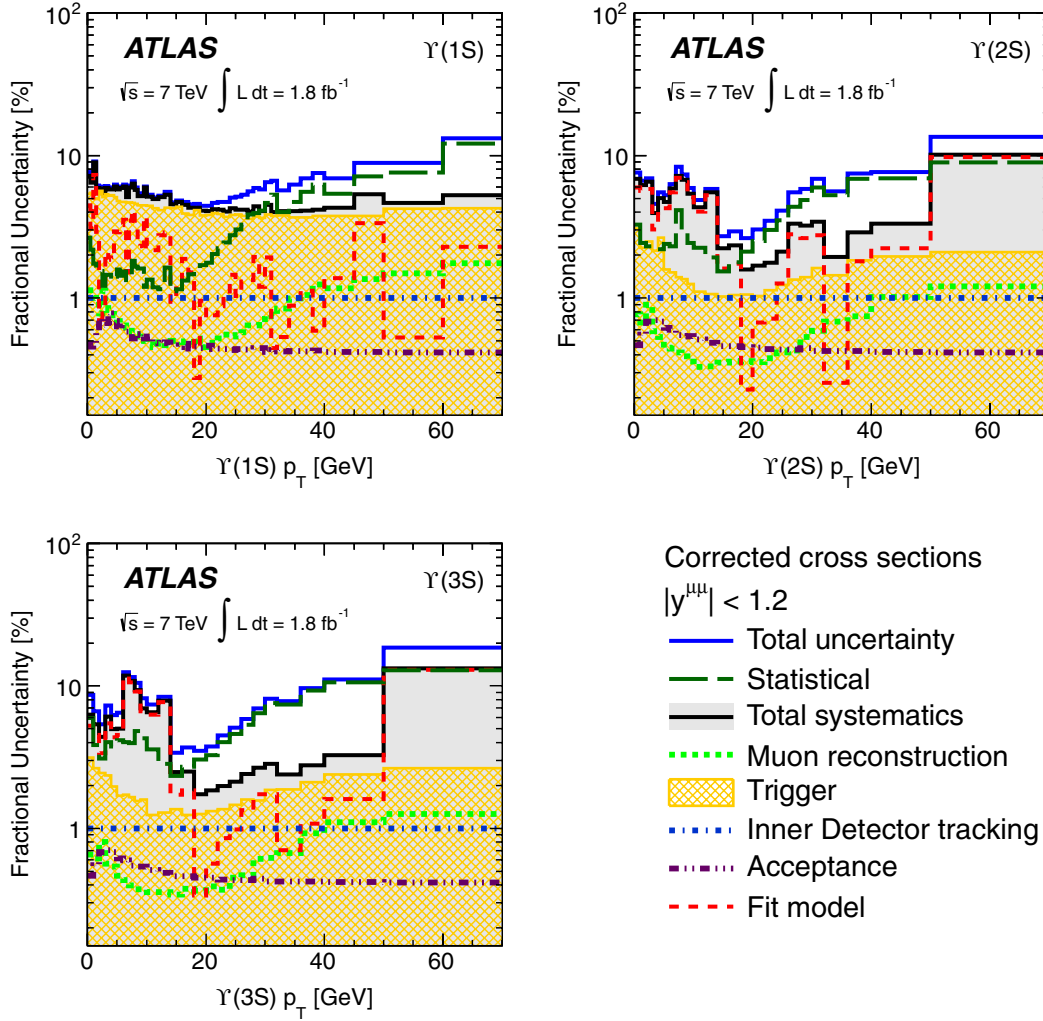


FIG. 5 (color online). Sources of statistical and systematic uncertainty on the corrected $Y(nS)$ production cross section measurements in the central rapidity region. A common luminosity uncertainty of $\pm 3.9\%$ is not included.

alignment by comparing results obtained using the unpolarized assumption ($\lambda_\theta = \lambda_\phi = \lambda_{\theta\phi} = 0$) to those derived under the other four extreme parameter combinations. The size of the possible variation in each bin is taken to be the largest positive and negative deviation from the unpolarized baseline result. We provide the cross section results for each of the spin-alignment scenarios along with tabulated values [26] of the weight corrections so that the corrected data can be determined in terms of any spin-alignment scenario.

VI. RESULTS AND DISCUSSION

We measure the differential cross section multiplied by the dimuon branching fractions of $Y(1S)$, $Y(2S)$, and $Y(3S)$ mesons as a function of Y transverse momentum and rapidity, both in a fiducial region defined by $p_T^\mu > 4$ GeV, $|\eta^\mu| < 2.3$ (free from spin-alignment uncertainties) and corrected back to the full muon decay phase

space with $|y^Y| < 2.25$. We additionally present measurements of the production cross sections of the $Y(2S)$ and $Y(3S)$ relative to the $Y(1S)$ as a function of $Y(1S)$ transverse momentum and rapidity. Tabulated results of all measurements presented in this paper are available in HEPDATA [26].

A. Fiducial cross sections

Differential cross sections multiplied by the $Y \rightarrow \mu^+ \mu^-$ branching fractions, $d^2\sigma/dp_T dy \times \text{Br}(Y \rightarrow \mu^+ \mu^-)$, are calculated within the fiducial acceptance of our analysis ($p_T^\mu > 4$ GeV, $|\eta^\mu| < 2.3$) using the results of fits to dimuon candidates in data corrected, candidate by candidate, for efficiencies using the fiducial weights, w_{fid} , defined in Eq. (2). These differential fiducial cross sections along with total uncertainties are shown in Figs. 8 and 9 and span 4 orders of magnitude across the p_T range studied.

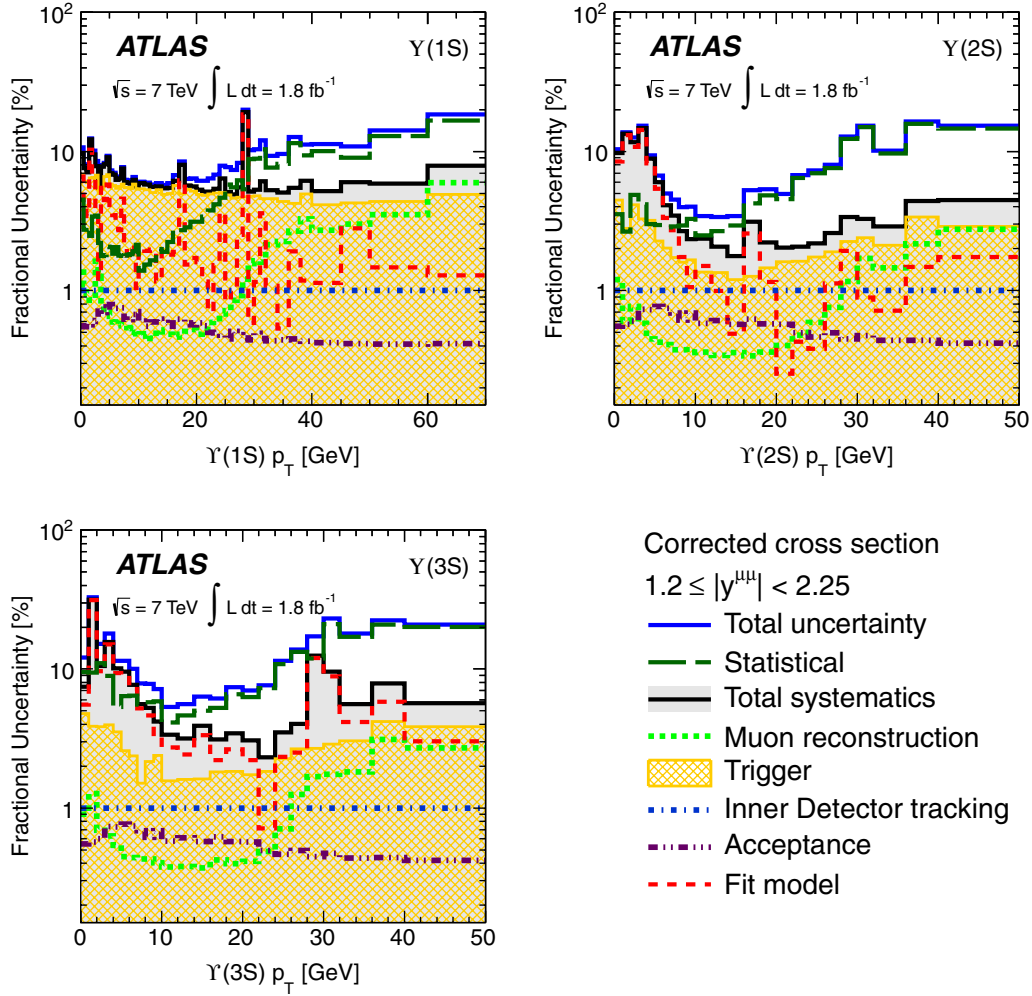


FIG. 6 (color online). Sources of statistical and systematic uncertainty on the corrected $Y(nS)$ production cross section measurements in the forward rapidity region. A common luminosity uncertainty of $\pm 3.9\%$ is not included.

Integrating over all p_T^Y and both rapidity bins we find cross sections within the fiducial acceptance of the detector as shown in Table II. The results for the $Y(1S)$ are consistent with our previous measurement [8] but extend to a significantly higher p_T^Y and with increased precision.

Presenting the results in a restricted kinematic phase space removes any uncertainty due to the spin alignment of quarkonia. This allows unambiguous comparison of differential spectra with any theoretical approaches that can provide predictions with kinematic restrictions applied to the decay products of the Y .

NLO color-singlet [14] predictions [30] have previously been compared to differential $Y(1S)$ fiducial production cross sections [8] and were found to underestimate the measured production rates by approximately an order of magnitude and to not reflect the p_T dependence of the data. This is not surprising as it has been known [16] for some time that higher-order corrections are both large and necessary in order to adequately describe quarkonium production at high p_T with color-singlet terms. At this time, no color-singlet calculations beyond NLO are available for quarkonium

production measurements quoted in a restricted muon acceptance, nor are color octet [17] or color evaporation [19] approaches currently able to account for the kinematics of leptons from the quarkonium decay. The fiducial measurements presented here are precise and free from any assumptions on the angular dependencies of the dimuon system, accurately reflecting the production dynamics in proton-proton collisions at $\sqrt{s} = 7 \text{ TeV}$.

B. Corrected cross sections

We also calculate differential cross sections multiplied by the $Y \rightarrow \mu^+ \mu^-$ branching fractions extrapolated to the full muon phase space within $|y^Y| < 2.25$. For these corrected cross sections, the results of fits to dimuon candidates in data are corrected, candidate by candidate, for efficiencies using the total weights, w_{tot} , defined in Eq. (2). Results are shown for the isotropic spin-alignment scenario in Figs. 10 and 11 as a function of Y p_T and y for all three states and, integrated over all p_T^Y and both rapidity bins, in Table III.

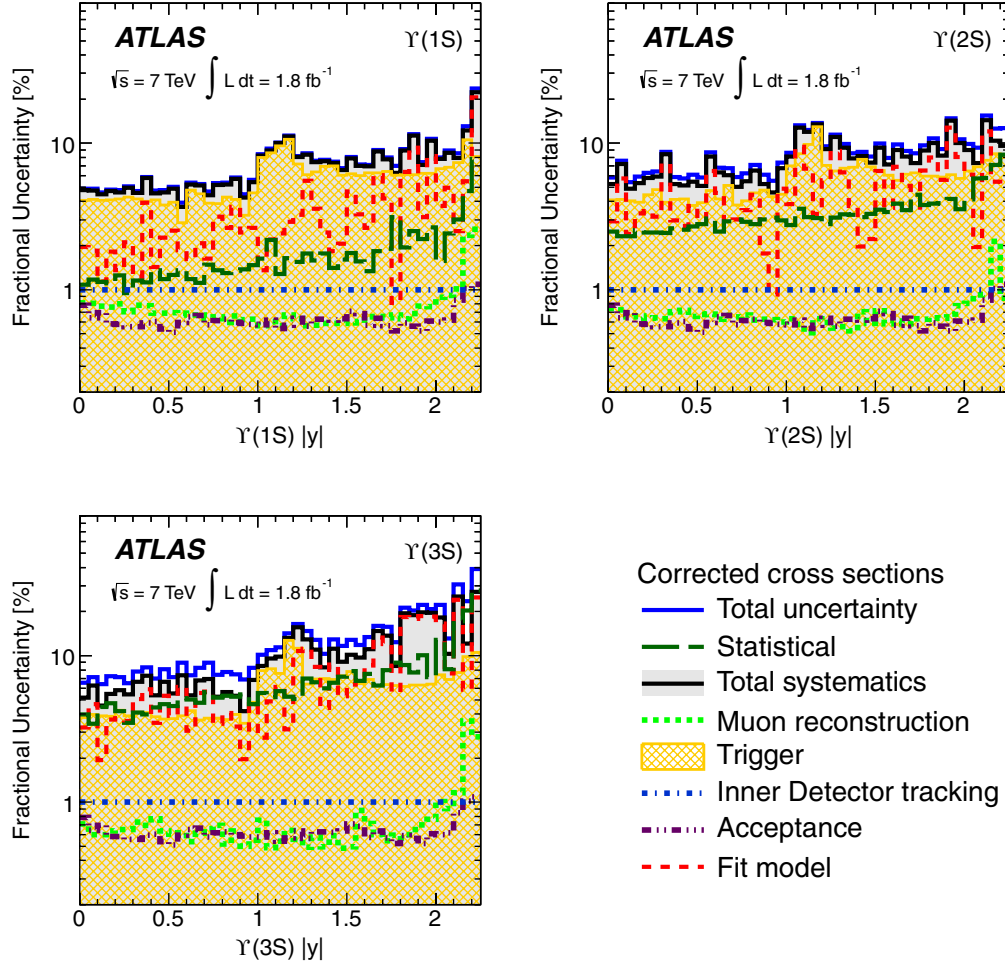


FIG. 7 (color online). Sources of statistical and systematic uncertainty on the corrected $Y(nS)$ production cross section measurements as a function of Y rapidity. A common luminosity uncertainty of $\pm 3.9\%$ is not included.

Our results are consistent with measurements by CMS [6] and, in the small region of rapidity overlap from $2.0 < |y| < 2.25$, with LHCb [11]. These results allow us to test phenomenological models of Y production not just at low p_T (for complementarity with results from the Tevatron experiments) but in a newly-probed region of significantly boosted Y , where higher-order contributions become particularly important.

Figures 12–17 show the differential cross sections as a function of p_T and rapidity for each of the Y states in comparison with theoretical predictions. The effects of varying spin-alignment assumptions from the nominal assumption of isotropic muon angular distributions independent of θ^* and ϕ^* are indicated by a shaded band.

Clearly, spin alignment has a large effect on the Y production cross sections, especially at low p_T^Y , and, in particular, if there is a nontrivial azimuthal component to the spin alignment. New results [4,12] of Y spin alignment from CDF and CMS suggest that the spin alignment is consistent with unpolarized production. Our central assumption of isotropic Y decays is consistent with these results. Nevertheless, as these spin-alignment

measurements are made at different center-of-mass energies or in a restricted phase space in both p_T^Y and rapidity with respect to measurements presented here, we provide the results under a variety of polarization scenarios so that the impact of spin alignment on the corrected cross sections can be quantified across the full range of study.

The contributions of the five polarization scenarios can be seen in the lower panes of each plot where the ratio of the differential cross section under these spin-alignment assumptions to the unpolarized scenario is shown. Across the whole p_T range studied the envelope is bounded from above by the $T++$ ($\lambda_\theta = +1$, $\lambda_\phi = +1$, $\lambda_{\theta\phi} = 0$) scenario with a maximal ϕ^* variation. From below, the cross section envelope is bounded by fully longitudinal spin alignment at very low p_T , with the $T+-$ ($\lambda_\theta = +1$, $\lambda_\phi = -1$, $\lambda_{\theta\phi} = 0$) scenario resulting in the largest downward variation at $p_T \gtrsim 4$ GeV. In this measurement we extend the p_T range above 45 GeV where the maximal possible impact due to the unknown spin alignment of Y is below $\pm 10\%$. This is significantly smaller than the theoretical uncertainties and is of similar magnitude to current

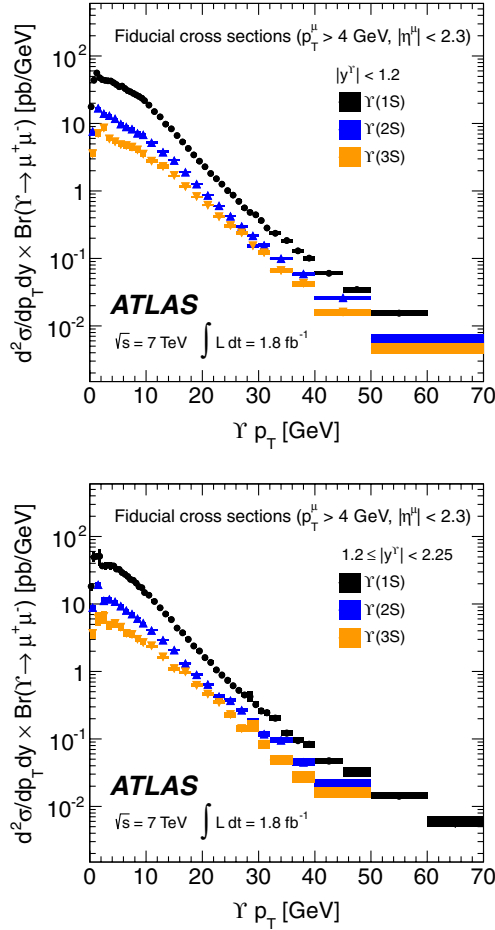


FIG. 8 (color online). Differential cross sections multiplied by the dimuon branching fraction, $d^2\sigma/dp_T dy \times \text{Br}(Y \rightarrow \mu^+ \mu^-)$, for central (top) and forward (bottom) rapidities, for $Y(1S)$, $Y(2S)$, $Y(3S)$ production within the fiducial acceptance. Points with error bars indicate results of the measurements with statistical uncertainties while shaded areas correspond to total uncertainties on the measurement, including systematic effects.

experimental uncertainties. As such, this region will offer a precision environment to compare future theoretical studies of Y production to data.

In Figs. 12–14 a comparison is also made to two theoretical predictions of Y production. The first [16] is a QCD-based calculation using the color-singlet mechanism [14], referred to as NNLO* CSM, and presumes that Y meson production occurs via a color-singlet state and includes full corrections up to next-to-leading order (NLO), as well as some of the most important next-to-next-to-leading-order (NNLO) terms. This inclusion significantly modifies the prediction. The partial nature of the higher-order calculation limits the applicability of the calculation to values above a particular Y p_T threshold and increases the sensitivity of the prediction to the choice of renormalization and factorization scales. The second prediction, known as the color evaporation model [19,31], labeled as CEM, is a phenomenological model for inclusive Y

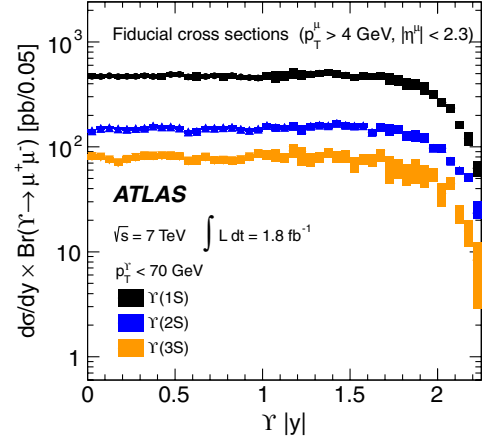


FIG. 9 (color online). Differential cross sections multiplied by the dimuon branching fraction, $d\sigma/dy \times \text{Br}(Y \rightarrow \mu^+ \mu^-)$ (p_T -integrated) $d\sigma/dy \times \text{Br}(Y \rightarrow \mu^+ \mu^-)$ for $Y(1S)$, $Y(2S)$, $Y(3S)$ production within the fiducial acceptance. Points with error bars indicate results of the measurements with statistical uncertainties while shaded areas correspond to total uncertainties on the measurement, including systematic effects.

production based on quark-hadron duality. This model assumes that any heavy $Q\bar{Q}$ pair produced in the initial hard scattering evolves to a quarkonium state if its mass is below the threshold of open heavy-flavor meson pairs. Predictions of the CEM model involve a single constant that must be determined from corrected cross section measurements for each quarkonium state and use a b -quark mass of 4.75 GeV. As in the case of the CSM, divergences in the predictions restrict the applicability of the model at low Y p_T . Uncertainties from factorization and renormalization scales are estimated from varying the scales independently up and down by a factor of 2 and additional uncertainties are estimated from varying the b -quark mass [32].

Color-singlet calculations at NLO/NNLO* predict a largely longitudinal polarization of direct Y particularly at high p_T (although the effect of feed-down introduces large uncertainties to this prediction). The color evaporation model offers no explicit prediction of the spin-alignment evolution of Y , but the nature of the model suggests no strong polarization should be observed as no single production mechanism dominates.

TABLE II. Integrated fiducial cross section measurements for $Y(nS)$. Uncertainties quoted represent statistical, systematic, and luminosity terms, respectively.

State	Integrated fiducial cross sections $p_T^\mu > 4 \text{ GeV}$, $ \eta^\mu < 2.3$ $\sigma_{\text{fid}}(pp \rightarrow Y) \times \text{Br}(Y \rightarrow \mu^+ \mu^-)$ Range: $p_T^Y < 70 \text{ GeV}$, $ y^Y < 2.25$	
$Y(1S)$	$1.890 \pm 0.007 \pm 0.095 \pm 0.074 \text{ nb}$	
$Y(2S)$	$0.601 \pm 0.003 \pm 0.040 \pm 0.023 \text{ nb}$	
$Y(3S)$	$0.304 \pm 0.003 \pm 0.021 \pm 0.012 \text{ nb}$	

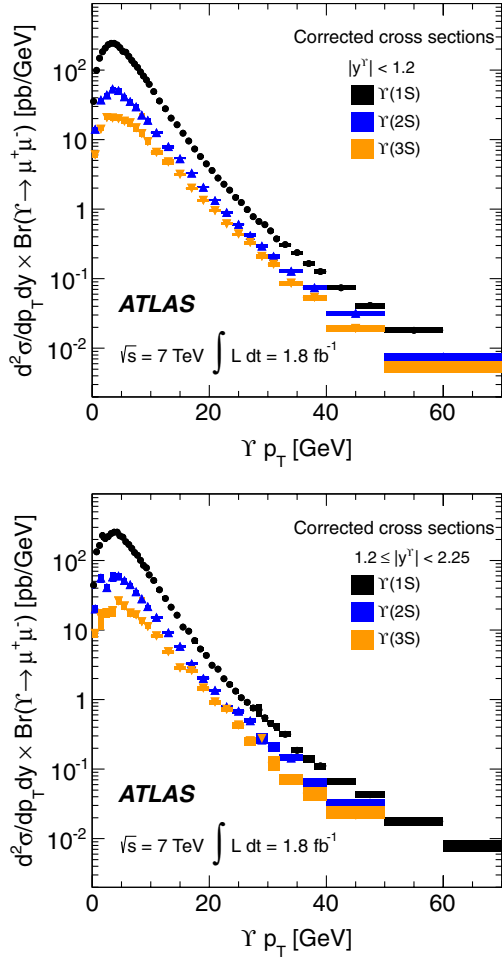


FIG. 10 (color online). Differential cross sections multiplied by the dimuon branching fraction, for $Y(1S)$, $Y(2S)$, and $Y(3S)$ production extrapolated to the full phase space for the (top) $|y^Y| < 1.2$, (bottom) $1.2 \leq |y^Y| < 2.25$ rapidity intervals. Points with error bars indicate the results of the measurements with total statistical and systematic errors. Results are shown assuming an isotropic spin-alignment scenario.

As can be seen in Figs. 12–14, the two models provide quite different descriptions of Y production. Predictions from CSM are for direct Y production only and so do not account for Y production that arises from feed-down from the production of higher Y states or from radiative decays of the $\chi_{bj}(nP)$. From previous measurements [33] the contribution of feed-down to $Y(1S)$ production is known to be approximately 50%, but the p_T dependence of the feed-down is not well known and cannot be reliably predicted, and so no explicit correction is made to the CSM predictions shown. No correction is needed for the CEM as this is already an inclusive calculation. Feed-down contributions are expected to similarly contribute to $Y(2S)$ production, but no measurement or reliable prediction for the relative contribution exists, so we do not apply a correction to the direct $Y(2S)$ CSM predictions either. For $Y(3S)$ there is no feed-down from higher Y states.

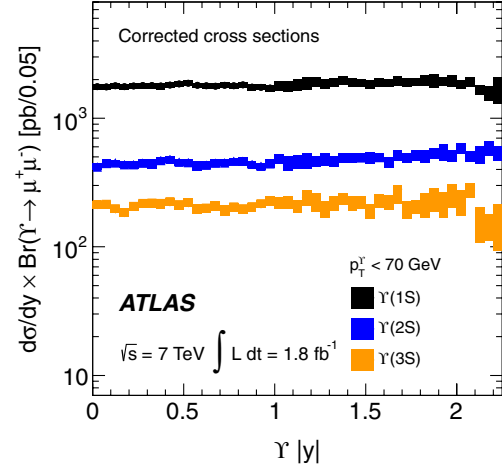


FIG. 11 (color online). Differential cross sections multiplied by the dimuon branching fraction, for $Y(1S)$, $Y(2S)$, and $Y(3S)$ production extrapolated to the full phase space, p_T -integrated as a function of absolute Y rapidity. Points with error bars indicate the results of the measurements with total statistical and systematic errors. Results are shown assuming an isotropic spin-alignment scenario.

Recently, the ATLAS experiment discovered [34] the existence of a state or states interpreted as the $\chi_{bj}(3P)$ below the $B\bar{B}$ threshold that are expected to have a significant branching fraction for radiative decays into $Y(3S) + \gamma$ and thus induce a feed-down contribution to $Y(3S)$ (and other Y states). As the relative production and decay rates of these states are also as yet unknown, no correction is applied to the CSM predictions for $Y(3S)$ production either.

For each of the three $Y(nS)$ states, the NNLO* CSM predictions (considering also the additional normalization uncertainty due to the poorly known contributions from feed-down) fit our data well in the moderate p_T^Y region but exhibit a steeper p_T dependence than seen in data. The predictions therefore significantly underestimate the cross section at high p_T . Theoretical developments in the prediction of feed-down contributions may improve this description. CEM predictions appear to show a better match with data at high p_T^Y . These predictions underestimate the rate (favoring a smaller choice of renormalization/factorization scale or larger b -quark mass) and have

TABLE III. Corrected cross section measurements in the isotropic spin-alignment scenario. Uncertainties quoted represent statistical, systematic, and luminosity terms, respectively.

State	Integrated corrected cross sections	
	$\sigma(pp \rightarrow Y) \times \text{Br}(Y \rightarrow \mu^+ \mu^-)$ Range: $p_T^Y < 70 \text{ GeV}$, $ y^Y < 2.25$	
$Y(1S)$	$8.01 \pm 0.02 \pm 0.36 \pm 0.31 \text{ nb}$	
$Y(2S)$	$2.05 \pm 0.01 \pm 0.12 \pm 0.08 \text{ nb}$	
$Y(3S)$	$0.92 \pm 0.01 \pm 0.07 \pm 0.04 \text{ nb}$	

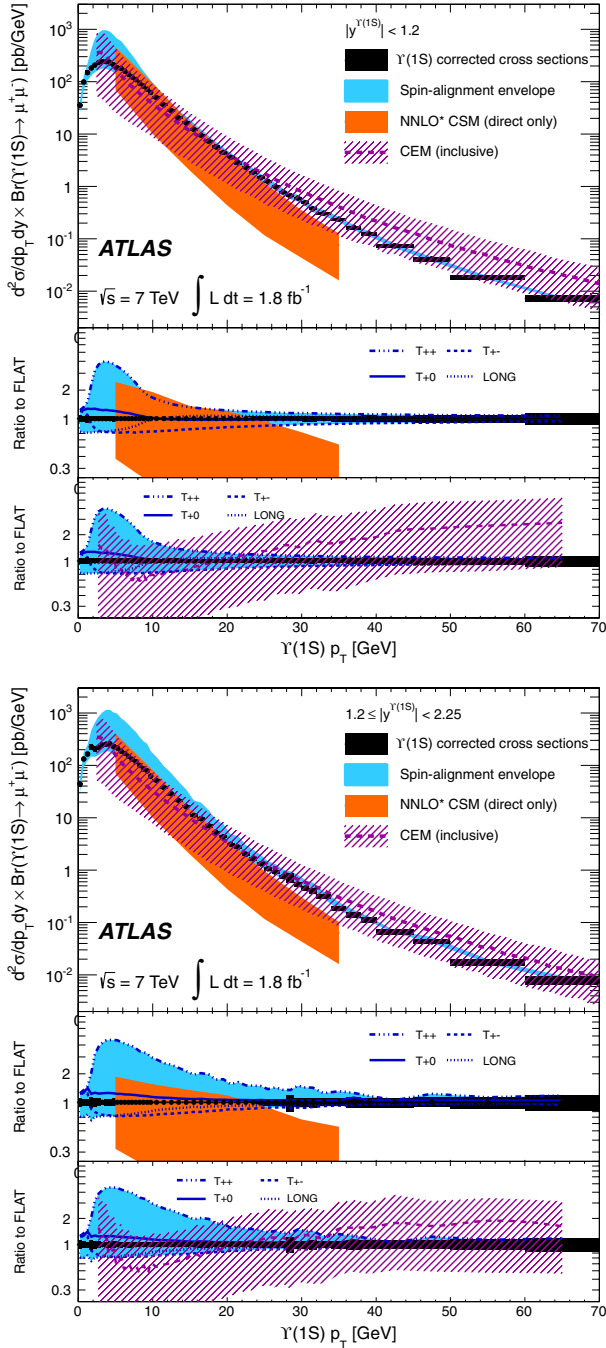


FIG. 12 (color online). Differential cross sections multiplied by the dimuon branching fraction, $d^2\sigma/dp_T dy \times \text{Br}(Y \rightarrow \mu^+ \mu^-)$, for $Y(1S)$ production extrapolated to the full phase space for (top) central and (bottom) forward rapidities. Points with error bars indicate results of the measurements with total (statistical and systematic) uncertainties. The maximal envelope of variation of the result due to spin-alignment uncertainty is indicated by the solid band. Also shown are predictions of direct production with the NNLO* color-singlet mechanism (CSM) and inclusive predictions from the color evaporation model (CEM). These theory predictions are shown as a ratio to the data in the lower panes for CEM (middle) and CSM (bottom), along with detail of the variations of the cross section measurement under the four anisotropic spin-alignment scenarios as a ratio to the nominal data.

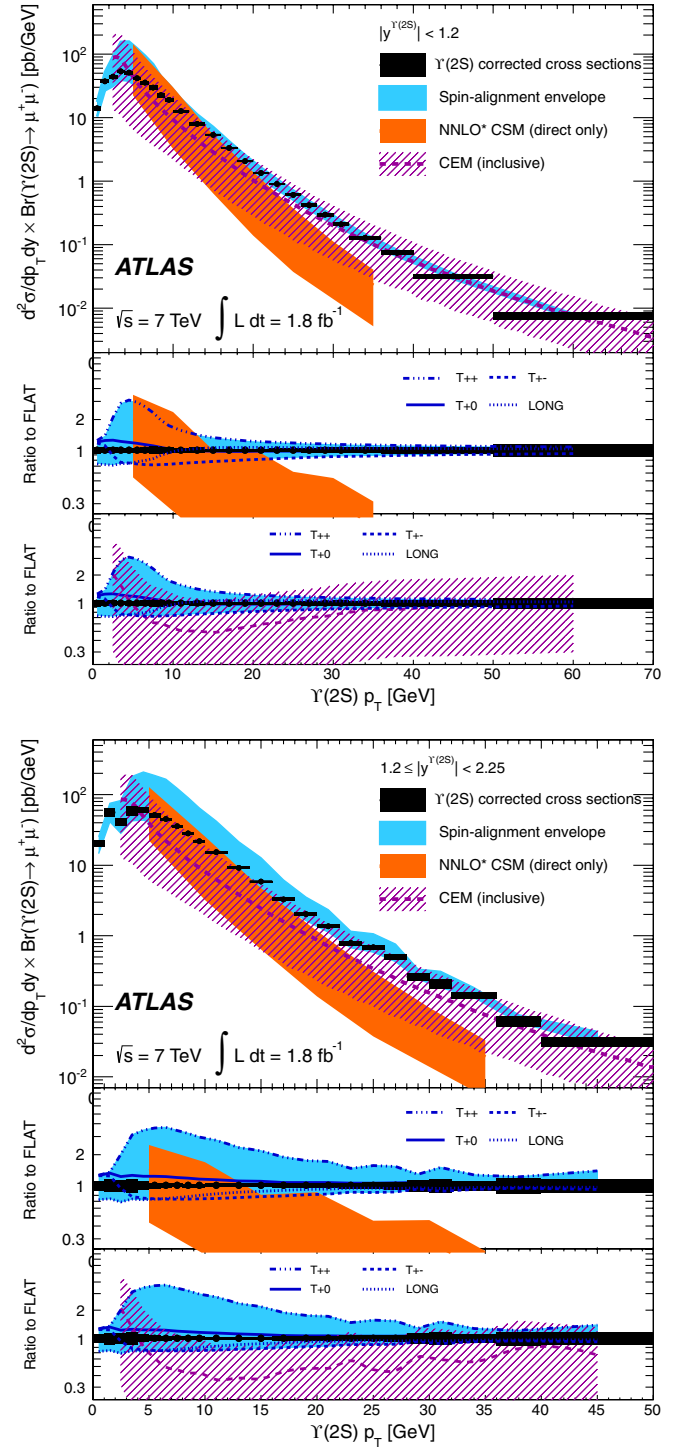
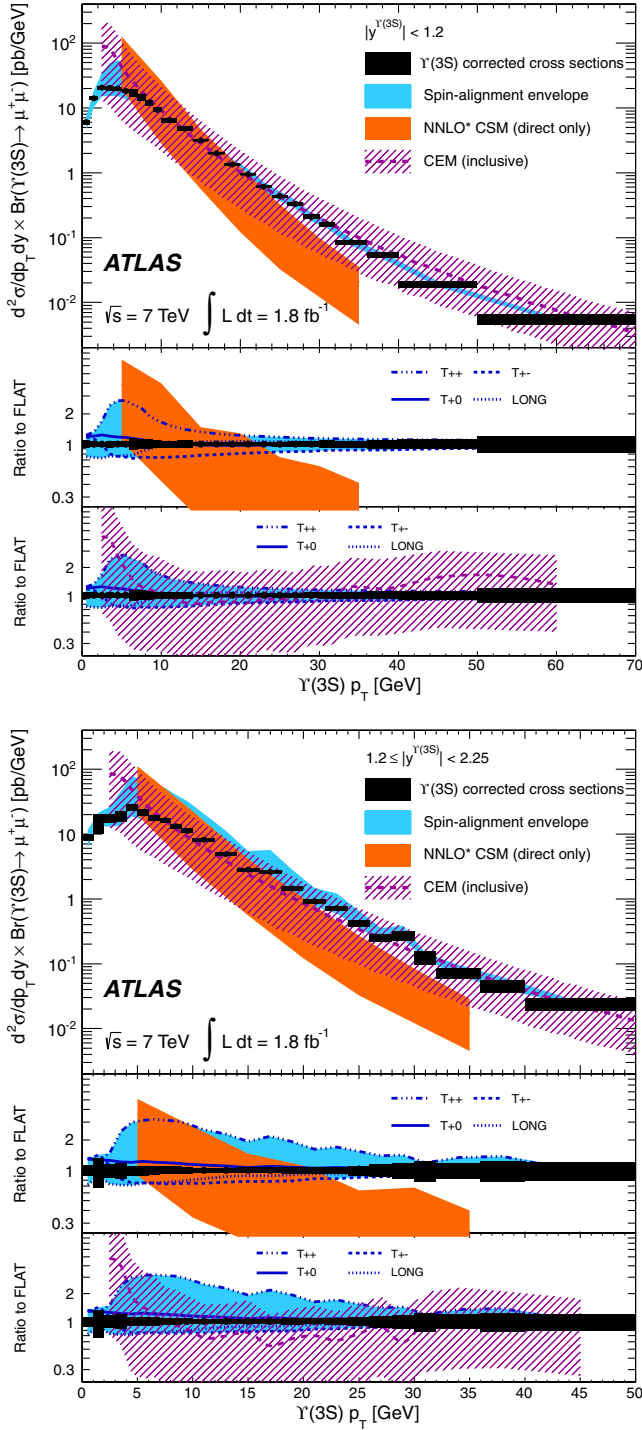


FIG. 13 (color online). As for Fig. 12, but for $Y(2S)$ production.

problems in modeling the shape of the spectrum, particularly at lower p_T . Shape discrepancies cannot be accommodated within the uncertainties quoted as changes in the scale choice introduce correlated changes in the prediction as a function of p_T .

Figures 15–17 show the variation of the production cross section as a function of absolute Y rapidity integrated

FIG. 14 (color online). As for Fig. 12, but for $Y(3S)$ production.

across all p_T . The dependence on rapidity is relatively flat in the interval of rapidities in the ATLAS acceptance.

Variations between spin-alignment scenarios lead largely to a change in the normalization of the distributions with little variation in shape except at high rapidity. There, the $T++$ scenario leads to an increase in the cross section with increasing rapidity, while the fully longitudinal scenario leads to a drop in cross section at high ($|y| \gtrsim 1.7$) rapidity.

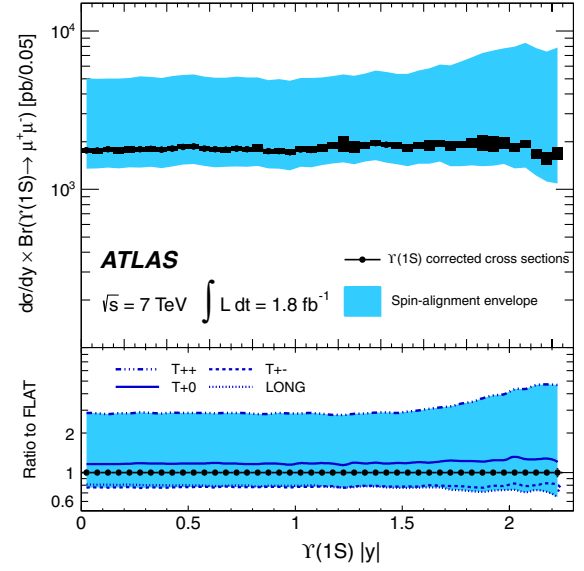


FIG. 15 (color online). Differential cross sections multiplied by the dimuon branching fraction, $d\sigma/dy \times \text{Br}(Y \rightarrow \mu^+ \mu^-)$, for $Y(1S)$ production extrapolated to the full phase space. Points with error bars indicate results of the measurements with total (statistical and systematic) uncertainties. The maximal envelope of variation of the result due to spin-alignment uncertainty is indicated by the solid band. The variations of the cross section measurement under the four anisotropic spin-alignment scenarios are shown in the lower pane as ratios to the unpolarized scenario.

C. Cross section ratios

From our differential cross section measurements, we explore the p_T and rapidity dependence of $Y(2S)$ and $Y(3S)$ production relative to the $Y(1S)$ by deriving the ratios

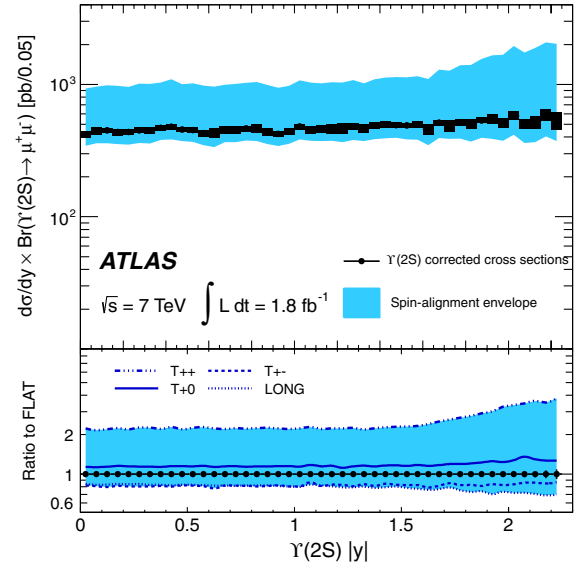
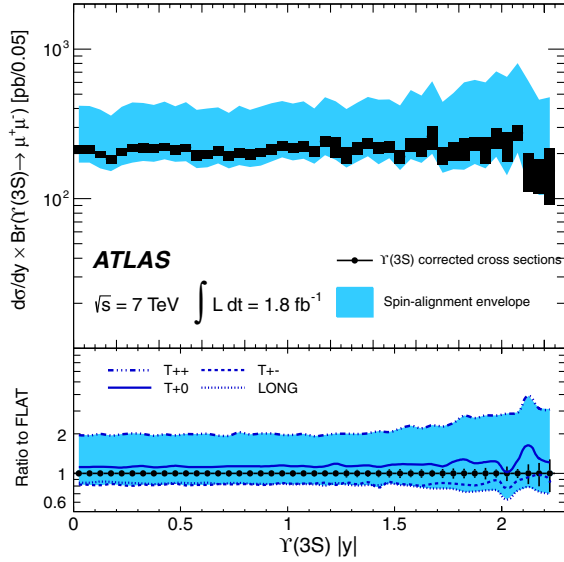


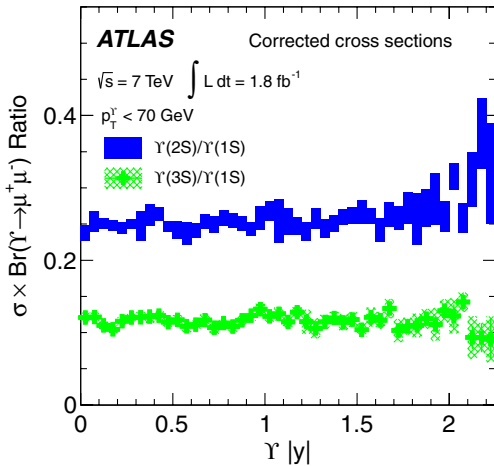
FIG. 16 (color online). As for Fig. 15, but for $Y(2S)$ production.

FIG. 17 (color online). As for Fig. 15, but for $Y(3S)$ production.

$$\frac{d^2\sigma(pp \rightarrow Y(nS)/dp_T dy}{d^2\sigma(pp \rightarrow Y(1S)/dp_T dy} \times \frac{\text{Br}(Y(nS) \rightarrow \mu^+\mu^-)}{\text{Br}(Y(1S) \rightarrow \mu^+\mu^-)} \quad (9)$$

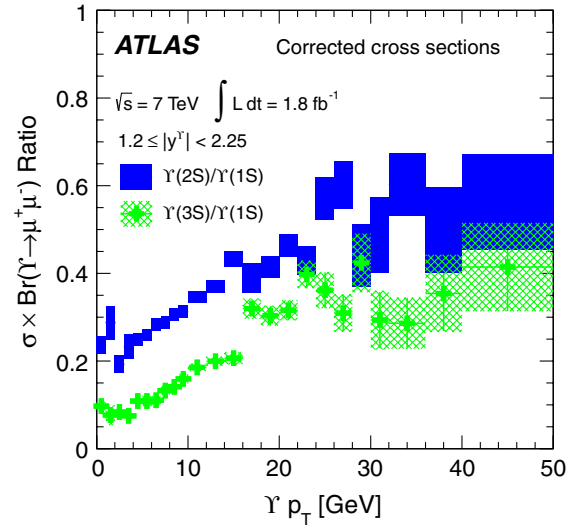
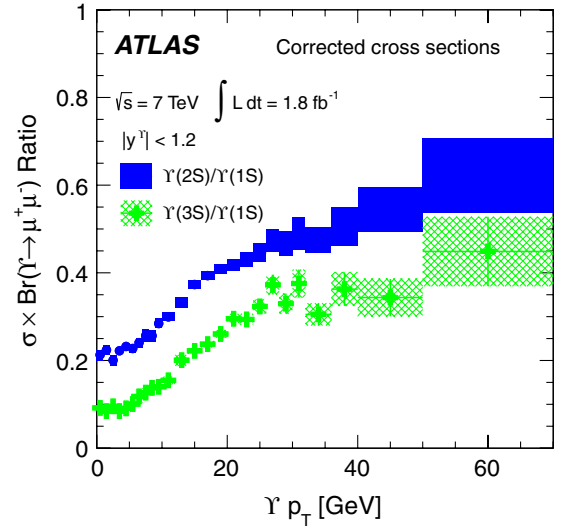
for $|y^Y| < 2.25$ with $n = 2, 3$. Such observables are sensitive to the magnitude and kinematic dependencies of feed-down contributions between the three Y states. Results of the differential cross section ratio measurements are presented in Figs. 18 and 19.

These measurements are made under the assumption of unpolarized $Y(nS)$ mesons, and take into account statistical correlations between the fitted numbers of $Y(1S)$,

FIG. 18 (color online). Ratios of differential $Y(2S)/Y(1S)$ and $Y(3S)/Y(1S)$ cross sections multiplied by the dimuon branching fractions as a function of dimuon rapidity. Points with error bars indicate results of the measurements with statistical uncertainties while shaded areas correspond to total uncertainties on each point, including systematic effects, but excluding spin-alignment effects.

$Y(2S)$, and $Y(3S)$ mesons. Systematic uncertainties are estimated by varying acceptance, efficiency, and fit model assumptions coherently in the numerator and denominator when calculating the ratios, thereby partially canceling uncertainties in the ratio. Luminosity uncertainties cancel entirely.

The measured $Y(nS)/Y(1S)$ ratios are relatively constant in the $0 < p_T < 5$ GeV interval at $\sim 20\%$ and $\sim 7\%$, respectively, for the $Y(2S)$ and $Y(3S)$. At higher p_T a significant and steady rise in the relative production rates of higher Y states is apparent, in agreement with measurements by CMS [6]. However, at the larger p_T^Y values (above

FIG. 19 (color online). Ratios of differential $Y(2S)/Y(1S)$ and $Y(3S)/Y(1S)$ cross sections multiplied by the dimuon branching fractions versus $Y p_T$ in the (top) central and (bottom) forward rapidity regions. Points with error bars indicate results of the measurements with statistical uncertainties while shaded areas correspond to total uncertainties on each point, including systematic effects, but excluding spin-alignment effects.

p_T^Y of 30–40 GeV) accessible for the first time with these measurements, evidence of a saturation in this rise is apparent, suggesting that we are probing a regime where direct production dominates over contributions from the decays of excited states. In contrast, the rapidity dependence of these production ratios is quite flat across the full $|y| < 2.25$ rapidity interval.

Higher-order color-singlet calculations are not currently able to predict the evolution of these production ratios in p_T^Y due to the significant feed-down contributions. At leading order in the quark velocity in the perturbative expansion, the production ratio of the *direct* contributions is proportional to the ratio of the squares of the magnitudes of the wave function at the origin (or the partial decay widths), multiplied by the branching fractions to dimuons for each of the states in question. The predicted ratios then are 36% for $Y(2S)/Y(1S)$ and 29% for $Y(3S)/Y(1S)$ for direct production. At high p_T , where the measured production ratio plateaus, the values are somewhat higher than these predictions suggesting that there is some enhancement (with respect to the simple picture above) of the $Y(2S)$ and $Y(3S)$ production relative to $Y(1S)$ production.

VII. CONCLUSIONS

We have measured differential production cross sections and relative production rates for $Y(1S)$, $Y(2S)$, and $Y(3S)$ mesons in pp collisions at $\sqrt{s} = 7$ TeV at the LHC up to $p_T^Y < 70$ GeV in the rapidity interval $|y^Y| < 2.25$. The possible impact of the Y spin alignment on these measured spectra is also quantified. These measurements are compatible with measurements by the CMS and LHCb collaborations. We have measured integrated corrected cross sections multiplied by the $Y \rightarrow \mu^+ \mu^-$ branching fractions, within the rapidity region $|y^Y| < 2.25$ of $8.01 \pm 0.02 \pm 0.36 \pm 0.31$ nb, $2.05 \pm 0.01 \pm 0.12 \pm 0.08$ nb, and $0.92 \pm 0.01 \pm 0.07 \pm 0.04$ nb for the $Y(1S)$, $Y(2S)$, and $Y(3S)$, respectively. Uncertainties correspond to statistical, systematic, and luminosity measurement effects.

These cross section estimates assume unpolarized production corresponding to $\lambda_\theta = \lambda_\phi = \lambda_{\theta\phi} = 0$ in Eq. (3). If the production polarization is fully transverse or longitudinal with no dependence on the azimuthal decay angle ϕ^* , corresponding to $\lambda_\theta = \pm 1$, $\lambda_\phi = \lambda_{\theta\phi} = 0$, the integrated cross sections may vary by up to $(+19, -23)\%$, $(+18, -21)\%$, and $(+17, -19)\%$, respectively, for the $Y(1S)$, $Y(2S)$, and $Y(3S)$. However, acceptances corresponding to certain nonzero values of λ_ϕ can become extremely low, especially at low transverse momenta of the muon pair. This would lead to a significant increase of the corrected cross sections in these configurations, up to $+217\%$, $+155\%$, and $+126\%$ for the three Y states.

We compare our differential cross section results to predictions from two theoretical approaches describing Y production. Our measurements find both the NNLO* CSM and the CEM predictions have some problems in describ-

ing the normalization and shape of the differential spectra. In particular, NNLO* dramatically underestimates the rate at high transverse momenta, where the data tend to agree better with the CEM. The inclusion of P -wave feed-down contributions in the theoretical calculation may help to improve the description. Large scale uncertainties in these predictions allow possible contributions from color-octet terms to contribute to the production rate in addition to singlet diagrams. The differential production ratios indicate that the increase in the production of higher Y states as a function of p_T^Y relative to the $Y(1S)$ observed previously begins to saturate at 30–40 GeV. Above ~ 40 GeV, the envelope of possible variations in the differential cross sections due to spin alignment is reduced to below $\pm 10\%$. This, along with the expected reduction in feed-down contributions, results in a relatively well-controlled region in which to study quarkonium production without the dominant experimental and theoretical effects that complicate such studies at lower p_T .

ACKNOWLEDGMENTS

We thank CERN for the very successful operation of the LHC, as well as the support staff from our institutions without whom ATLAS could not be operated efficiently. We acknowledge the support of ANPCyT, Argentina; YerPhI, Armenia; ARC, Australia; BMWF and FWF, Austria; ANAS, Azerbaijan; SSTC, Belarus; CNPq and FAPESP, Brazil; NSERC, NRC and CFI, Canada; CERN; CONICYT, Chile; CAS, MOST and NSFC, China; COLCIENCIAS, Colombia; MSMT CR, MPO CR and VSC CR, Czech Republic; DNRF, DNSRC and Lundbeck Foundation, Denmark; EPLANET, ERC, and NSRF, European Union; IN2P3-CNRS, CEA-DSM/IRFU, France; GNSF, Georgia; BMBF, DFG, HGF, MPG, and AvH Foundation, Germany; GSRT and NSRF, Greece; ISF, MINERVA, GIF, DIP, and Benoziyo Center, Israel; INFN, Italy; MEXT and JSPS, Japan; CNRST, Morocco; FOM and NWO, Netherlands; BRF and RCN, Norway; MNiSW, Poland; GRICES and FCT, Portugal; MERYS (MECTS), Romania; MES of Russia and ROSATOM, Russian Federation; JINR; MSTB, Serbia; MSSR, Slovakia; ARRS and MVZT, Slovenia; DST/NRF, South Africa; MICINN, Spain; SRC and Wallenberg Foundation, Sweden; SER, SNSF, and Cantons of Bern and Geneva, Switzerland; NSC, Taiwan; TAEK, Turkey; STFC, the Royal Society and Leverhulme Trust, United Kingdom; DOE and NSF, United States of America. The crucial computing support from all WLCG partners is acknowledged gratefully, in particular, from CERN and the ATLAS Tier-1 facilities at TRIUMF (Canada), NDGF (Denmark, Norway, Sweden), CC-IN2P3 (France), KIT/GridKA (Germany), INFN-CNAF (Italy), NL-T1 (Netherlands), PIC (Spain), ASGC (Taiwan), RAL (UK), and BNL (USA) and in the Tier-2 facilities worldwide.

- [1] J. J. Aubert *et al.*, *Phys. Rev. Lett.* **33**, 1404 (1974); J. E. Augustin *et al.*, *Phys. Rev. Lett.* **33**, 1406 (1974).
- [2] D. C. Hom *et al.*, *Phys. Rev. Lett.* **39**, 252 (1977).
- [3] T. Aaltonen *et al.* (CDF Collaboration), *Phys. Rev. D* **71**, 032001 (2005); V. M. Abazov *et al.* (D0 Collaboration), *Phys. Rev. Lett.* **94**, 232001 (2005); **100**, 049902(E) (2008); V. M. Abazov *et al.* (D0 Collaboration), *Phys. Rev. Lett.* **101**, 182004 (2008); T. Aaltonen *et al.* (CDF Collaboration), *Phys. Rev. Lett.* **99**, 132001 (2007); *Phys. Rev. D* **80**, 031103 (2009).
- [4] T. Aaltonen *et al.* (CDF Collaboration), *Phys. Rev. Lett.* **108**, 151802 (2012).
- [5] V. Khachatryan *et al.*, (CMS Collaboration), *Eur. Phys. J. C* **71**, 1575 (2011); V. Khachatryan *et al.*, (CMS Collaboration), *J. High Energy Phys.* **02** (2012) 011.
- [6] CMS Collaboration, *Phys. Rev. D* **83**, 112004 (2011).
- [7] ATLAS Collaboration, *Nucl. Phys.* **B850**, 387 (2011).
- [8] ATLAS Collaboration, *Phys. Lett. B* **705**, 9 (2011).
- [9] K. Aamodt *et al.* (ALICE Collaboration), *Phys. Lett. B* **704**, 442 (2011); B. Abelev *et al.* (ALICE Collaboration), *J. High Energy Phys.* **11** (2012) 065.
- [10] R. Aaij *et al.* (LHCb Collaboration), *Eur. Phys. J. C* **71**, 1645 (2011).
- [11] R. Aaij *et al.* (LHCb Collaboration), *Eur. Phys. J. C* **72**, 2025 (2012).
- [12] CMS Collaboration, [arXiv:1209.2922](https://arxiv.org/abs/1209.2922).
- [13] N. Brambilla *et al.*, *Eur. Phys. J. C* **71**, 1534 (2011).
- [14] J. F. Owens, E. Reya, and M. Gluck, *Phys. Rev. D* **18**, 1501 (1978); V. G. Kartvelishvili, A. K. Likhoded, and S. R. Slabospitsky, *Yad. Fiz.* **28**, 1315 (1978) [*Sov. J. Nucl. Phys.* **28**, 678 (1978)]; C. H. Chang, *Nucl. Phys.* **B172**, 425 (1980); E. L. Berger and D. L. Jones, *Phys. Rev. D* **23**, 1521 (1981); R. Baier and R. Ruckl, *Nucl. Phys.* **B201**, 1 (1982); *Z. Phys. C* **19**, 251 (1983).
- [15] P. Artoisenet, J. P. Lansberg, and F. Maltoni, *Phys. Lett. B* **653**, 60 (2007).
- [16] P. Artoisenet, J. M. Campbell, J. P. Lansberg, F. Maltoni, and F. Tramontano, *Phys. Rev. Lett.* **101**, 152001 (2008); J. P. Lansberg, *Eur. Phys. J. C* **61**, 693 (2009).
- [17] G. T. Bodwin, E. Braaten, and G. P. Lepage, *Phys. Rev. D* **51**, 1125 (1995); **55**, 5853(E) (1997); P. L. Cho and A. K. Leibovich, *Phys. Rev. D* **53**, 150 (1996); **53**, 6203 (1996); B. Gong, J. X. Wang, and H. F. Zhang, *Phys. Rev. D* **83**, 114021 (2011).
- [18] P. Hagler, R. Kirschner, A. Schafer, L. Szymanowski, and O. V. Teryaev, *Phys. Rev. Lett.* **86**, 1446 (2001); S. P. Baranov and N. P. Zotov, *JETP Lett.* **86**, 435 (2007); **88**, 711 (2008).
- [19] H. Fritzsch, *Phys. Lett.* **67B**, 217 (1977); F. Halzen, *Phys. Lett.* **69B**, 105 (1977); M. Gluck, J. F. Owens, and E. Reya, *Phys. Rev. D* **17**, 2324 (1978); V. D. Barger, W. Y. Keung, and R. J. N. Phillips, *Phys. Lett.* **91B**, 253 (1980); J. F. Amundson, O. J. P. Eboli, E. M. Gregores, and F. Halzen, *Phys. Lett. B* **372**, 127 (1996); **390**, 323 (1997).
- [20] ATLAS uses a right-handed coordinate system with its origin at the nominal interaction point (IP) in the center of the detector, and the z axis along the beam line. The x axis points from the IP to the center of the LHC ring, and the y axis points upwards. Cylindrical coordinates (r, ϕ) are used in the transverse plane, ϕ being the azimuthal angle around the beam line. Observables labeled transverse are projected into the x - y plane. The pseudorapidity is defined in terms of the polar angle as $\eta = -\ln \tan(\theta/2)$. Rapidity is defined as $y = \frac{1}{2} \ln \frac{E+p_z}{E-p_z}$ where E is the energy and p_z is the momentum parallel to the beam axis.
- [21] N. Brambilla *et al.* (Quarkonium Working Group Collaboration) [arXiv:hep-ph/0412158](https://arxiv.org/abs/hep-ph/0412158) (and references therein).
- [22] ATLAS Collaboration, *JINST* **3**, S08003 (2008).
- [23] ATLAS Collaboration, *Eur. Phys. J. C* **72**, 1849 (2012).
- [24] P. Faccioli, C. Lourenco, J. Seixas, and H. K. Wohri, *Eur. Phys. J. C* **69**, 657 (2010).
- [25] S. Palestini, *Phys. Rev. D* **83**, 031503 (2011).
- [26] hepdata repository for results in this paper: <http://hepdata.cedar.ac.uk/view/red6042>.
- [27] These corrections introduce a negligible anticorrelation between the measured values of ϵ_{ROI} and those of c_a and $c_{\Delta R}$.
- [28] K. Nakamura *et al.* (PDG Collaboration), *J. Phys. G* **37**, 075021 (2010).
- [29] ATLAS Collaboration, *Eur. Phys. J. C* **71**, 1630 (2011); ATLAS Collaboration, Report No. ATLAS-CONF-2011-116 (2011).
- [30] J. M. Campbell, F. Maltoni, and F. Tramontano, *Phys. Rev. Lett.* **98**, 252002 (2007).
- [31] A. D. Frawley, T. Ullrich, and R. Vogt, *Phys. Rep.* **462**, 125 (2008).
- [32] M. Cacciari, P. Nason, and R. Vogt, *Phys. Rev. Lett.* **95**, 122001 (2005).
- [33] T. Aaltonen *et al.* (CDF Collaboration), *Phys. Rev. Lett.* **84**, 2094 (2000); R. Aaij (LHCb Collaboration), *J. High Energy Phys.* **11** (2012) 031.
- [34] ATLAS Collaboration, *Phys. Rev. Lett.* **108**, 152001 (2012).

G. Aad,⁴⁸ T. Abajyan,²¹ B. Abbott,¹¹¹ J. Abdallah,¹² S. Abdel Khalek,¹¹⁵ A. A. Abdelalim,⁴⁹ O. Abidinov,¹¹ R. Aben,¹⁰⁵ B. Abi,¹¹² M. Abolins,⁸⁸ O. S. AbouZeid,¹⁵⁸ H. Abramowicz,¹⁵³ H. Abreu,¹³⁶ B. S. Acharya,^{164a,164b,b} L. Adamczyk,³⁸ D. L. Adams,²⁵ T. N. Addy,⁵⁶ J. Adelman,¹⁷⁶ S. Adomeit,⁹⁸ P. Adragna,⁷⁵ T. Adye,¹²⁹ S. Aefsky,²³ J. A. Aguilar-Saavedra,^{124b,c} M. Agustoni,¹⁷ M. Aharrouche,⁸¹ S. P. Ahlen,²² F. Ahles,⁴⁸ A. Ahmad,¹⁴⁸ M. Ahsan,⁴¹ G. Aielli,^{133a,133b} T. P. A. Åkesson,⁷⁹ G. Akimoto,¹⁵⁵ A. V. Akimov,⁹⁴ M. S. Alam,² M. A. Alam,⁷⁶ J. Albert,¹⁶⁹ S. Albrand,⁵⁵ M. Aleksa,³⁰ I. N. Aleksandrov,⁶⁴ F. Alessandria,^{89a} C. Alexa,^{26a} G. Alexander,¹⁵³ G. Alexandre,⁴⁹ T. Alexopoulos,¹⁰ M. Alhroob,^{164a,164c} M. Aliev,¹⁶ G. Alimonti,^{89a} J. Alison,¹²⁰ B. M. M. Allbrooke,¹⁸ P. P. Allport,⁷³ S. E. Allwood-Spiers,⁵³ J. Almond,⁸² A. Aloisio,^{102a,102b} R. Alon,¹⁷² A. Alonso,⁷⁹ F. Alonso,⁷⁰ A. Altheimer,³⁵ B. Alvarez Gonzalez,⁸⁸ M. G. Alviggi,^{102a,102b} K. Amako,⁶⁵ C. Amelung,²³ V. V. Ammosov,^{128,a}

- S. P. Amor Dos Santos,^{124a} A. Amorim,^{124a,d} N. Amram,¹⁵³ C. Anastopoulos,³⁰ L. S. Ancu,¹⁷ N. Andari,¹¹⁵
 T. Andeen,³⁵ C. F. Anders,^{58b} G. Anders,^{58a} K. J. Anderson,³¹ A. Andreazza,^{89a,89b} V. Andrei,^{58a} M-L. Andrieux,⁹⁵
 X. S. Anduaga,⁷⁰ S. Angelidakis,⁹ P. Anger,⁴⁴ A. Angerami,³⁵ F. Anghinolfi,³⁰ A. Anisenkov,¹⁰⁷ N. Anjos,^{124a}
 A. Annovi,⁴⁷ A. Antonaki,⁹ M. Antonelli,⁴⁷ A. Antonov,⁹⁶ J. Antos,^{144b} F. Anulli,^{132a} M. Aoki,¹⁰¹ S. Aoun,⁸³
 L. Aperio Bella,⁵ R. Apolle,^{118,e} G. Arabidze,⁸⁸ I. Aracena,¹⁴³ Y. Arai,⁶⁵ A. T. H. Arce,⁴⁵ S. Arfaoui,¹⁴⁸ J-F. Arguin,⁹³
 S. Argyropoulos,⁴² E. Arik,^{19a,a} M. Arik,^{19a} A. J. Armbruster,⁸⁷ O. Arnaez,⁸¹ V. Arnal,⁸⁰ A. Artamonov,⁹⁵
 G. Artoni,^{132a,132b} D. Arutinov,²¹ S. Asai,¹⁵⁵ S. Ask,²⁸ B. Åsman,^{146a,146b} L. Asquith,⁶ K. Assamagan,^{25,f}
 A. Astbury,¹⁶⁹ M. Atkinson,¹⁶⁵ B. Aubert,⁵ E. Auge,¹¹⁵ K. Augsten,¹²⁷ M. Aurousseau,^{145a} G. Avolio,³⁰ D. Axen,¹⁶⁸
 G. Azuelos,^{93,g} Y. Azuma,¹⁵⁵ M. A. Baak,³⁰ G. Baccaglioni,^{89a} C. Bacci,^{134a,134b} A. M. Bach,¹⁵ H. Bachacou,¹³⁶
 K. Bachas,³⁰ M. Backes,⁴⁹ M. Backhaus,²¹ J. Backus Mayes,¹⁴³ E. Badescu,^{26a} P. Bagnaia,^{132a,132b} S. Bahinipati,³
 Y. Bai,^{33a} D. C. Bailey,¹⁵⁸ T. Bain,¹⁵⁸ J. T. Baines,¹²⁹ O. K. Baker,¹⁷⁶ M. D. Baker,²⁵ S. Baker,⁷⁷ P. Balek,¹²⁶
 E. Banas,³⁹ P. Banerjee,⁹³ Sw. Banerjee,¹⁷³ D. Banfi,³⁰ A. Bangert,¹⁵⁰ V. Bansal,¹⁶⁹ H. S. Bansil,¹⁸ L. Barak,¹⁷²
 S. P. Baranov,⁹⁴ A. Barbaro Galtieri,¹⁵ T. Barber,⁴⁸ E. L. Barberio,⁸⁶ D. Barberis,^{50a,50b} M. Barbero,²¹ D. Y. Bardin,⁶⁴
 T. Barillari,⁹⁹ M. Barisonzi,¹⁷⁵ T. Barklow,¹⁴³ N. Barlow,²⁸ B. M. Barnett,¹²⁹ R. M. Barnett,¹⁵ A. Baroncelli,^{134a}
 G. Barone,⁴⁹ A. J. Barr,¹¹⁸ F. Barreiro,⁸⁰ J. Barreiro Guimarães da Costa,⁵⁷ R. Bartoldus,¹⁴³ A. E. Barton,⁷¹
 V. Bartsch,¹⁴⁹ A. Basye,¹⁶⁵ R. L. Bates,⁵³ L. Batkova,^{144a} J. R. Batley,²⁸ A. Battaglia,¹⁷ M. Battistin,³⁰ F. Bauer,¹³⁶
 H. S. Bawa,^{143,h} S. Beale,⁹⁸ T. Beau,⁷⁸ P. H. Beauchemin,¹⁶¹ R. Beccherle,^{50a} P. Bechtle,²¹ H. P. Beck,¹⁷
 K. Becker,¹⁷⁵ S. Becker,⁹⁸ M. Beckingham,¹³⁸ K. H. Becks,¹⁷⁵ A. J. Beddall,^{19c} A. Beddall,^{19c} S. Bedikian,¹⁷⁶
 V. A. Bednyakov,⁶⁴ C. P. Bee,⁸³ L. J. Beemster,¹⁰⁵ M. Begel,²⁵ S. Behar Harpaz,¹⁵² P. K. Behera,⁶² M. Beimforde,⁹⁹
 C. Belanger-Champagne,⁸⁵ P. J. Bell,⁴⁹ W. H. Bell,⁴⁹ G. Bella,¹⁵³ L. Bellagamba,^{20a} M. Bellomo,³⁰ A. Belloni,⁵⁷
 O. Beloborodova,^{107,i} K. Belotskiy,⁹⁶ O. Beltramello,³⁰ O. Benary,¹⁵³ D. Bencheekroun,^{135a} K. Bendtz,^{146a,146b}
 N. Benekos,¹⁶⁵ Y. Benhammou,¹⁵³ E. Benhar Noccioli,⁴⁹ J. A. Benitez Garcia,^{159b} D. P. Benjamin,⁴⁵ M. Benoit,¹¹⁵
 J. R. Bensinger,²³ K. Benslama,¹³⁰ S. Bentvelsen,¹⁰⁵ D. Berge,³⁰ E. Bergeaas Kuutmann,⁴² N. Berger,⁵
 F. Berghaus,¹⁶⁹ E. Berglund,¹⁰⁵ J. Beringer,¹⁵ P. Bernat,⁷⁷ R. Bernhard,⁴⁸ C. Bernius,²⁵ T. Berry,⁷⁶ C. Bertella,⁸³
 A. Bertin,^{20a,20b} F. Bertolucci,^{122a,122b} M. I. Besana,^{89a,89b} G. J. Besjes,¹⁰⁴ N. Besson,¹³⁶ S. Bethke,⁹⁹ W. Bhimji,⁴⁶
 R. M. Bianchi,³⁰ L. Bianchini,²³ M. Bianco,^{72a,72b} O. Biebel,⁹⁸ S. P. Bieniek,⁷⁷ K. Bierwagen,⁵⁴ J. Biesiada,¹⁵
 M. Biglietti,^{134a} H. Bilokon,⁴⁷ M. Bindi,^{20a,20b} S. Binet,¹¹⁵ A. Bingul,^{19c} C. Bini,^{132a,132b} C. Biscarat,¹⁷⁸ B. Bittner,⁹⁹
 C. W. Black,¹⁵⁰ K. M. Black,²² R. E. Blair,⁶ J.-B. Blanchard,¹³⁶ G. Blanchot,³⁰ T. Blazek,^{144a} I. Bloch,⁴² C. Blocker,²³
 J. Blocki,³⁹ A. Blondel,⁴⁹ W. Blum,⁸¹ U. Blumenschein,⁵⁴ G. J. Bobbink,¹⁰⁵ V. S. Bobrovnikov,¹⁰⁷ S. S. Bocchetta,⁷⁹
 A. Bocci,⁴⁵ C. R. Boddy,¹¹⁸ M. Boehler,⁴⁸ J. Boek,¹⁷⁵ T. T. Boek,¹⁷⁵ N. Boelaert,³⁶ J. A. Bogaerts,³⁰
 A. Bogdanchikov,¹⁰⁷ A. Bogouch,^{90,a} C. Bohm,^{146a} J. Bohm,¹²⁵ V. Boisvert,⁷⁶ T. Bold,³⁸ V. Boldea,^{26a}
 N. M. Bolnet,¹³⁶ M. Bomben,⁷⁸ M. Bona,⁷⁵ M. Boonekamp,¹³⁶ S. Bordini,⁷⁸ C. Borer,¹⁷ A. Borisov,¹²⁸
 G. Borissov,⁷¹ I. Borjanovic,^{13a} M. Borri,⁸² S. Borroni,⁸⁷ J. Bortfeldt,⁹⁸ V. Bortolotto,^{134a,134b} K. Bos,¹⁰⁵
 D. Boscherini,^{20a} M. Bosman,¹² H. Boterenbrood,¹⁰⁵ J. Bouchami,⁹³ J. Boudreau,¹²³ E. V. Bouhova-Thacker,⁷¹
 D. Boumediene,³⁴ C. Bourdarios,¹¹⁵ N. Bousson,⁸³ A. Boveia,³¹ J. Boyd,³⁰ I. R. Boyko,⁶⁴ I. Bozovic-Jelisavcic,^{13b}
 J. Bracinik,¹⁸ P. Branchini,^{134a} A. Brandt,⁸ G. Brandt,¹¹⁸ O. Brandt,⁵⁴ U. Bratzler,¹⁵⁶ B. Brau,⁸⁴ J. E. Brau,¹¹⁴
 H. M. Braun,^{175,a} S. F. Brazzale,^{164a,164c} B. Breliev,¹⁵⁸ J. Bremer,³⁰ K. Brendlinger,¹²⁰ R. Brenner,¹⁶⁶ S. Bressler,¹⁷²
 D. Britton,⁵³ F. M. Brochu,²⁸ I. Brock,²¹ R. Brock,⁸⁸ F. Broggi,^{89a} C. Bromberg,⁸⁸ J. Bronner,⁹⁹ G. Brooijmans,³⁵
 T. Brooks,⁷⁶ W. K. Brooks,^{32b} G. Brown,⁸² P. A. Bruckman de Renstrom,³⁹ D. Bruncko,^{144b} R. Bruneliere,⁴⁸
 S. Brunet,⁶⁰ A. Bruni,^{20a} G. Bruni,^{20a} M. Bruschi,^{20a} L. Bryngemark,⁷⁹ T. Buanes,¹⁴ Q. Buat,⁵⁵ F. Bucci,⁴⁹
 J. Buchanan,¹¹⁸ P. Buchholz,¹⁴¹ R. M. Buckingham,¹¹⁸ A. G. Buckley,⁴⁶ S. I. Buda,^{26a} I. A. Budagov,⁶⁴ B. Budick,¹⁰⁸
 V. Büscher,⁸¹ L. Bugge,¹¹⁷ O. Bulekov,⁹⁶ A. C. Bundock,⁷³ M. Bunse,⁴³ T. Buran,¹¹⁷ H. Burckhart,³⁰ S. Burdin,⁷³
 T. Burgess,¹⁴ S. Burke,¹²⁹ E. Busato,³⁴ P. Bussey,⁵³ C. P. Buszello,¹⁶⁶ B. Butler,¹⁴³ J. M. Butler,²² C. M. Buttar,⁵³
 J. M. Butterworth,⁷⁷ W. Buttinger,²⁸ M. Byszewski,³⁰ S. Cabrera Urbán,¹⁶⁷ D. Caforio,^{20a,20b} O. Cakir,^{4a}
 P. Calafiura,¹⁵ G. Calderini,⁷⁸ P. Calfayan,⁹⁸ R. Calkins,¹⁰⁶ L. P. Caloba,^{24a} R. Caloi,^{132a,132b} D. Calvet,³⁴ S. Calvet,³⁴
 R. Camacho Toro,³⁴ P. Camarri,^{133a,133b} D. Cameron,¹¹⁷ L. M. Caminada,¹⁵ R. Caminal Armadans,¹² S. Campana,³⁰
 M. Campanelli,⁷⁷ V. Canale,^{102a,102b} F. Canelli,³¹ A. Canepa,^{159a} J. Cantero,⁸⁰ R. Cantrill,⁷⁶ L. Capasso,^{102a,102b}
 M. D. M. Capeans Garrido,³⁰ I. Caprini,^{26a} M. Caprini,^{26a} D. Capriotti,⁹⁹ M. Capua,^{37a,37b} R. Caputo,⁸¹
 R. Cardarelli,^{133a} T. Carli,³⁰ G. Carlino,^{102a} L. Carminati,^{89a,89b} B. Caron,⁸⁵ S. Caron,¹⁰⁴ E. Carquin,^{32b}
 G. D. Carrillo-Montoya,^{145b} A. A. Carter,⁷⁵ J. R. Carter,²⁸ J. Carvalho,^{124a,j} D. Casadei,¹⁰⁸ M. P. Casado,¹²
 M. Cascella,^{122a,122b} C. Caso,^{50a,50b,a} A. M. Castaneda Hernandez,^{173,k} E. Castaneda-Miranda,¹⁷³

- V. Castillo Gimenez,¹⁶⁷ N. F. Castro,^{124a} G. Cataldi,^{72a} P. Catastini,⁵⁷ A. Catinaccio,³⁰ J. R. Catmore,³⁰ A. Cattai,³⁰ G. Cattani,^{133a,133b} S. Caughron,⁸⁸ V. Cavaliere,¹⁶⁵ P. Cavalleri,⁷⁸ D. Cavalli,^{89a} M. Cavalli-Sforza,¹² V. Cavasinni,^{122a,122b} F. Ceradini,^{134a,134b} A. S. Cerqueira,^{24b} A. Cerri,¹⁵ L. Cerrito,⁷⁵ F. Cerutti,¹⁵ S. A. Cetin,^{19b} A. Chafaq,^{135a} D. Chakraborty,¹⁰⁶ I. Chalupkova,¹²⁶ K. Chan,³ P. Chang,¹⁶⁵ B. Chapleau,⁸⁵ J. D. Chapman,²⁸ J. W. Chapman,⁸⁷ D. G. Charlton,¹⁸ V. Chavda,⁸² C. A. Chavez Barajas,³⁰ S. Cheatham,⁸⁵ S. Chekanov,⁶ S. V. Chekulaev,^{159a} G. A. Chelkov,⁶⁴ M. A. Chelstowska,¹⁰⁴ C. Chen,⁶³ H. Chen,²⁵ S. Chen,^{33c} X. Chen,¹⁷³ Y. Chen,³⁵ Y. Cheng,³¹ A. Cheplakov,⁶⁴ R. Cherkaoui El Moursli,^{135e} V. Chernyatin,²⁵ E. Cheu,⁷ S. L. Cheung,¹⁵⁸ L. Chevalier,¹³⁶ G. Chiefari,^{102a,102b} L. Chikovani,^{51a,} J. T. Childers,³⁰ A. Chilingarov,⁷¹ G. Chiodini,^{72a} A. S. Chisholm,¹⁸ R. T. Chislett,⁷⁷ A. Chitan,^{26a} M. V. Chizhov,⁶⁴ G. Choudalakis,³¹ S. Chouridou,¹³⁷ I. A. Christidi,⁷⁷ A. Christov,⁴⁸ D. Chromek-Burckhart,³⁰ M. L. Chu,¹⁵¹ J. Chudoba,¹²⁵ G. Ciapetti,^{132a,132b} A. K. Ciftci,^{4a} R. Ciftci,^{4a} D. Cinca,³⁴ V. Cindro,⁷⁴ A. Ciochio,¹⁵ M. Cirilli,⁸⁷ P. Cirkovic,^{13b} Z. H. Citron,¹⁷² M. Citterio,^{89a} M. Ciubancan,^{26a} A. Clark,⁴⁹ P. J. Clark,⁴⁶ R. N. Clarke,¹⁵ W. Cleland,¹²³ J. C. Clemens,⁸³ B. Clement,⁵⁵ C. Clement,^{146a,146b} Y. Coadou,⁸³ M. Cobal,^{164a,164c} A. Coccaro,¹³⁸ J. Cochran,⁶³ L. Coffey,²³ J. G. Cogan,¹⁴³ J. Coggeshall,¹⁶⁵ J. Colas,⁵ S. Cole,¹⁰⁶ A. P. Colijn,¹⁰⁵ N. J. Collins,¹⁸ C. Collins-Tooth,⁵³ J. Collot,⁵⁵ T. Colombo,^{119a,119b} G. Colon,⁸⁴ G. Compostella,⁹⁹ P. Conde Muiño,^{124a} E. Coniavitis,¹⁶⁶ M. C. Conidi,¹² S. M. Consonni,^{89a,89b} V. Consorti,⁴⁸ S. Constantinescu,^{26a} C. Conta,^{119a,119b} G. Conti,⁵⁷ F. Conventi,^{102a,1} M. Cooke,¹⁵ B. D. Cooper,⁷⁷ A. M. Cooper-Sarkar,¹¹⁸ K. Copic,¹⁵ T. Cornelissen,¹⁷⁵ M. Corradi,^{20a} F. Corriveau,^{85,m} A. Cortes-Gonzalez,¹⁶⁵ G. Cortiana,⁹⁹ G. Costa,^{89a} M. J. Costa,¹⁶⁷ D. Costanzo,¹³⁹ D. Côté,³⁰ L. Courneyea,¹⁶⁹ G. Cowan,⁷⁶ B. E. Cox,⁸² K. Cranmer,¹⁰⁸ F. Crescioli,⁷⁸ M. Cristinziani,²¹ G. Crosetti,^{37a,37b} S. Crépe-Renaudin,⁵⁵ C.-M. Cuciuc,^{26a} C. Cuenca Almenar,¹⁷⁶ T. Cuhadar Donszelmann,¹³⁹ J. Cummings,¹⁷⁶ M. Curatolo,⁴⁷ C. J. Curtis,¹⁸ C. Cuthbert,¹⁵⁰ P. Cwetanski,⁶⁰ H. Czirr,¹⁴¹ P. Czodrowski,⁴⁴ Z. Czyczula,¹⁷⁶ S. D'Auria,⁵³ M. D'Onofrio,⁷³ A. D'Orazio,^{132a,132b} M. J. Da Cunha Sargedas De Sousa,^{124a} C. Da Via,⁸² W. Dabrowski,³⁸ A. Dafinca,¹¹⁸ T. Dai,⁸⁷ F. Dallaire,⁹³ C. Dallapiccola,⁸⁴ M. Dam,³⁶ M. Dameri,^{50a,50b} D. S. Damiani,¹³⁷ H. O. Danielsson,³⁰ V. Dao,⁴⁹ G. Darbo,^{50a} G. L. Darlea,^{26b} J. A. Dassoulas,⁴² W. Davey,²¹ T. Davidek,¹²⁶ N. Davidson,⁸⁶ R. Davidson,⁷¹ E. Davies,^{118,e} M. Davies,⁹³ O. Davignon,⁷⁸ A. R. Davison,⁷⁷ Y. Davygora,^{58a} E. Dawe,¹⁴² I. Dawson,¹³⁹ R. K. Daya-Ishmukhametova,²³ K. De,⁸ R. de Asmundis,^{102a} S. De Castro,^{20a,20b} S. De Cecco,⁷⁸ J. de Graat,⁹⁸ N. De Groot,¹⁰⁴ P. de Jong,¹⁰⁵ C. De La Taille,¹¹⁵ H. De la Torre,⁸⁰ F. De Lorenzi,⁶³ L. de Mora,⁷¹ L. De Noij,¹⁰⁵ D. De Pedis,^{132a} A. De Salvo,^{132a} U. De Sanctis,^{164a,164c} A. De Santo,¹⁴⁹ J. B. De Vivie De Regie,¹¹⁵ G. De Zorzi,^{132a,132b} W. J. Dearnaley,⁷¹ R. Debbe,²⁵ C. Debenedetti,⁴⁶ B. Dechenaux,⁵⁵ D. V. Dedovich,⁶⁴ J. Degenhardt,¹²⁰ J. Del Peso,⁸⁰ T. Del Prete,^{122a,122b} T. Delemontex,⁵⁵ M. Deliyergiyev,⁷⁴ A. Dell'Acqua,³⁰ L. Dell'Asta,²² M. Della Pietra,^{102a,1} D. della Volpe,^{102a,102b} M. Delmastro,⁵ P. A. Delsart,⁵⁵ C. Deluca,¹⁰⁵ S. Demers,¹⁷⁶ M. Demichev,⁶⁴ B. Demirköz,^{12,n} S. P. Denisov,¹²⁸ D. Derendarz,³⁹ J. E. Derkaoui,^{135d} F. Derue,⁷⁸ P. Dervan,⁷³ K. Desch,²¹ E. Devetak,¹⁴⁸ P. O. Deviveiros,¹⁰⁵ A. Dewhurst,¹²⁹ B. DeWilde,¹⁴⁸ S. Dhaliwal,¹⁵⁸ R. Dhullipudi,^{25,o} A. Di Ciaccio,^{133a,133b} L. Di Ciaccio,⁵ C. Di Donato,^{102a,102b} A. Di Girolamo,³⁰ B. Di Girolamo,³⁰ S. Di Luise,^{134a,134b} A. Di Mattia,¹⁵² B. Di Micco,³⁰ R. Di Nardo,⁴⁷ A. Di Simone,^{133a,133b} R. Di Sipio,^{20a,20b} M. A. Diaz,^{32a} E. B. Diehl,⁸⁷ J. Dietrich,⁴² T. A. Dietzsch,^{58a} S. Diglio,⁸⁶ K. Dindar Yagci,⁴⁰ J. Dingfelder,²¹ F. Dinut,^{26a} C. Dionisi,^{132a,132b} P. Dita,^{26a} S. Dita,^{26a} F. Dittus,³⁰ F. Djama,⁸³ T. Djobava,^{51b} M. A. B. do Vale,^{24c} A. Do Valle Wemans,^{124a,p} T. K. O. Doan,⁵ M. Dobbs,⁸⁵ D. Dobos,³⁰ E. Dobson,^{30,q} J. Dodd,³⁵ C. Doglioni,⁴⁹ T. Doherty,⁵³ Y. Doi,^{65,a} J. Dolejsi,¹²⁶ Z. Dolezal,¹²⁶ B. A. Dolgoshein,^{96,a} T. Dohmae,¹⁵⁵ M. Donadelli,^{24d} J. Donini,³⁴ J. Dopke,³⁰ A. Doria,^{102a} A. Dos Anjos,¹⁷³ A. Dotti,^{122a,122b} M. T. Dova,⁷⁰ A. D. Doxiadis,¹⁰⁵ A. T. Doyle,⁵³ N. Dressnandt,¹²⁰ M. Dris,¹⁰ J. Dubbert,⁹⁹ S. Dube,¹⁵ E. Duchovni,¹⁷² G. Duckeck,⁹⁸ D. Duda,¹⁷⁵ A. Dudarev,³⁰ F. Dudziak,⁶³ M. Dührssen,³⁰ I. P. Duerdoth,⁸² L. Duflot,¹¹⁵ M.-A. Dufour,⁸⁵ L. Duguid,⁷⁶ M. Dunford,^{58a} H. Duran Yildiz,^{4a} R. Duxfield,¹³⁹ M. Dwuznik,³⁸ M. Düren,⁵² W. L. Ebenstein,⁴⁵ J. Ebke,⁹⁸ S. Eckweiler,⁸¹ K. Edmonds,⁸¹ W. Edson,² C. A. Edwards,⁷⁶ N. C. Edwards,⁵³ W. Ehrenfeld,⁴² T. Eifert,¹⁴³ G. Eigen,¹⁴ K. Einsweiler,¹⁵ E. Eisenhandler,⁷⁵ T. Ekelof,¹⁶⁶ M. El Kacimi,^{135c} M. Ellert,¹⁶⁶ S. Elles,⁵ F. Ellinghaus,⁸¹ K. Ellis,⁷⁵ N. Ellis,³⁰ J. Elmsheuser,⁹⁸ M. Elsing,³⁰ D. Emelianov,¹²⁹ R. Engelmann,¹⁴⁸ A. Engl,⁹⁸ B. Epp,⁶¹ J. Erdmann,¹⁷⁶ A. Ereditato,¹⁷ D. Eriksson,^{146a} J. Ernst,² M. Ernst,²⁵ J. Ernwein,¹³⁶ D. Errede,¹⁶⁵ S. Errede,¹⁶⁵ E. Ertel,⁸¹ M. Escalier,¹¹⁵ H. Esch,⁴³ C. Escobar,¹²³ X. Espinal Curull,¹² B. Esposito,⁴⁷ F. Etienne,⁸³ A. I. Etievre,¹³⁶ E. Etzion,¹⁵³ D. Evangelakou,⁵⁴ H. Evans,⁶⁰ L. Fabbri,^{20a,20b} C. Fabre,³⁰ R. M. Fakhruddinov,¹²⁸ S. Falciano,^{132a} Y. Fang,^{33a} M. Fanti,^{89a,89b} A. Farbin,⁸ A. Farilla,^{134a} J. Farley,¹⁴⁸ T. Farooque,¹⁵⁸ S. Farrell,¹⁶³ S. M. Farrington,¹⁷⁰ P. Farthouat,³⁰ F. Fassi,¹⁶⁷ P. Fassnacht,³⁰ D. Fassouliotis,⁹ B. Fathollahzadeh,¹⁵⁸

- A. Favareto,^{89a,89b} L. Fayard,¹¹⁵ S. Fazio,^{37a,37b} P. Federic,^{144a} O. L. Fedin,¹²¹ W. Fedorko,⁸⁸ M. Fehling-Kaschek,⁴⁸ L. Feligioni,⁸³ C. Feng,^{33d} E. J. Feng,⁶ A. B. Fenyuk,¹²⁸ J. Ferencei,^{144b} W. Fernando,⁶ S. Ferrag,⁵³ J. Ferrando,⁵³ V. Ferrara,⁴² A. Ferrari,¹⁶⁶ P. Ferrari,¹⁰⁵ R. Ferrari,^{119a} D. E. Ferreira de Lima,⁵³ A. Ferrer,¹⁶⁷ D. Ferrere,⁴⁹ C. Ferretti,⁸⁷ A. Ferretto Parodi,^{50a,50b} M. Fiascaris,³¹ F. Fiedler,⁸¹ A. Filipčič,⁷⁴ F. Filthaut,¹⁰⁴ M. Fincke-Keeler,¹⁶⁹ M. C. N. Fiolhais,^{124a,j} L. Fiorini,¹⁶⁷ A. Firan,⁴⁰ G. Fischer,⁴² M. J. Fisher,¹⁰⁹ M. Flechl,⁴⁸ I. Fleck,¹⁴¹ J. Fleckner,⁸¹ P. Fleischmann,¹⁷⁴ S. Fleischmann,¹⁷⁵ T. Flick,¹⁷⁵ A. Floderus,⁷⁹ L. R. Flores Castillo,¹⁷³ A. C. Florez Bustos,^{159b} M. J. Flowerdew,⁹⁹ T. Fonseca Martin,¹⁷ A. Formica,¹³⁶ A. Forti,⁸² D. Fortin,^{159a} D. Fournier,¹¹⁵ A. J. Fowler,⁴⁵ H. Fox,⁷¹ P. Francavilla,¹² M. Franchini,^{20a,20b} S. Franchino,^{119a,119b} D. Francis,³⁰ T. Frank,¹⁷² M. Franklin,⁵⁷ S. Franz,³⁰ M. Fraternali,^{119a,119b} S. Fratina,¹²⁰ S. T. French,²⁸ C. Friedrich,⁴² F. Friedrich,⁴⁴ D. Froidevaux,³⁰ J. A. Frost,²⁸ C. Fukunaga,¹⁵⁶ E. Fullana Torregrosa,¹²⁶ B. G. Fulsom,¹⁴³ J. Fuster,¹⁶⁷ C. Gabaldon,³⁰ O. Gabizon,¹⁷² T. Gadfort,²⁵ S. Gadomski,⁴⁹ G. Gagliardi,^{50a,50b} P. Gagnon,⁶⁰ C. Galea,⁹⁸ B. Galhardo,^{124a} E. J. Gallas,¹¹⁸ V. Gallo,¹⁷ B. J. Gallop,¹²⁹ P. Gallus,¹²⁵ K. K. Gan,¹⁰⁹ Y. S. Gao,^{143,h} A. Gaponenko,¹⁵ F. Garbersen,¹⁷⁶ M. Garcia-Sciveres,¹⁵ C. García,¹⁶⁷ J. E. García Navarro,¹⁶⁷ R. W. Gardner,³¹ N. Garelli,³⁰ H. Garitaonandia,¹⁰⁵ V. Garonne,³⁰ C. Gatti,⁴⁷ G. Gaudio,^{119a} B. Gaur,¹⁴¹ L. Gauthier,¹³⁶ P. Gauzzi,^{132a,132b} I. L. Gavrilenko,⁹⁴ C. Gay,¹⁶⁸ G. Gaycken,²¹ E. N. Gazis,¹⁰ P. Ge,^{33d} Z. Gecse,¹⁶⁸ C. N. P. Gee,¹²⁹ D. A. A. Geerts,¹⁰⁵ Ch. Geich-Gimbel,²¹ K. Gellerstedt,^{146a,146b} C. Gemme,^{50a} A. Gemmell,⁵³ M. H. Genest,⁵⁵ S. Gentile,^{132a,132b} M. George,⁵⁴ S. George,⁷⁶ D. Gerbaudo,¹² P. Gerlach,¹⁷⁵ A. Gershon,¹⁵³ C. Geweniger,^{58a} H. Ghazlane,^{135b} N. Ghodbane,³⁴ B. Giacobbe,^{20a} S. Giagu,^{132a,132b} V. Giangiobbe,¹² F. Gianotti,³⁰ B. Gibbard,²⁵ A. Gibson,¹⁵⁸ S. M. Gibson,³⁰ M. Gilchriese,¹⁵ D. Gillberg,²⁹ A. R. Gillman,¹²⁹ D. M. Gingrich,^{3,g} J. Ginzburg,¹⁵³ N. Giokaris,⁹ M. P. Giordani,^{164c} R. Giordano,^{102a,102b} F. M. Giorgi,¹⁶ P. Giovannini,⁹⁹ P. F. Giraud,¹³⁶ D. Giugni,^{89a} M. Giunta,⁹³ B. K. Gjelsten,¹¹⁷ L. K. Gladilin,⁹⁷ C. Glasman,⁸⁰ J. Glatzer,²¹ A. Glazov,⁴² K. W. Glitza,¹⁷⁵ G. L. Glonti,⁶⁴ J. R. Goddard,⁷⁵ J. Godfrey,¹⁴² J. Godlewski,³⁰ M. Goebel,⁴² T. Göpfert,⁴⁴ C. Goeringer,⁸¹ C. Gössling,⁴³ S. Goldfarb,⁸⁷ T. Golling,¹⁷⁶ D. Golubkov,¹²⁸ A. Gomes,^{124a,d} L. S. Gomez Fajardo,⁴² R. Gonçalves,⁷⁶ J. Goncalves Pinto Firmino Da Costa,⁴² L. Gonella,²¹ S. González de la Hoz,¹⁶⁷ G. Gonzalez Parra,¹² M. L. Gonzalez Silva,²⁷ S. Gonzalez-Sevilla,⁴⁹ J. J. Goodson,¹⁴⁸ L. Goossens,³⁰ P. A. Gorbounov,⁹⁵ H. A. Gordon,²⁵ I. Gorelov,¹⁰³ G. Gorfine,¹⁷⁵ B. Gorini,³⁰ E. Gorini,^{72a,72b} A. Gorišek,⁷⁴ E. Gornicki,³⁹ A. T. Goshaw,⁶ M. Gosselink,¹⁰⁵ M. I. Gostkin,⁶⁴ I. Gough Eschrich,¹⁶³ M. Goughri,^{135a} D. Goujdami,^{135c} M. P. Goulette,⁴⁹ A. G. Goussiou,¹³⁸ C. Goy,⁵ S. Gozpinar,²³ I. Grabowska-Bold,³⁸ P. Grafström,^{20a,20b} K.-J. Grahm,⁴² E. Gramstad,¹¹⁷ F. Grancagnolo,^{72a} S. Grancagnolo,¹⁶ V. Grassi,¹⁴⁸ V. Gratchev,¹²¹ N. Grau,³⁵ H. M. Gray,³⁰ J. A. Gray,¹⁴⁸ E. Graziani,^{134a} O. G. Grebenyuk,¹²¹ T. Greenshaw,⁷³ Z. D. Greenwood,^{25,o} K. Gregersen,³⁶ I. M. Gregor,⁴² P. Grenier,¹⁴³ J. Griffiths,⁸ N. Grigalashvili,⁶⁴ A. A. Grillo,¹³⁷ S. Grinstein,¹² Ph. Gris,³⁴ Y. V. Grishkevich,⁹⁷ J.-F. Grivaz,¹¹⁵ E. Gross,¹⁷² J. Grosse-Knetter,⁵⁴ J. Groth-Jensen,¹⁷² K. Grybel,¹⁴¹ D. Guest,¹⁷⁶ C. Guicheney,³⁴ E. Guido,^{50a,50b} S. Guindon,⁵⁴ U. Gul,⁵³ J. Gunther,¹²⁵ B. Guo,¹⁵⁸ J. Guo,³⁵ P. Gutierrez,¹¹¹ N. Guttman,¹⁵³ O. Gutzwiller,¹⁷³ C. Guyot,¹³⁶ C. Gwenlan,¹¹⁸ C. B. Gwilliam,⁷³ A. Haas,¹⁰⁸ S. Haas,³⁰ C. Haber,¹⁵ H. K. Hadavand,⁸ D. R. Hadley,¹⁸ P. Haefner,²¹ F. Hahn,³⁰ Z. Hajduk,³⁹ H. Hakobyan,¹⁷⁷ D. Hall,¹¹⁸ K. Hamacher,¹⁷⁵ P. Hamal,¹¹³ K. Hamano,⁸⁶ M. Hamer,⁵⁴ A. Hamilton,^{145b,r} S. Hamilton,¹⁶¹ L. Han,^{33b} K. Hanagaki,¹¹⁶ K. Hanawa,¹⁶⁰ M. Hance,¹⁵ C. Handel,⁸¹ P. Hanke,^{58a} J. R. Hansen,³⁶ J. B. Hansen,³⁶ J. D. Hansen,³⁶ P. H. Hansen,³⁶ P. Hansson,¹⁴³ K. Hara,¹⁶⁰ T. Harenberg,¹⁷⁵ S. Harkusha,⁹⁰ D. Harper,⁸⁷ R. D. Harrington,⁴⁶ O. M. Harris,¹³⁸ J. Hartert,⁴⁸ F. Hartjes,¹⁰⁵ T. Haruyama,⁶⁵ A. Harvey,⁵⁶ S. Hasegawa,¹⁰¹ Y. Hasegawa,¹⁴⁰ S. Hassani,¹³⁶ S. Haug,¹⁷ M. Hauschild,³⁰ R. Hauser,⁸⁸ M. Havranek,²¹ C. M. Hawkes,¹⁸ R. J. Hawkins,³⁰ A. D. Hawkins,⁷⁹ T. Hayakawa,⁶⁶ T. Hayashi,¹⁶⁰ D. Hayden,⁷⁶ C. P. Hays,¹¹⁸ H. S. Hayward,⁷³ S. J. Haywood,¹²⁹ S. J. Head,¹⁸ V. Hedberg,⁷⁹ L. Heelan,⁸ S. Heim,¹²⁰ B. Heinemann,¹⁵ S. Heisterkamp,³⁶ L. Helary,²² C. Heller,⁹⁸ M. Heller,³⁰ S. Hellman,^{146a,146b} D. Hellmich,²¹ C. Helsens,¹² R. C. W. Henderson,⁷¹ M. Henke,^{58a} A. Henrichs,¹⁷⁶ A. M. Henriques Correia,³⁰ S. Henrot-Versille,¹¹⁵ C. Hensel,⁵⁴ C. M. Hernandez,⁸ Y. Hernández Jiménez,¹⁶⁷ R. Herrberg,¹⁶ G. Herten,⁴⁸ R. Hertenberger,⁹⁸ L. Hervas,³⁰ G. G. Hesketh,⁷⁷ N. P. Hessey,¹⁰⁵ E. Higón-Rodriguez,¹⁶⁷ J. C. Hill,²⁸ K. H. Hiller,⁴² S. Hillert,²¹ S. J. Hillier,¹⁸ I. Hinchliffe,¹⁵ E. Hines,¹²⁰ M. Hirose,¹¹⁶ F. Hirsch,⁴³ D. Hirschbuehl,¹⁷⁵ J. Hobbs,¹⁴⁸ N. Hod,¹⁵³ M. C. Hodgkinson,¹³⁹ P. Hodgson,¹³⁹ A. Hoecker,³⁰ M. R. Hoefkamp,¹⁰³ J. Hoffman,⁴⁰ D. Hoffmann,⁸³ M. Hohlfield,⁸¹ M. Holder,¹⁴¹ S. O. Holmgren,^{146a} T. Holy,¹²⁷ J. L. Holzbauer,⁸⁸ T. M. Hong,¹²⁰ L. Hooft van Huysduynen,¹⁰⁸ S. Horner,⁴⁸ J.-Y. Hostachy,⁵⁵ S. Hou,¹⁵¹ A. Hoummada,^{135a} J. Howard,¹¹⁸ J. Howarth,⁸² I. Hristova,¹⁶ J. Hrivnac,¹¹⁵ T. Hryn'ova,⁵ P. J. Hsu,⁸¹ S.-C. Hsu,¹³⁸ D. Hu,³⁵ Z. Hubacek,¹²⁷ F. Hubaut,⁸³ F. Huegging,²¹ A. Huettmann,⁴² T. B. Huffman,¹¹⁸ E. W. Hughes,³⁵ G. Hughes,⁷¹ M. Huhtinen,³⁰

- M. Hurlwitz,¹⁵ N. Huseynov,^{64,s} J. Huston,⁸⁸ J. Huth,⁵⁷ G. Iacobucci,⁴⁹ G. Iakovidis,¹⁰ M. Ibbotson,⁸² I. Ibragimov,¹⁴¹ L. Iconomidou-Fayard,¹¹⁵ J. Idarraga,¹¹⁵ P. Iengo,^{102a} O. Igonkina,¹⁰⁵ Y. Ikegami,⁶⁵ M. Ikeno,⁶⁵ D. Iliadis,¹⁵⁴ N. Ilic,¹⁵⁸ T. Ince,⁹⁹ P. Ioannou,⁹ M. Iodice,^{134a} K. Iordanidou,⁹ V. Ippolito,^{132a,132b} A. Irles Quiles,¹⁶⁷ C. Isaksson,¹⁶⁶ M. Ishino,⁶⁷ M. Ishitsuka,¹⁵⁷ R. Ishmukhametov,¹⁰⁹ C. Issever,¹¹⁸ S. Istin,^{19a} A. V. Ivashin,¹²⁸ W. Iwanski,³⁹ H. Iwasaki,⁶⁵ J. M. Izen,⁴¹ V. Izzo,^{102a} B. Jackson,¹²⁰ J. N. Jackson,⁷³ P. Jackson,¹ M. R. Jaekel,³⁰ V. Jain,² K. Jakobs,⁴⁸ S. Jakobsen,³⁶ T. Jakoubek,¹²⁵ J. Jakubek,¹²⁷ D. O. Jamin,¹⁵¹ D. K. Jana,¹¹¹ E. Jansen,⁷⁷ H. Jansen,³⁰ J. Janssen,²¹ A. Jantsch,⁹⁹ M. Janus,⁴⁸ R. C. Jared,¹⁷³ G. Jarlskog,⁷⁹ L. Jeanty,⁵⁷ I. Jen-La Plante,³¹ D. Jennens,⁸⁶ P. Jenni,³⁰ A. E. Loevschall-Jensen,³⁶ P. Jež,³⁶ S. Jézéquel,⁵ M. K. Jha,^{20a} H. Ji,¹⁷³ W. Ji,⁸¹ J. Jia,¹⁴⁸ Y. Jiang,^{33b} M. Jimenez Belenguer,⁴² S. Jin,^{33a} O. Jinnouchi,¹⁵⁷ M. D. Joergensen,³⁶ D. Joffe,⁴⁰ M. Johansen,^{146a,146b} K. E. Johansson,^{146a} P. Johansson,¹³⁹ S. Johnert,⁴² K. A. Johns,⁷ K. Jon-And,^{146a,146b} G. Jones,¹⁷⁰ R. W. L. Jones,⁷¹ T. J. Jones,⁷³ C. Joram,³⁰ P. M. Jorge,^{124a} K. D. Joshi,⁸² J. Jovicevic,¹⁴⁷ T. Jovin,^{13b} X. Ju,¹⁷³ C. A. Jung,⁴³ R. M. Jungst,³⁰ V. Juranek,¹²⁵ P. Jussel,⁶¹ A. Juste Rozas,¹² S. Kabana,¹⁷ M. Kaci,¹⁶⁷ A. Kaczmarek,³⁹ P. Kadlecik,³⁶ M. Kado,¹¹⁵ H. Kagan,¹⁰⁹ M. Kagan,⁵⁷ E. Kajomovitz,¹⁵² S. Kalinin,¹⁷⁵ L. V. Kalinovskaya,⁶⁴ S. Kama,⁴⁰ N. Kanaya,¹⁵⁵ M. Kaneda,³⁰ S. Kaneti,²⁸ T. Kanno,¹⁵⁷ V. A. Kantserov,⁹⁶ J. Kanzaki,⁶⁵ B. Kaplan,¹⁰⁸ A. Kapliy,³¹ J. Kaplon,³⁰ D. Kar,⁵³ M. Karagounis,²¹ K. Karakostas,¹⁰ M. Karnevskiy,^{58b} V. Kartvelishvili,⁷¹ A. N. Karyukhin,¹²⁸ L. Kashif,¹⁷³ G. Kasieczka,^{58b} R. D. Kass,¹⁰⁹ A. Kastanas,¹⁴ M. Kataoka,⁵ Y. Kataoka,¹⁵⁵ J. Katzy,⁴² V. Kaushik,⁷ K. Kawagoe,⁶⁹ T. Kawamoto,¹⁵⁵ G. Kawamura,⁸¹ M. S. Kayl,¹⁰⁵ S. Kazama,¹⁵⁵ V. F. Kazanin,¹⁰⁷ M. Y. Kazarinov,⁶⁴ R. Keeler,¹⁶⁹ P. T. Keener,¹²⁰ R. Kehoe,⁴⁰ M. Keil,⁵⁴ G. D. Kekelidze,⁶⁴ J. S. Keller,¹³⁸ M. Kenyon,⁵³ O. Kepka,¹²⁵ N. Kerschen,³⁰ B. P. Kerševan,⁷⁴ S. Kersten,¹⁷⁵ K. Kessoku,¹⁵⁵ J. Keung,¹⁵⁸ F. Khalil-zada,¹¹ H. Khandanyan,^{146a,146b} A. Khanov,¹¹² D. Kharchenko,⁶⁴ A. Khodinov,⁹⁶ A. Khomich,^{58a} T. J. Khoo,²⁸ G. Khorauli,²¹ A. Khoroshilov,¹⁷⁵ V. Khovanskii,⁹⁵ E. Khramov,⁶⁴ J. Khubua,^{51b} H. Kim,^{146a,146b} S. H. Kim,¹⁶⁰ N. Kimura,¹⁷¹ O. Kind,¹⁶ B. T. King,⁷³ M. King,⁶⁶ R. S. B. King,¹¹⁸ J. Kirk,¹²⁹ A. E. Kiryunin,⁹⁹ T. Kishimoto,⁶⁶ D. Kisieleska,³⁸ T. Kitamura,⁶⁶ T. Kittelmann,¹²³ K. Kiuchi,¹⁶⁰ E. Kladiva,^{144b} M. Klein,⁷³ U. Klein,⁷³ K. Kleinknecht,⁸¹ M. Klemetti,⁸⁵ A. Klier,¹⁷² P. Klimek,^{146a,146b} A. Klimontov,²⁵ R. Klingenberg,⁴³ J. A. Klinger,⁸² E. B. Klinkby,³⁶ T. Klioutchnikova,³⁰ P. F. Klok,¹⁰⁴ S. Klous,¹⁰⁵ E.-E. Kluge,^{58a} T. Kluge,⁷³ P. Kluit,¹⁰⁵ S. Kluth,⁹⁹ E. Kneringer,⁶¹ E. B. F. G. Knoops,⁸³ A. Knue,⁵⁴ B. R. Ko,⁴⁵ T. Kobayashi,¹⁵⁵ M. Kobel,⁴⁴ M. Kocian,¹⁴³ P. Kodys,¹²⁶ K. Köneke,³⁰ A. C. König,¹⁰⁴ S. Koenig,⁸¹ L. Köpke,⁸¹ F. Koetsveld,¹⁰⁴ P. Koevesarki,²¹ T. Koffas,²⁹ E. Koffeman,¹⁰⁵ L. A. Kogan,¹¹⁸ S. Kohlmann,¹⁷⁵ F. Kohn,⁵⁴ Z. Kohout,¹²⁷ T. Kohriki,⁶⁵ T. Koi,¹⁴³ G. M. Kolachev,^{107,a} H. Kolanoski,¹⁶ V. Kolesnikov,⁶⁴ I. Koletsou,^{89a} J. Koll,⁸⁸ A. A. Komar,⁹⁴ Y. Komori,¹⁵⁵ T. Kondo,⁶⁵ T. Kono,^{42,t} A. I. Kononov,⁴⁸ R. Konoplich,^{108,u} N. Konstantinidis,⁷⁷ R. Kopeliansky,¹⁵² S. Koperny,³⁸ K. Korcyl,³⁹ K. Kordas,¹⁵⁴ A. Korn,¹¹⁸ A. Korol,¹⁰⁷ I. Korolkov,¹² E. V. Korolkova,¹³⁹ V. A. Korotkov,¹²⁸ O. Kortner,⁹⁹ S. Kortner,⁹⁹ V. V. Kostyukhin,²¹ S. Kotov,⁹⁹ V. M. Kotov,⁶⁴ A. Kotwal,⁴⁵ C. Kourkoumelis,⁹ V. Kouskoura,¹⁵⁴ A. Koutsman,^{159a} R. Kowalewski,¹⁶⁹ T. Z. Kowalski,³⁸ W. Kozanecki,¹³⁶ A. S. Kozhin,¹²⁸ V. Kral,¹²⁷ V. A. Kramarenko,⁹⁷ G. Kramberger,⁷⁴ M. W. Krasny,⁷⁸ A. Krasznahorkay,¹⁰⁸ J. K. Kraus,²¹ A. Kravchenko,²⁵ S. Kreiss,¹⁰⁸ F. Krejci,¹²⁷ J. Kretzschmar,⁷³ K. Kreutzfeldt,⁵² N. Krieger,⁵⁴ P. Krieger,¹⁵⁸ K. Kroeninger,⁵⁴ H. Kroha,⁹⁹ J. Kroll,¹²⁰ J. Kroseberg,²¹ J. Krstic,^{13a} U. Kruchonak,⁶⁴ H. Krüger,²¹ T. Kruker,¹⁷ N. Krumnack,⁶³ Z. V. Krumshteyn,⁶⁴ M. K. Kruse,⁴⁵ T. Kubota,⁸⁶ S. Kuday,^{4a} S. Kuehn,⁴⁸ A. Kugel,^{58c} T. Kuhl,⁴² D. Kuhn,⁶¹ V. Kukhtin,⁶⁴ Y. Kulchitsky,⁹⁰ S. Kuleshov,^{32b} C. Kummer,⁹⁸ M. Kuna,⁷⁸ J. Kunkle,¹²⁰ A. Kupco,¹²⁵ H. Kurashige,⁶⁶ M. Kurata,¹⁶⁰ Y. A. Kurochkin,⁹⁰ V. Kus,¹²⁵ E. S. Kuwertz,¹⁴⁷ M. Kuze,¹⁵⁷ J. Kvita,¹⁴² R. Kwee,¹⁶ A. La Rosa,⁴⁹ L. La Rotonda,^{37a,37b} L. Labarga,⁸⁰ S. Lablak,^{135a} C. Lacasta,¹⁶⁷ F. Lacava,^{132a,132b} J. Lacey,²⁹ H. Lacker,¹⁶ D. Lacour,⁷⁸ V. R. Lacuesta,¹⁶⁷ E. Ladygin,⁶⁴ R. Lafaye,⁵ B. Laforge,⁷⁸ T. Lagouri,¹⁷⁶ S. Lai,⁴⁸ E. Laisne,⁵⁵ L. Lambourne,⁷⁷ C. L. Lampen,⁷ W. Lampl,⁷ E. Lancon,¹³⁶ U. Landgraf,⁴⁸ M. P. J. Landon,⁷⁵ V. S. Lang,^{58a} C. Lange,⁴² A. J. Lankford,¹⁶³ F. Lanni,²⁵ K. Lantzsch,¹⁷⁵ A. Lanza,^{119a} S. Laplace,⁷⁸ C. Lapoire,²¹ J. F. Laporte,¹³⁶ T. Lari,^{89a} A. Larter,¹¹⁸ M. Lassnig,³⁰ P. Laurelli,⁴⁷ V. Lavorini,^{37a,37b} W. Lavrijsen,¹⁵ P. Laycock,⁷³ O. Le Dortz,⁷⁸ E. Le Guirriec,⁸³ E. Le Menedeu,¹² T. LeCompte,⁶ F. Ledroit-Guillon,⁵⁵ H. Lee,¹⁰⁵ J. S. H. Lee,¹¹⁶ S. C. Lee,¹⁵¹ L. Lee,¹⁷⁶ M. Lefebvre,¹⁶⁹ M. Legendre,¹³⁶ F. Legger,⁹⁸ C. Leggett,¹⁵ M. Lehmann,²¹ G. Lehmann Miotto,³⁰ A. G. Leister,¹⁷⁶ M. A. L. Leite,^{24d} R. Leitner,¹²⁶ D. Lellouch,¹⁷² B. Lemmer,⁵⁴ V. Lendermann,^{58a} K. J. C. Leney,^{145b} T. Lenz,¹⁰⁵ G. Lenzen,¹⁷⁵ B. Lenzi,³⁰ K. Leonhardt,⁴⁴ S. Leontsinis,¹⁰ F. Lepold,^{58a} C. Leroy,⁹³ J.-R. Lessard,¹⁶⁹ C. G. Lester,²⁸ C. M. Lester,¹²⁰ J. Levêque,⁵ D. Levin,⁸⁷ L. J. Levinson,¹⁷² A. Lewis,¹¹⁸ G. H. Lewis,¹⁰⁸ A. M. Leyko,²¹ M. Leyton,¹⁶ B. Li,^{33b} B. Li,⁸³ H. Li,¹⁴⁸ H. L. Li,³¹ S. Li,^{33b,v} X. Li,⁸⁷ Z. Liang,^{118,w} H. Liao,³⁴ B. Liberti,^{133a} P. Lichard,³⁰ M. Lichtnecker,⁹⁸ K. Lie,¹⁶⁵ W. Liebig,¹⁴ C. Limbach,²¹ A. Limosani,⁸⁶ M. Limper,⁶² S. C. Lin,^{151,x} F. Linde,¹⁰⁵

- J. T. Linnemann,⁸⁸ E. Lipeles,¹²⁰ A. Lipniacka,¹⁴ T. M. Liss,¹⁶⁵ D. Lissauer,²⁵ A. Lister,⁴⁹ A. M. Litke,¹³⁷ C. Liu,²⁹ D. Liu,¹⁵¹ J. B. Liu,⁸⁷ L. Liu,⁸⁷ M. Liu,^{33b} Y. Liu,^{33b} M. Livan,^{119a,119b} S. S. A. Livermore,¹¹⁸ A. Lleres,⁵⁵ J. Llorente Merino,⁸⁰ S. L. Lloyd,⁷⁵ E. Lobodzinska,⁴² P. Loch,⁷ W. S. Lockman,¹³⁷ T. Loddenkoetter,²¹ F. K. Loebinger,⁸² A. Loginov,¹⁷⁶ C. W. Loh,¹⁶⁸ T. Lohse,¹⁶ K. Lohwasser,⁴⁸ M. Lokajicek,¹²⁵ V. P. Lombardo,⁵ R. E. Long,⁷¹ L. Lopes,^{124a} D. Lopez Mateos,⁵⁷ J. Lorenz,⁹⁸ N. Lorenzo Martinez,¹¹⁵ M. Losada,¹⁶² P. Loscutoff,¹⁵ F. Lo Sterzo,^{132a,132b} M. J. Losty,^{159a,a} X. Lou,⁴¹ A. Lounis,¹¹⁵ K. F. Loureiro,¹⁶² J. Love,⁶ P. A. Love,⁷¹ A. J. Lowe,^{143,h} F. Lu,^{33a} H. J. Lubatti,¹³⁸ C. Luci,^{132a,132b} A. Lucotte,⁵⁵ A. Ludwig,⁴⁴ D. Ludwig,⁴² I. Ludwig,⁴⁸ J. Ludwig,⁴⁸ F. Luehring,⁶⁰ G. Luijkx,¹⁰⁵ W. Lukas,⁶¹ L. Luminari,^{132a} E. Lund,¹¹⁷ B. Lund-Jensen,¹⁴⁷ B. Lundberg,⁷⁹ J. Lundberg,^{146a,146b} O. Lundberg,^{146a,146b} J. Lundquist,³⁶ M. Lungwitz,⁸¹ D. Lynn,²⁵ E. Lytken,⁷⁹ H. Ma,²⁵ L. L. Ma,¹⁷³ G. Maccarrone,⁴⁷ A. Macchiolo,⁹⁹ B. Maček,⁷⁴ J. Machado Miguens,^{124a} D. Macina,³⁰ R. Mackeprang,³⁶ R. J. Madaras,¹⁵ H. J. Maddocks,⁷¹ W. F. Mader,⁴⁴ R. Maenner,^{58c} T. Maeno,²⁵ P. Mättig,¹⁷⁵ S. Mättig,⁴² L. Magnoni,¹⁶³ E. Magradze,⁵⁴ K. Mahboubi,⁴⁸ J. Mahlstedt,¹⁰⁵ S. Mahmoud,⁷³ G. Mahout,¹⁸ C. Maiani,¹³⁶ C. Maidantchik,^{24a} A. Maio,^{124a,d} S. Majewski,²⁵ Y. Makida,⁶⁵ N. Makovec,¹¹⁵ P. Mal,¹³⁶ B. Malaescu,³⁰ Pa. Malecki,³⁹ P. Malecki,³⁹ V. P. Maleev,¹²¹ F. Malek,⁵⁵ U. Mallik,⁶² D. Malon,⁶ C. Malone,¹⁴³ S. Maltezos,¹⁰ V. Malyshev,¹⁰⁷ S. Malyukov,³⁰ J. Mamuzic,^{13b} A. Manabe,⁶⁵ L. Mandelli,^{89a} I. Mandić,⁷⁴ R. Mandrysch,⁶² J. Maneira,^{124a} A. Manfredini,⁹⁹ L. Manhaes de Andrade Filho,^{24b} J. A. Manjarres Ramos,¹³⁶ A. Mann,⁹⁸ P. M. Manning,¹³⁷ A. Manousakis-Katsikakis,⁹ B. Mansoulie,¹³⁶ A. Mapelli,³⁰ L. Mapelli,³⁰ L. March,¹⁶⁷ J. F. Marchand,²⁹ F. Marchese,^{133a,133b} G. Marchiori,⁷⁸ M. Marcisovsky,¹²⁵ C. P. Marino,¹⁶⁹ F. Marroquim,^{24a} Z. Marshall,³⁰ L. F. Marti,¹⁷ S. Marti-Garcia,¹⁶⁷ B. Martin,³⁰ B. Martin,⁸⁸ J. P. Martin,⁹³ T. A. Martin,¹⁸ V. J. Martin,⁴⁶ B. Martin dit Latour,⁴⁹ S. Martin-Haugh,¹⁴⁹ M. Martinez,¹² V. Martinez Outschoorn,⁵⁷ A. C. Martyniuk,¹⁶⁹ M. Marx,⁸² F. Marzano,^{132a} A. Marzin,¹¹¹ L. Masetti,⁸¹ T. Mashimo,¹⁵⁵ R. Mashinistov,⁹⁴ J. Masik,⁸² A. L. Maslennikov,¹⁰⁷ I. Massa,^{20a,20b} G. Massaro,¹⁰⁵ N. Massol,⁵ P. Mastrandrea,¹⁴⁸ A. Mastroberardino,^{37a,37b} T. Masubuchi,¹⁵⁵ H. Matsunaga,¹⁵⁵ T. Matsushita,⁶⁶ C. Mattravers,^{118,e} J. Maurer,⁸³ S. J. Maxfield,⁷³ D. A. Maximov,^{107,i} A. Mayne,¹³⁹ R. Mazini,¹⁵¹ M. Mazur,²¹ L. Mazzaferro,^{133a,133b} M. Mazzanti,^{89a} J. Mc Donald,⁸⁵ S. P. Mc Kee,⁸⁷ A. McCarn,¹⁶⁵ R. L. McCarthy,¹⁴⁸ T. G. McCarthy,²⁹ N. A. McCubbin,¹²⁹ K. W. McFarlane,^{56,a} J. A. Mcfayden,¹³⁹ G. Mchedlidze,^{51b} T. McLaughlan,¹⁸ S. J. McMahon,¹²⁹ R. A. McPherson,^{169,m} A. Meade,⁸⁴ J. Mechnich,¹⁰⁵ M. Mechtel,¹⁷⁵ M. Medinnis,⁴² S. Meehan,³¹ R. Meera-Lebbai,¹¹¹ T. Meguro,¹¹⁶ S. Mehlhase,³⁶ A. Mehta,⁷³ K. Meier,^{58a} B. Meirose,⁷⁹ C. Melachrinou,³¹ B. R. Mellado Garcia,¹⁷³ F. Meloni,^{89a,89b} L. Mendoza Navas,¹⁶² Z. Meng,^{151,y} A. Mengarelli,^{20a,20b} S. Menke,⁹⁹ E. Meoni,¹⁶¹ K. M. Mercurio,⁵⁷ P. Mermod,⁴⁹ L. Merola,^{102a,102b} C. Meroni,^{89a} F. S. Merritt,³¹ H. Merritt,¹⁰⁹ A. Messina,^{30,z} J. Metcalfe,²⁵ A. S. Mete,¹⁶³ C. Meyer,⁸¹ C. Meyer,³¹ J.-P. Meyer,¹³⁶ J. Meyer,¹⁷⁴ J. Meyer,⁵⁴ S. Michal,³⁰ L. Micu,^{26a} R. P. Middleton,¹²⁹ S. Migas,⁷³ L. Mijović,¹³⁶ G. Mikenberg,¹⁷² M. Mikestikova,¹²⁵ M. Mikuž,⁷⁴ D. W. Miller,³¹ R. J. Miller,⁸⁸ W. J. Mills,¹⁶⁸ C. Mills,⁵⁷ A. Milov,¹⁷² D. A. Milstead,^{146a,146b} D. Milstein,¹⁷² A. A. Minaenko,¹²⁸ M. Miñano Moya,¹⁶⁷ I. A. Minashvili,⁶⁴ A. I. Mincer,¹⁰⁸ B. Mindur,³⁸ M. Mineev,⁶⁴ Y. Ming,¹⁷³ L. M. Mir,¹² G. Mirabelli,^{132a} J. Mitrevski,¹³⁷ V. A. Mitsou,¹⁶⁷ S. Mitsui,⁶⁵ P. S. Miyagawa,¹³⁹ J. U. Mjörnmark,⁷⁹ T. Moa,^{146a,146b} V. Moeller,²⁸ K. Mönig,⁴² N. Möser,²¹ S. Mohapatra,¹⁴⁸ W. Mohr,⁴⁸ R. Moles-Valls,¹⁶⁷ A. Molfetas,³⁰ J. Monk,⁷⁷ E. Monnier,⁸³ J. Montejo Berlingen,¹² F. Monticelli,⁷⁰ S. Monzani,^{20a,20b} R. W. Moore,³ G. F. Moorhead,⁸⁶ C. Mora Herrera,⁴⁹ A. Moraes,⁵³ N. Morange,¹³⁶ J. Morel,⁵⁴ G. Morello,^{37a,37b} D. Moreno,⁸¹ M. Moreno Llacer,¹⁶⁷ P. Morettini,^{50a} M. Morgenstern,⁴⁴ M. Morii,⁵⁷ A. K. Morley,³⁰ G. Mornacchi,³⁰ J. D. Morris,⁷⁵ L. Morvaj,¹⁰¹ H. G. Moser,⁹⁹ M. Mosidze,^{51b} J. Moss,¹⁰⁹ R. Mount,¹⁴³ E. Mountricha,^{10,aa} S. V. Mouraviev,^{94,a} E. J. W. Moyse,⁸⁴ F. Mueller,^{58a} J. Mueller,¹²³ K. Mueller,²¹ T. A. Müller,⁹⁸ T. Mueller,⁸¹ D. Muenstermann,³⁰ Y. Munwes,¹⁵³ W. J. Murray,¹²⁹ I. Mussche,¹⁰⁵ E. Musto,¹⁵² A. G. Myagkov,¹²⁸ M. Myska,¹²⁵ O. Nackenhorst,⁵⁴ J. Nadal,¹² K. Nagai,¹⁶⁰ R. Nagai,¹⁵⁷ K. Nagano,⁶⁵ A. Nagarkar,¹⁰⁹ Y. Nagasaka,⁵⁹ M. Nagel,⁹⁹ A. M. Nairz,³⁰ Y. Nakahama,³⁰ K. Nakamura,¹⁵⁵ T. Nakamura,¹⁵⁵ I. Nakano,¹¹⁰ G. Nanava,²¹ A. Napier,¹⁶¹ R. Narayan,^{58b} M. Nash,^{77,c} T. Nattermann,²¹ T. Naumann,⁴² G. Navarro,¹⁶² H. A. Neal,⁸⁷ P. Yu. Nechaeva,⁹⁴ T. J. Neep,⁸² A. Negri,^{119a,119b} G. Negri,³⁰ M. Negrini,^{20a} S. Nektarijevic,⁴⁹ A. Nelson,¹⁶³ T. K. Nelson,¹⁴³ S. Nemecek,¹²⁵ P. Nemethy,¹⁰⁸ A. A. Nepomuceno,^{24a} M. Nessi,^{30,bb} M. S. Neubauer,¹⁶⁵ M. Neumann,¹⁷⁵ A. Neusiedl,⁸¹ R. M. Neves,¹⁰⁸ P. Nevski,²⁵ F. M. Newcomer,¹²⁰ P. R. Newman,¹⁸ V. Nguyen Thi Hong,¹³⁶ R. B. Nickerson,¹¹⁸ R. Nicolaidou,¹³⁶ B. Nicquevert,³⁰ F. Niedercorn,¹¹⁵ J. Nielsen,¹³⁷ N. Nikiforou,³⁵ A. Nikiforov,¹⁶ V. Nikolaenko,¹²⁸ I. Nikolic-Audit,⁷⁸ K. Nikolics,⁴⁹ K. Nikolopoulos,¹⁸ H. Nilsen,⁴⁸ P. Nilsson,⁸ Y. Ninomiya,¹⁵⁵ A. Nisati,^{132a} R. Nisius,⁹⁹ T. Nobe,¹⁵⁷ L. Nodulman,⁶ M. Nomachi,¹¹⁶

- I. Nomidis,¹⁵⁴ S. Norberg,¹¹¹ M. Nordberg,³⁰ P. R. Norton,¹²⁹ J. Novakova,¹²⁶ M. Nozaki,⁶⁵ L. Nozka,¹¹³
 I. M. Nugent,^{159a} A.-E. Nuncio-Quiroz,²¹ G. Nunes Hanninger,⁸⁶ T. Nunnemann,⁹⁸ E. Nurse,⁷⁷ B. J. O'Brien,⁴⁶
 D. C. O'Neil,¹⁴² V. O'Shea,⁵³ L. B. Oakes,⁹⁸ F. G. Oakham,^{29,g} H. Oberlack,⁹⁹ J. Ocariz,⁷⁸ A. Ochi,⁶⁶ S. Oda,⁶⁹
 S. Odaka,⁶⁵ J. Odier,⁸³ H. Ogren,⁶⁰ A. Oh,⁸² S. H. Oh,⁴⁵ C. C. Ohm,³⁰ T. Ohshima,¹⁰¹ W. Okamura,¹¹⁶ H. Okawa,²⁵
 Y. Okumura,³¹ T. Okuyama,¹⁵⁵ A. Olariu,^{26a} A. G. Olchevski,⁶⁴ S. A. Olivares Pino,^{32a} M. Oliveira,^{124a,j}
 D. Oliveira Damazio,²⁵ E. Oliver Garcia,¹⁶⁷ D. Olivito,¹²⁰ A. Olszewski,³⁹ J. Olszowska,³⁹ A. Onofre,^{124a,cc}
 P. U. E. Onyisi,^{31,dd} C. J. Oram,^{159a} M. J. Oreglia,³¹ Y. Oren,¹⁵³ D. Orestano,^{134a,134b} N. Orlando,^{72a,72b} I. Orlov,¹⁰⁷
 C. Oropeza Barrera,⁵³ R. S. Orr,¹⁵⁸ B. Osculati,^{50a,50b} R. Ospanov,¹²⁰ C. Osuna,¹² G. Otero y Garzon,²⁷
 J. P. Ottersbach,¹⁰⁵ M. Ouchrif,^{135d} E. A. Ouellette,¹⁶⁹ F. Ould-Saada,¹¹⁷ A. Ouraou,¹³⁶ Q. Ouyang,^{33a}
 A. Ovcharova,¹⁵ M. Owen,⁸² S. Owen,¹³⁹ V. E. Ozcan,^{19a} N. Ozturk,⁸ A. Pacheco Pages,¹² C. Padilla Aranda,¹²
 S. Pagan Griso,¹⁵ E. Paganis,¹³⁹ C. Pahl,⁹⁹ F. Paige,²⁵ P. Pais,⁸⁴ K. Pajchel,¹¹⁷ G. Palacino,^{159b} C. P. Paleari,⁷
 S. Palestini,³⁰ D. Pallin,³⁴ A. Palma,^{124a} J. D. Palmer,¹⁸ Y. B. Pan,¹⁷³ E. Panagiotopoulou,¹⁰ J. G. Panduro Vazquez,⁷⁶
 P. Pani,¹⁰⁵ N. Panikashvili,⁸⁷ S. Panitkin,²⁵ D. Pantea,^{26a} A. Papadelis,^{146a} Th. D. Papadopoulou,¹⁰ A. Paramonov,⁶
 D. Paredes Hernandez,³⁴ W. Park,^{25,ee} M. A. Parker,²⁸ F. Parodi,^{50a,50b} J. A. Parsons,³⁵ U. Parzefall,⁴⁸ S. Pashapour,⁵⁴
 E. Pasqualucci,^{132a} S. Passaggio,^{50a} A. Passeri,^{134a} F. Pastore,^{134a,134b,a} Fr. Pastore,⁷⁶ G. Pásztor,^{49,ff} S. Patariaia,¹⁷⁵
 N. Patel,¹⁵⁰ J. R. Pater,⁸² S. Patricelli,^{102a,102b} T. Pauly,³⁰ M. Pecsny,^{144a} S. Pedraza Lopez,¹⁶⁷
 M. I. Pedraza Morales,¹⁷³ S. V. Peleganchuk,¹⁰⁷ D. Pelikan,¹⁶⁶ H. Peng,^{33b} B. Penning,³¹ A. Penson,³⁵ J. Penwell,⁶⁰
 M. Perantoni,^{24a} K. Perez,^{35,gg} T. Perez Cavalcanti,⁴² E. Perez Codina,^{159a} M. T. Pérez García-Estañ,¹⁶⁷
 V. Perez Reale,³⁵ L. Perini,^{89a,89b} H. Pernegger,³⁰ R. Perrino,^{72a} P. Perrodo,⁵ V. D. Peshekhonov,⁶⁴ K. Peters,³⁰
 B. A. Petersen,³⁰ J. Petersen,³⁰ T. C. Petersen,³⁶ E. Petit,⁵ A. Petridis,¹⁵⁴ C. Petridou,¹⁵⁴ E. Petrolo,^{132a}
 F. Petrucci,^{134a,134b} D. Petschull,⁴² M. Petteni,¹⁴² R. Pezoa,^{32b} A. Phan,⁸⁶ P. W. Phillips,¹²⁹ G. Piacquadio,³⁰
 A. Picazio,⁴⁹ E. Piccaro,⁷⁵ M. Piccinini,^{20a,20b} S. M. Piec,⁴² R. Piegaiia,²⁷ D. T. Pignotti,¹⁰⁹ J. E. Pilcher,³¹
 A. D. Pilkington,⁸² J. Pina,^{124a,d} M. Pinamonti,^{164a,164c} A. Pinder,¹¹⁸ J. L. Pinfold,³ A. Pingel,³⁶ B. Pinto,^{124a}
 C. Pizio,^{89a,89b} M.-A. Pleier,²⁵ E. Plotnikova,⁶⁴ A. Poblaguev,²⁵ S. Poddar,^{58a} F. Podlyski,³⁴ L. Poggioli,¹¹⁵ D. Pohl,²¹
 M. Pohl,⁴⁹ G. Polesello,^{119a} A. Policicchio,^{37a,37b} A. Polini,^{20a} J. Poll,⁷⁵ V. Polychronakos,²⁵ D. Pomeroy,²³
 K. Pommès,³⁰ L. Pontecorvo,^{132a} B. G. Pope,⁸⁸ G. A. Popeneciu,^{26a} D. S. Popovic,^{13a} A. Poppleton,³⁰
 X. Portell Bueso,³⁰ G. E. Pospelov,⁹⁹ S. Pospisil,¹²⁷ I. N. Potrap,⁹⁹ C. J. Potter,¹⁴⁹ C. T. Potter,¹¹⁴ G. Poulard,³⁰
 J. Poveda,⁶⁰ V. Pozdnyakov,⁶⁴ R. Prabhu,⁷⁷ P. Pralavorio,⁸³ A. Pranko,¹⁵ S. Prasad,³⁰ R. Pravahan,²⁵ S. Prell,⁶³
 K. Pretzl,¹⁷ D. Price,⁶⁰ J. Price,⁷³ L. E. Price,⁶ D. Prieur,¹²³ M. Primavera,^{72a} K. Prokofiev,¹⁰⁸ F. Prokoshin,^{32b}
 S. Protopopescu,²⁵ J. Proudfoot,⁶ X. Prudent,⁴⁴ M. Przybycien,³⁸ H. Przysieszniak,⁵ S. Psoroulas,²¹ E. Ptacek,¹¹⁴
 E. Pueschel,⁸⁴ J. Purdham,⁸⁷ M. Purohit,^{25,ee} P. Puzo,¹¹⁵ Y. Pylypchenko,⁶² J. Qian,⁸⁷ A. Quadt,⁵⁴ D. R. Quarrie,¹⁵
 W. B. Quayle,¹⁷³ M. Raas,¹⁰⁴ V. Radeka,²⁵ V. Radescu,⁴² P. Radloff,¹¹⁴ F. Ragusa,^{89a,89b} G. Rahal,¹⁷⁸
 A. M. Rahimi,¹⁰⁹ D. Rahm,²⁵ S. Rajagopalan,²⁵ M. Rammensee,⁴⁸ M. Rammes,¹⁴¹ A. S. Randle-Conde,⁴⁰
 K. Randrianarivony,²⁹ K. Rao,¹⁶³ F. Rauscher,⁹⁸ T. C. Rave,⁴⁸ M. Raymond,³⁰ A. L. Read,¹¹⁷ D. M. Rebuzzi,^{119a,119b}
 A. Redelbach,¹⁷⁴ G. Redlinger,²⁵ R. Reece,¹²⁰ K. Reeves,⁴¹ A. Reinsch,¹¹⁴ I. Reisinger,⁴³ C. Rembser,³⁰ Z. L. Ren,¹⁵¹
 A. Renaud,¹¹⁵ M. Rescigno,^{132a} S. Resconi,^{89a} B. Resende,¹³⁶ P. Reznicek,⁹⁸ R. Rezvani,¹⁵⁸ R. Richter,⁹⁹
 E. Richter-Was,^{5,hh} M. Ridet,⁷⁸ M. Rijpstra,¹⁰⁵ M. Rijssenbeek,¹⁴⁸ A. Rimoldi,^{119a,119b} L. Rinaldi,^{20a} R. R. Rios,⁴⁰
 I. Riu,¹² G. Rivoltella,^{89a,89b} F. Rizatdinova,¹¹² E. Rizvi,⁷⁵ S. H. Robertson,^{85,m} A. Robichaud-Veronneau,¹¹⁸
 D. Robinson,²⁸ J. E. M. Robinson,⁸² A. Robson,⁵³ J. G. Rocha de Lima,¹⁰⁶ C. Roda,^{122a,122b} D. Roda Dos Santos,³⁰
 A. Roe,⁵⁴ S. Roe,³⁰ O. Røhne,¹¹⁷ S. Rolli,¹⁶¹ A. Romaniouk,⁹⁶ M. Romano,^{20a,20b} G. Romeo,²⁷ E. Romero Adam,¹⁶⁷
 N. Rempotis,¹³⁸ L. Roos,⁷⁸ E. Ros,¹⁶⁷ S. Rosati,^{132a} K. Rosbach,⁴⁹ A. Rose,¹⁴⁹ M. Rose,⁷⁶ G. A. Rosenbaum,¹⁵⁸
 E. I. Rosenberg,⁶³ P. L. Rosendahl,¹⁴ O. Rosenthal,¹⁴¹ L. Rosselet,⁴⁹ V. Rossetti,¹² E. Rossi,^{132a,132b} L. P. Rossi,^{50a}
 M. Rotaru,^{26a} I. Roth,¹⁷² J. Rothberg,¹³⁸ D. Rousseau,¹¹⁵ C. R. Royon,¹³⁶ A. Rozanov,⁸³ Y. Rozen,¹⁵² X. Ruan,^{33a,ii}
 F. Rubbo,¹² I. Rubinskiy,⁴² N. Ruckstuhl,¹⁰⁵ V. I. Rud,⁹⁷ C. Rudolph,⁴⁴ G. Rudolph,⁶¹ F. Rühr,⁷ A. Ruiz-Martinez,⁶³
 L. Rumyantsev,⁶⁴ Z. Rurikova,⁴⁸ N. A. Rusakovich,⁶⁴ A. Ruschke,⁹⁸ J. P. Rutherford,⁷ P. Ruzicka,¹²⁵
 Y. F. Ryabov,¹²¹ M. Rybar,¹²⁶ G. Rybkin,¹¹⁵ N. C. Ryder,¹¹⁸ A. F. Saavedra,¹⁵⁰ I. Sadeh,¹⁵³ H. F.-W. Sadrozinski,¹³⁷
 R. Sadykov,⁶⁴ F. Safai Tehrani,^{132a} H. Sakamoto,¹⁵⁵ G. Salamanna,⁷⁵ A. Salamon,^{133a} M. Saleem,¹¹¹ D. Salek,³⁰
 D. Salihagic,⁹⁹ A. Salnikov,¹⁴³ J. Salt,¹⁶⁷ B. M. Salvachua Ferrando,⁶ D. Salvatore,^{37a,37b} F. Salvatore,¹⁴⁹
 A. Salvucci,¹⁰⁴ A. Salzburger,³⁰ D. Sampsonidis,¹⁵⁴ B. H. Samset,¹¹⁷ A. Sanchez,^{102a,102b} V. Sanchez Martinez,¹⁶⁷
 H. Sandaker,¹⁴ H. G. Sander,⁸¹ M. P. Sanders,⁹⁸ M. Sandhoff,¹⁷⁵ T. Sandoval,²⁸ C. Sandoval,¹⁶² R. Sandstroem,⁹⁹
 D. P. C. Sankey,¹²⁹ A. Sansoni,⁴⁷ C. Santamarina Rios,⁸⁵ C. Santoni,³⁴ R. Santonico,^{133a,133b} H. Santos,^{124a}

- I. Santoyo Castillo,¹⁴⁹ J. G. Saraiva,^{124a} T. Sarangi,¹⁷³ E. Sarkisyan-Grinbaum,⁸ B. Sarrazin,²¹ F. Sarri,^{122a,122b}
 G. Sartisohn,¹⁷⁵ O. Sasaki,⁶⁵ Y. Sasaki,¹⁵⁵ N. Sasao,⁶⁷ I. Satsounkevitch,⁹⁰ G. Sauvage,^{5,a} E. Sauvan,⁵
 J. B. Sauvan,¹¹⁵ P. Savard,^{158,g} V. Savinov,¹²³ D. O. Savu,³⁰ L. Sawyer,^{25,o} D. H. Saxon,⁵³ J. Saxon,¹²⁰ C. Sbarra,^{20a}
 A. Sbrizzi,^{20a,20b} D. A. Scannicchio,¹⁶³ M. Scarcella,¹⁵⁰ J. Schaarschmidt,¹¹⁵ P. Schacht,⁹⁹ D. Schaefer,¹²⁰
 U. Schäfer,⁸¹ A. Schaelicke,⁴⁶ S. Schaepe,²¹ S. Schaetzel,^{58b} A. C. Schaffer,¹¹⁵ D. Schaile,⁹⁸ R. D. Schamberger,¹⁴⁸
 A. G. Schamov,¹⁰⁷ V. Scharf,^{58a} V. A. Schegelsky,¹²¹ D. Scheirich,⁸⁷ M. Schernau,¹⁶³ M. I. Scherzer,³⁵
 C. Schiavi,^{50a,50b} J. Schieck,⁹⁸ M. Schioppa,^{37a,37b} S. Schlenker,³⁰ E. Schmidt,⁴⁸ K. Schmieden,²¹ C. Schmitt,⁸¹
 S. Schmitt,^{58b} B. Schneider,¹⁷ U. Schnoor,⁴⁴ L. Schoeffel,¹³⁶ A. Schoening,^{58b} A. L. S. Schorlemmer,⁵⁴ M. Schott,³⁰
 D. Schouten,^{159a} J. Schovancova,¹²⁵ M. Schram,⁸⁵ C. Schroeder,⁸¹ N. Schroer,^{58c} M. J. Schultens,²¹ J. Schultes,¹⁷⁵
 H.-C. Schultz-Coulon,^{58a} H. Schulz,¹⁶ M. Schumacher,⁴⁸ B. A. Schumm,¹³⁷ Ph. Schune,¹³⁶ A. Schwartzman,¹⁴³
 Ph. Schwegler,⁹⁹ Ph. Schwemling,⁷⁸ R. Schwienhorst,⁸⁸ R. Schwierz,⁴⁴ J. Schwindling,¹³⁶ T. Schwindt,²¹
 M. Schwoerer,⁵ F. G. Sciaccia,¹⁷ G. Sciolla,²³ W. G. Scott,¹²⁹ J. Searcy,¹¹⁴ G. Sedov,⁴² E. Sedykh,¹²¹ S. C. Seidel,¹⁰³
 A. Seiden,¹³⁷ F. Seifert,⁴⁴ J. M. Seixas,^{24a} G. Sekhniaidze,^{102a} S. J. Sekula,⁴⁰ K. E. Selbach,⁴⁶ D. M. Seliverstov,¹²¹
 B. Sellden,^{146a} G. Sellers,⁷³ M. Seman,^{144b} N. Semprini-Cesari,^{20a,20b} C. Serfon,⁹⁸ L. Serin,¹¹⁵ L. Serkin,⁵⁴
 R. Seuster,^{159a} H. Severini,¹¹¹ A. Sfyrila,³⁰ E. Shabalina,⁵⁴ M. Shamim,¹¹⁴ L. Y. Shan,^{33a} J. T. Shank,²² Q. T. Shao,⁸⁶
 M. Shapiro,¹⁵ P. B. Shatalov,⁹⁵ K. Shaw,^{164a,164c} D. Sherman,¹⁷⁶ P. Sherwood,⁷⁷ S. Shimizu,¹⁰¹ M. Shimojima,¹⁰⁰
 T. Shin,⁵⁶ M. Shiyakova,⁶⁴ A. Shmeleva,⁹⁴ M. J. Shochet,³¹ D. Short,¹¹⁸ S. Shrestha,⁶³ E. Shulga,⁹⁶ M. A. Shupe,⁷
 P. Sicho,¹²⁵ A. Sidoti,^{132a} F. Siegert,⁴⁸ Dj. Sijacki,^{13a} O. Silbert,¹⁷² J. Silva,^{124a} Y. Silver,¹⁵³ D. Silverstein,¹⁴³
 S. B. Silverstein,^{146a} V. Simak,¹²⁷ O. Simard,¹³⁶ Lj. Simic,^{13a} S. Simion,¹¹⁵ E. Simioni,⁸¹ B. Simmons,⁷⁷
 R. Simoniello,^{89a,89b} M. Simonyan,³⁶ P. Sinervo,¹⁵⁸ N. B. Sinev,¹¹⁴ V. Sipica,¹⁴¹ G. Siragusa,¹⁷⁴ A. Sircar,²⁵
 A. N. Sisakyan,^{64,a} S. Yu. Sivoklov,⁹⁷ J. Sjölin,^{146a,146b} T. B. Sjursen,¹⁴ L. A. Skinnari,¹⁵ H. P. Skottowe,⁵⁷
 K. Skovpen,¹⁰⁷ P. Skubic,¹¹¹ M. Slater,¹⁸ T. Slavicek,¹²⁷ K. Sliwa,¹⁶¹ V. Smakhtin,¹⁷² B. H. Smart,⁴⁶ L. Smestad,¹¹⁷
 S. Yu. Smirnov,⁹⁶ Y. Smirnov,⁹⁶ L. N. Smirnova,⁹⁷ O. Smirnova,⁷⁹ B. C. Smith,⁵⁷ D. Smith,¹⁴³ K. M. Smith,⁵³
 M. Smizanska,⁷¹ K. Smolek,¹²⁷ A. A. Snesarev,⁹⁴ S. W. Snow,⁸² J. Snow,¹¹¹ S. Snyder,²⁵ R. Sobie,^{169,m}
 J. Sodomka,¹²⁷ A. Soffer,¹⁵³ C. A. Solans,¹⁶⁷ M. Solar,¹²⁷ J. Solc,¹²⁷ E. Yu. Soldatov,⁹⁶ U. Soldevila,¹⁶⁷
 E. Solfaroli Camillocci,^{132a,132b} A. A. Solodkov,¹²⁸ O. V. Solovyanov,¹²⁸ V. Solovyev,¹²¹ N. Soni,¹ A. Sood,¹⁵
 V. Sopko,¹²⁷ B. Sopko,¹²⁷ M. Sosebee,⁸ R. Soualah,^{164a,164c} P. Soueid,⁹³ A. Soukharev,¹⁰⁷ S. Spagnolo,^{72a,72b}
 F. Spanò,⁷⁶ R. Spighi,^{20a} G. Spigo,³⁰ R. Spiwoks,³⁰ M. Spousta,^{126,jj} T. Spreitzer,¹⁵⁸ B. Spurlock,⁸ R. D. St. Denis,⁵³
 J. Stahlman,¹²⁰ R. Stamen,^{58a} E. Stanecka,³⁹ R. W. Stanek,⁶ C. Stancu,^{134a} M. Stancu-Bellu,⁴² M. M. Stanitzki,⁴²
 S. Stapnes,¹¹⁷ E. A. Starchenko,¹²⁸ J. Stark,⁵⁵ P. Staroba,¹²⁵ P. Starovoitov,⁴² R. Staszewski,³⁹ A. Staude,⁹⁸
 P. Stavina,^{144a,a} G. Steele,⁵³ P. Steinbach,⁴⁴ P. Steinberg,²⁵ I. Stekl,¹²⁷ B. Stelzer,¹⁴² H. J. Stelzer,⁸⁸
 O. Stelzer-Chilton,^{159a} H. Stenzel,⁵² S. Stern,⁹⁹ G. A. Stewart,³⁰ J. A. Stillings,²¹ M. C. Stockton,⁸⁵ K. Stoerig,⁴⁸
 G. Stoicea,^{26a} S. Stonjek,⁹⁹ P. Strachota,¹²⁶ A. R. Stradling,⁸ A. Straessner,⁴⁴ J. Strandberg,¹⁴⁷ S. Strandberg,^{146a,146b}
 A. Strandlie,¹¹⁷ M. Strang,¹⁰⁹ E. Strauss,¹⁴³ M. Strauss,¹¹¹ P. Strizenec,^{144b} R. Ströhmer,¹⁷⁴ D. M. Strom,¹¹⁴
 J. A. Strong,^{76,a} R. Stroynowski,⁴⁰ B. Stugu,¹⁴ I. Stumer,^{25,a} J. Stupak,¹⁴⁸ P. Sturm,¹⁷⁵ N. A. Styles,⁴² D. A. Soh,^{151,w}
 D. Su,¹⁴³ H. S. Subramania,³ R. Subramaniam,²⁵ A. Succurro,¹² Y. Sugaya,¹¹⁶ C. Suhr,¹⁰⁶ M. Suk,¹²⁶ V. V. Sulin,⁹⁴
 S. Sultansoy,^{4d} T. Sumida,⁶⁷ X. Sun,⁵⁵ J. E. Sundermann,⁴⁸ K. Suruliz,¹³⁹ G. Susinno,^{37a,37b} M. R. Sutton,¹⁴⁹
 Y. Suzuki,⁶⁵ Y. Suzuki,⁶⁶ M. Svatos,¹²⁵ S. Swedish,¹⁶⁸ I. Sykora,^{144a} T. Sykora,¹²⁶ J. Sánchez,¹⁶⁷ D. Ta,¹⁰⁵
 K. Tackmann,⁴² A. Taffard,¹⁶³ R. Tafirout,^{159a} N. Taiblum,¹⁵³ Y. Takahashi,¹⁰¹ H. Takai,²⁵ R. Takashima,⁶⁸
 H. Takeda,⁶⁶ T. Takeshita,¹⁴⁰ Y. Takubo,⁶⁵ M. Talby,⁸³ A. Talyshev,^{107,i} M. C. Tamsett,²⁵ K. G. Tan,⁸⁶ J. Tanaka,¹⁵⁵
 R. Tanaka,¹¹⁵ S. Tanaka,¹³¹ S. Tanaka,⁶⁵ A. J. Tanasijczuk,¹⁴² K. Tani,⁶⁶ N. Tannoury,⁸³ S. Tapprogge,⁸¹ D. Tardif,¹⁵⁸
 S. Tarem,¹⁵² F. Tarrade,²⁹ G. F. Tartarelli,^{89a} P. Tas,¹²⁶ M. Tasevsky,¹²⁵ E. Tassi,^{37a,37b} Y. Tayalati,^{135d} C. Taylor,⁷⁷
 F. E. Taylor,⁹² G. N. Taylor,⁸⁶ W. Taylor,^{159b} M. Teinturier,¹¹⁵ F. A. Teischinger,³⁰ M. Teixeira Dias Castanheira,⁷⁵
 P. Teixeira-Dias,⁷⁶ K. K. Temming,⁴⁸ H. Ten Kate,³⁰ P. K. Teng,¹⁵¹ S. Terada,⁶⁵ K. Terashi,¹⁵⁵ J. Terron,⁸⁰ M. Testa,⁴⁷
 R. J. Teuscher,^{158,m} J. Therhaag,²¹ T. Theveneaux-Pelzer,⁷⁸ S. Thoma,⁴⁸ J. P. Thomas,¹⁸ E. N. Thompson,³⁵
 P. D. Thompson,¹⁸ P. D. Thompson,¹⁵⁸ A. S. Thompson,⁵³ L. A. Thomsen,³⁶ E. Thomson,¹²⁰ M. Thomson,²⁸
 W. M. Thong,⁸⁶ R. P. Thun,⁸⁷ F. Tian,³⁵ M. J. Tibbetts,¹⁵ T. Tic,¹²⁵ V. O. Tikhomirov,⁹⁴ Y. A. Tikhonov,^{107,i}
 S. Timoshenko,⁹⁶ E. Tiouchichine,⁸³ P. Tipton,¹⁷⁶ S. Tisserant,⁸³ T. Todorov,⁵ S. Todorova-Nova,¹⁶¹ B. Toggerson,¹⁶³
 J. Tojo,⁶⁹ S. Tokár,^{144a} K. Tokushuku,⁶⁵ K. Tollefson,⁸⁸ M. Tomoto,¹⁰¹ L. Tompkins,³¹ K. Toms,¹⁰³ A. Tonoyan,¹⁴
 C. Topfel,¹⁷ N. D. Topilin,⁶⁴ E. Torrence,¹¹⁴ H. Torres,⁷⁸ E. Torró Pastor,¹⁶⁷ J. Toth,^{83,ff} F. Touchard,⁸³ D. R. Tovey,¹³⁹
 T. Trefzger,¹⁷⁴ L. Tremblet,³⁰ A. Tricoli,³⁰ I. M. Trigger,^{159a} S. Trincaz-Duvold,⁷⁸ M. F. Tripiana,⁷⁰ N. Triplett,²⁵

W. Trischuk,¹⁵⁸ B. Trocmé,⁵⁵ C. Troncon,^{89a} M. Trottier-McDonald,¹⁴² P. True,⁸⁸ M. Trzebinski,³⁹ A. Trzupek,³⁹ C. Tsarouchas,³⁰ J. C.-L. Tseng,¹¹⁸ M. Tsiakiris,¹⁰⁵ P. V. Tsiarehska,⁹⁰ D. Tsiou, ^{5,kk} G. Tsipolitis,¹⁰ S. Tsiskaridze,¹² V. Tsiskaridze,⁴⁸ E. G. Tskhadadze,^{51a} I. I. Tsukerman,⁹⁵ V. Tsulaia,¹⁵ J.-W. Tsung,²¹ S. Tsuno,⁶⁵ D. Tsybychev,¹⁴⁸ A. Tua,¹³⁹ A. Tudorache,^{26a} V. Tudorache,^{26a} J. M. Tuggle,³¹ M. Turala,³⁹ D. Turecek,¹²⁷ I. Turk Cakir,^{4e} E. Turlay,¹⁰⁵ R. Turra,^{89a,89b} P. M. Tuts,³⁵ A. Tykhonov,⁷⁴ M. Tylmad,^{146a,146b} M. Tyndel,¹²⁹ G. Tzanakos,⁹ K. Uchida,²¹ I. Ueda,¹⁵⁵ R. Ueno,²⁹ M. Ughetto,⁸³ M. Ugland,¹⁴ M. Uhlenbrock,²¹ M. Uhrmacher,⁵⁴ F. Ukegawa,¹⁶⁰ G. Unal,³⁰ A. Undrus,²⁵ G. Unel,¹⁶³ Y. Unno,⁶⁵ D. Urbaniec,³⁵ P. Urquijo,²¹ G. Usai,⁸ M. Uslenghi,^{119a,119b} L. Vacavant,⁸³ V. Vacek,¹²⁷ B. Vachon,⁸⁵ S. Vahsen,¹⁵ J. Valenta,¹²⁵ S. Valentinetti,^{20a,20b} A. Valero,¹⁶⁷ S. Valkar,¹²⁶ E. Valladolid Gallego,¹⁶⁷ S. Vallecorsa,¹⁵² J. A. Valls Ferrer,¹⁶⁷ R. Van Berg,¹²⁰ P. C. Van Der Deijl,¹⁰⁵ R. van der Geer,¹⁰⁵ H. van der Graaf,¹⁰⁵ R. Van Der Leeuw,¹⁰⁵ E. van der Poel,¹⁰⁵ D. van der Ster,³⁰ N. van Eldik,³⁰ P. van Gemmeren,⁶ J. Van Nieuwkoop,¹⁴² I. van Vulpen,¹⁰⁵ M. Vanadia,⁹⁹ W. Vandelli,³⁰ A. Vaniachine,⁶ P. Vankov,⁴² F. Vannucci,⁷⁸ R. Vari,^{132a} E. W. Varnes,⁷ T. Varol,⁸⁴ D. Varouchas,¹⁵ A. Vartapetian,⁸ K. E. Varvell,¹⁵⁰ V. I. Vassilikopoulos,⁵⁶ F. Vazeille,³⁴ T. Vazquez Schroeder,⁵⁴ G. Vegni,^{89a,89b} J. J. Veillet,¹¹⁵ F. Veloso,^{124a} R. Veness,³⁰ S. Veneziano,^{132a} A. Ventura,^{72a,72b} D. Ventura,⁸⁴ M. Venturi,⁴⁸ N. Venturi,¹⁵⁸ V. Vercesi,^{119a} M. Verducci,¹³⁸ W. Verkerke,¹⁰⁵ J. C. Vermeulen,¹⁰⁵ A. Vest,⁴⁴ M. C. Vetterli,^{142,g} I. Vichou,¹⁶⁵ T. Vickey,^{145b,II} O. E. Vickey Boeriu,^{145b} G. H. A. Viehhauser,¹¹⁸ S. Viel,¹⁶⁸ M. Villa,^{20a,20b} M. Villaplana Perez,¹⁶⁷ E. Vilucchi,⁴⁷ M. G. Vincet,²⁹ E. Vinek,³⁰ V. B. Vinogradov,⁶⁴ M. Virchaux,^{136,a} J. Virzi,¹⁵ O. Vitells,¹⁷² M. Viti,⁴² I. Vivarelli,⁴⁸ F. Vives Vaque,³ S. Vlachos,¹⁰ D. Vladoiu,⁹⁸ M. Vlasak,¹²⁷ A. Vogel,²¹ P. Vokac,¹²⁷ G. Volpi,⁴⁷ M. Volpi,⁸⁶ G. Volpini,^{89a} H. von der Schmitt,⁹⁹ H. von Radziewski,⁴⁸ E. von Toerne,²¹ V. Vorobel,¹²⁶ V. Vorwerk,¹² M. Vos,¹⁶⁷ R. Voss,³⁰ J. H. Vossebeld,⁷³ N. Vranjes,¹³⁶ M. Vranjes Milosavljevic,¹⁰⁵ V. Vrba,¹²⁵ M. Vreeswijk,¹⁰⁵ T. Vu Anh,⁴⁸ R. Vuillermet,³⁰ I. Vukotic,³¹ W. Wagner,¹⁷⁵ P. Wagner,¹²⁰ H. Wahlen,¹⁷⁵ S. Wahrmond,⁴⁴ J. Wakabayashi,¹⁰¹ S. Walch,⁸⁷ J. Walder,⁷¹ R. Walker,⁹⁸ W. Walkowiak,¹⁴¹ R. Wall,¹⁷⁶ P. Waller,⁷³ B. Walsh,¹⁷⁶ C. Wang,⁴⁵ H. Wang,¹⁷³ H. Wang,⁴⁰ J. Wang,¹⁵¹ J. Wang,^{33a} R. Wang,¹⁰³ S. M. Wang,¹⁵¹ T. Wang,²¹ A. Warburton,⁸⁵ C. P. Ward,²⁸ D. R. Wardrope,⁷⁷ M. Warsinsky,⁴⁸ A. Washbrook,⁴⁶ C. Wasicki,⁴² I. Watanabe,⁶⁶ P. M. Watkins,¹⁸ A. T. Watson,¹⁸ I. J. Watson,¹⁵⁰ M. F. Watson,¹⁸ G. Watts,¹³⁸ S. Watts,⁸² A. T. Waugh,¹⁵⁰ B. M. Waugh,⁷⁷ M. S. Weber,¹⁷ J. S. Webster,³¹ A. R. Weidberg,¹¹⁸ P. Weigell,⁹⁹ J. Weingarten,⁵⁴ C. Weiser,⁴⁸ P. S. Wells,³⁰ T. Wenaus,²⁵ D. Wendland,¹⁶ Z. Weng,^{151,w} T. Wengler,³⁰ S. Wenig,³⁰ N. Vermes,²¹ M. Werner,⁴⁸ P. Werner,³⁰ M. Werth,¹⁶³ M. Wessels,^{58a} J. Wetter,¹⁶¹ C. Weydert,⁵⁵ K. Whalen,²⁹ A. White,⁸ M. J. White,⁸⁶ S. White,^{122a,122b} S. R. Whitehead,¹¹⁸ D. Whiteson,¹⁶³ D. Whittington,⁶⁰ D. Wicke,¹⁷⁵ F. J. Wickens,¹²⁹ W. Wiedenmann,¹⁷³ M. Wielers,¹²⁹ P. Wienemann,²¹ C. Wiglesworth,⁷⁵ L. A. M. Wiik-Fuchs,²¹ P. A. Wijeratne,⁷⁷ A. Wildauer,⁹⁹ M. A. Wildt,^{42,t} I. Wilhelm,¹²⁶ H. G. Wilkens,³⁰ J. Z. Will,⁹⁸ E. Williams,³⁵ H. H. Williams,¹²⁰ W. Willis,³⁵ S. Willocq,⁸⁴ J. A. Wilson,¹⁸ M. G. Wilson,¹⁴³ A. Wilson,⁸⁷ I. Wingerter-Seez,⁵ S. Winkelmann,⁴⁸ F. Winklmeier,³⁰ M. Wittgen,¹⁴³ S. J. Wollstadt,⁸¹ M. W. Wolter,³⁹ H. Wolters,^{124a,j} W. C. Wong,⁴¹ G. Wooden,⁸⁷ B. K. Wosiek,³⁹ J. Wotschack,³⁰ M. J. Woudstra,⁸² K. W. Wozniak,³⁹ K. Wraight,⁵³ M. Wright,⁵³ B. Wrona,⁷³ S. L. Wu,¹⁷³ X. Wu,⁴⁹ Y. Wu,^{33b,mm} E. Wulf,³⁵ B. M. Wynne,⁴⁶ S. Xella,³⁶ M. Xiao,¹³⁶ S. Xie,⁴⁸ C. Xu,^{33b,aa} D. Xu,^{33a} L. Xu,^{33b} B. Yabsley,¹⁵⁰ S. Yacoob,^{145a,nn} M. Yamada,⁶⁵ H. Yamaguchi,¹⁵⁵ A. Yamamoto,⁶⁵ K. Yamamoto,⁶³ S. Yamamoto,¹⁵⁵ T. Yamamura,¹⁵⁵ T. Yamanaka,¹⁵⁵ T. Yamazaki,¹⁵⁵ Y. Yamazaki,⁶⁶ Z. Yan,²² H. Yang,⁸⁷ U. K. Yang,⁸² Y. Yang,¹⁰⁹ Z. Yang,^{146a,146b} S. Yanush,⁹¹ L. Yao,^{33a} Y. Yasu,⁶⁵ E. Yatsenko,⁴² J. Ye,⁴⁰ S. Ye,²⁵ A. L. Yen,⁵⁷ M. Yilmaz,^{4c} R. Yoosoofmiya,¹²³ K. Yorita,¹⁷¹ R. Yoshida,⁶ K. Yoshihara,¹⁵⁵ C. Young,¹⁴³ C. J. Young,¹¹⁸ S. Youssef,²² D. Yu,²⁵ D. R. Yu,¹⁵ J. Yu,⁸ J. Yu,¹¹² L. Yuan,⁶⁶ A. Yurkewicz,¹⁰⁶ B. Zabinski,³⁹ R. Zaidan,⁶² A. M. Zaitsev,¹²⁸ L. Zanello,^{132a,132b} D. Zanzi,⁹⁹ A. Zaytsev,²⁵ C. Zeitnitz,¹⁷⁵ M. Zeman,¹²⁵ A. Zemla,³⁹ O. Zenin,¹²⁸ T. Ženiš,^{144a} Z. Zinonos,^{122a,122b} D. Zerwas,¹¹⁵ G. Zevi della Porta,⁵⁷ D. Zhang,⁸⁷ H. Zhang,⁸⁸ J. Zhang,⁶ X. Zhang,^{33d} Z. Zhang,¹¹⁵ L. Zhao,¹⁰⁸ Z. Zhao,^{33b} A. Zhemchugov,⁶⁴ J. Zhong,¹¹⁸ B. Zhou,⁸⁷ N. Zhou,¹⁶³ Y. Zhou,¹⁵¹ C. G. Zhu,^{33d} H. Zhu,⁴² J. Zhu,⁸⁷ Y. Zhu,^{33b} X. Zhuang,⁹⁸ V. Zhuravlov,⁹⁹ A. Zibell,⁹⁸ D. Zieminska,⁶⁰ N. I. Zimin,⁶⁴ R. Zimmermann,²¹ S. Zimmermann,²¹ S. Zimmermann,⁴⁸ M. Ziolkowski,¹⁴¹ R. Zitoun,⁵ L. Živković,³⁵ V. V. Zmouchko,^{128,a} G. Zobernig,¹⁷³ A. Zoccoli,^{20a,20b} M. zur Nedden,¹⁶ V. Zutshi,¹⁰⁶ and L. Zwalinski³⁰

(ATLAS Collaboration)

¹*School of Chemistry and Physics, University of Adelaide, Adelaide, Australia*²*Physics Department, SUNY Albany, Albany New York, USA*³*Department of Physics, University of Alberta, Edmonton, Alberta, Canada*

- ^{4a}Department of Physics, Ankara University, Ankara, Turkey
^{4b}Department of Physics, Dumlupinar University, Kutahya, Turkey
^{4c}Department of Physics, Gazi University, Ankara, Turkey
^{4d}Division of Physics, TOBB University of Economics and Technology, Ankara, Turkey
^{4e}Turkish Atomic Energy Authority, Ankara, Turkey
⁵LAPP, CNRS/IN2P3 and Université de Savoie, Annecy-le-Vieux, France
⁶High Energy Physics Division, Argonne National Laboratory, Argonne, Illinois, USA
⁷Department of Physics, University of Arizona, Tucson, Arizona, USA
⁸Department of Physics, The University of Texas at Arlington, Arlington, Texas, USA
⁹Physics Department, University of Athens, Athens, Greece
¹⁰Physics Department, National Technical University of Athens, Zografou, Greece
¹¹Institute of Physics, Azerbaijan Academy of Sciences, Baku, Azerbaijan
¹²Institut de Física d'Altes Energies and Departament de Física de la Universitat Autònoma de Barcelona and ICREA, Barcelona, Spain
^{13a}Institute of Physics, University of Belgrade, Belgrade, Serbia
^{13b}Vinca Institute of Nuclear Sciences, University of Belgrade, Belgrade, Serbia
¹⁴Department for Physics and Technology, University of Bergen, Bergen, Norway
¹⁵Physics Division, Lawrence Berkeley National Laboratory and University of California, Berkeley, California, USA
¹⁶Department of Physics, Humboldt University, Berlin, Germany
¹⁷Albert Einstein Center for Fundamental Physics and Laboratory for High Energy Physics, University of Bern, Bern, Switzerland
¹⁸School of Physics and Astronomy, University of Birmingham, Birmingham, United Kingdom
^{19a}Department of Physics, Bogazici University, Istanbul, Turkey
^{19b}Division of Physics, Dogus University, Istanbul, Turkey
^{19c}Department of Physics Engineering, Gaziantep University, Gaziantep, Turkey
^{19d}Department of Physics, Istanbul Technical University, Istanbul, Turkey
^{20a}INFN Sezione di Bologna, Italy
^{20b}Dipartimento di Fisica, Università di Bologna, Bologna, Italy
²¹Physikalisches Institut, University of Bonn, Bonn, Germany
²²Department of Physics, Boston University, Boston, Massachusetts, USA
²³Department of Physics, Brandeis University, Waltham, Massachusetts, USA
^{24a}Universidade Federal do Rio De Janeiro COPPE/EE/IF, Rio de Janeiro, Brazil
^{24b}Federal University of Juiz de Fora (UFJF), Juiz de Fora, Brazil
^{24c}Federal University of Sao Joao del Rei (UFSJ), Sao Joao del Rei, Brazil
^{24d}Instituto de Física, Universidade de Sao Paulo, Sao Paulo, Brazil
²⁵Physics Department, Brookhaven National Laboratory, Upton, New York, USA
^{26a}National Institute of Physics and Nuclear Engineering, Bucharest, Romania
^{26b}University Politehnica Bucharest, Bucharest, Romania
^{26c}West University in Timisoara, Timisoara, Romania
²⁷Departamento de Física, Universidad de Buenos Aires, Buenos Aires, Argentina
²⁸Cavendish Laboratory, University of Cambridge, Cambridge, United Kingdom
²⁹Department of Physics, Carleton University, Ottawa, Ontario, Canada
³⁰CERN, Geneva, Switzerland
³¹Enrico Fermi Institute, University of Chicago, Chicago, Illinois, USA
^{32a}Departamento de Física, Pontificia Universidad Católica de Chile, Santiago, Chile
^{32b}Departamento de Física, Universidad Técnica Federico Santa María, Valparaíso, Chile
^{33a}Institute of High Energy Physics, Chinese Academy of Sciences, Beijing, China
^{33b}Department of Modern Physics, University of Science and Technology of China, Anhui, China
^{33c}Department of Physics, Nanjing University, Jiangsu, China
^{33d}School of Physics, Shandong University, Shandong, China
^{33e}Physics Department, Shanghai Jiao Tong University, Shanghai, China
³⁴Laboratoire de Physique Corpusculaire, Clermont Université and Université Blaise Pascal and CNRS/IN2P3, Clermont-Ferrand, France
³⁵Nevis Laboratory, Columbia University, Irvington, New York, USA
³⁶Niels Bohr Institute, University of Copenhagen, Copenhagen, Denmark
^{37a}INFN Gruppo Collegato di Cosenza, Italy
^{37b}Dipartimento di Fisica, Università della Calabria, Arcavata di Rende, Italy
³⁸AGH University of Science and Technology, Faculty of Physics and Applied Computer Science, Krakow, Poland
³⁹The Henryk Niewodniczanski Institute of Nuclear Physics, Polish Academy of Sciences, Krakow, Poland
⁴⁰Physics Department, Southern Methodist University, Dallas, Texas, USA
⁴¹Physics Department, University of Texas at Dallas, Richardson, Texas, USA
⁴²DESY, Hamburg and Zeuthen, Germany

- ⁴³*Institut für Experimentelle Physik IV, Technische Universität Dortmund, Dortmund, Germany*
- ⁴⁴*Institut für Kern- und Teilchenphysik, Technical University Dresden, Dresden, Germany*
- ⁴⁵*Department of Physics, Duke University, Durham, North Carolina, USA*
- ⁴⁶*SUPA - School of Physics and Astronomy, University of Edinburgh, Edinburgh, United Kingdom*
- ⁴⁷*INFN Laboratori Nazionali di Frascati, Frascati, Italy*
- ⁴⁸*Fakultät für Mathematik und Physik, Albert-Ludwigs-Universität, Freiburg, Germany*
- ⁴⁹*Section de Physique, Université de Genève, Geneva, Switzerland*
- ^{50a}*INFN Sezione di Genova, Italy*
- ^{50b}*Dipartimento di Fisica, Università di Genova, Genova, Italy*
- ^{51a}*E. Andronikashvili Institute of Physics, Iv. Javakishvili Tbilisi State University, Tbilisi, Georgia*
- ^{51b}*High Energy Physics Institute, Tbilisi State University, Tbilisi, Georgia*
- ⁵²*II Physikalisches Institut, Justus-Liebig-Universität Giessen, Giessen, Germany*
- ⁵³*SUPA-School of Physics and Astronomy, University of Glasgow, Glasgow, United Kingdom*
- ⁵⁴*II Physikalisches Institut, Georg-August-Universität, Göttingen, Germany*
- ⁵⁵*Laboratoire de Physique Subatomique et de Cosmologie, Université Joseph Fourier and CNRS/IN2P3 and Institut National Polytechnique de Grenoble, Grenoble, France*
- ⁵⁶*Department of Physics, Hampton University, Hampton, Virginia, USA*
- ⁵⁷*Laboratory for Particle Physics and Cosmology, Harvard University, Cambridge, Massachusetts, USA*
- ^{58a}*Kirchhoff-Institut für Physik, Ruprecht-Karls-Universität Heidelberg, Heidelberg, Germany*
- ^{58b}*Physikalisches Institut, Ruprecht-Karls-Universität Heidelberg, Heidelberg, Germany*
- ^{58c}*ZITI Institut für technische Informatik, Ruprecht-Karls-Universität Heidelberg, Mannheim, Germany*
- ⁵⁹*Faculty of Applied Information Science, Hiroshima Institute of Technology, Hiroshima, Japan*
- ⁶⁰*Department of Physics, Indiana University, Bloomington, Indiana, USA*
- ⁶¹*Institut für Astro- und Teilchenphysik, Leopold-Franzens-Universität, Innsbruck, Austria*
- ⁶²*University of Iowa, Iowa City, Iowa, USA*
- ⁶³*Department of Physics and Astronomy, Iowa State University, Ames, Iowa, USA*
- ⁶⁴*Joint Institute for Nuclear Research, JINR Dubna, Dubna, Russia*
- ⁶⁵*KEK, High Energy Accelerator Research Organization, Tsukuba, Japan*
- ⁶⁶*Graduate School of Science, Kobe University, Kobe, Japan*
- ⁶⁷*Faculty of Science, Kyoto University, Kyoto, Japan*
- ⁶⁸*Kyoto University of Education, Kyoto, Japan*
- ⁶⁹*Department of Physics, Kyushu University, Fukuoka, Japan*
- ⁷⁰*Instituto de Física La Plata, Universidad Nacional de La Plata and CONICET, La Plata, Argentina*
- ⁷¹*Physics Department, Lancaster University, Lancaster, United Kingdom*
- ^{72a}*INFN Sezione di Lecce, Italy*
- ^{72b}*Dipartimento di Matematica e Fisica, Università del Salento, Lecce, Italy*
- ⁷³*Oliver Lodge Laboratory, University of Liverpool, Liverpool, United Kingdom*
- ⁷⁴*Department of Physics, Jožef Stefan Institute and University of Ljubljana, Ljubljana, Slovenia*
- ⁷⁵*School of Physics and Astronomy, Queen Mary University of London, London, United Kingdom*
- ⁷⁶*Department of Physics, Royal Holloway University of London, Surrey, United Kingdom*
- ⁷⁷*Department of Physics and Astronomy, University College London, London, United Kingdom*
- ⁷⁸*Laboratoire de Physique Nucléaire et de Hautes Energies, UPMC and Université Paris-Diderot and CNRS/IN2P3, Paris, France*
- ⁷⁹*Fysiska institutionen, Lunds universitet, Lund, Sweden*
- ⁸⁰*Departamento de Física Teórica C-15, Universidad Autónoma de Madrid, Madrid, Spain*
- ⁸¹*Institut für Physik, Universität Mainz, Mainz, Germany*
- ⁸²*School of Physics and Astronomy, University of Manchester, Manchester, United Kingdom*
- ⁸³*CPPM, Aix-Marseille Université and CNRS/IN2P3, Marseille, France*
- ⁸⁴*Department of Physics, University of Massachusetts, Amherst, Massachusetts, USA*
- ⁸⁵*Department of Physics, McGill University, Montreal, Quebec, Canada*
- ⁸⁶*School of Physics, University of Melbourne, Victoria, Australia*
- ⁸⁷*Department of Physics, The University of Michigan, Ann Arbor, Michigan, USA*
- ⁸⁸*Department of Physics and Astronomy, Michigan State University, East Lansing, Michigan, USA*
- ^{89a}*INFN Sezione di Milano, Italy*
- ^{89b}*Dipartimento di Fisica, Università di Milano, Milano, Italy*
- ⁹⁰*B.I. Stepanov Institute of Physics, National Academy of Sciences of Belarus, Minsk, Republic of Belarus*
- ⁹¹*National Scientific and Educational Centre for Particle and High Energy Physics, Minsk, Republic of Belarus*
- ⁹²*Department of Physics, Massachusetts Institute of Technology, Cambridge, Massachusetts, USA*
- ⁹³*Group of Particle Physics, University of Montreal, Montreal, Quebec, Canada*
- ⁹⁴*P.N. Lebedev Institute of Physics, Academy of Sciences, Moscow, Russia*
- ⁹⁵*Institute for Theoretical and Experimental Physics (ITEP), Moscow, Russia*
- ⁹⁶*Moscow Engineering and Physics Institute (MEPhI), Moscow, Russia*

- ⁹⁷*Skobeltsyn Institute of Nuclear Physics, Lomonosov Moscow State University, Moscow, Russia*
- ⁹⁸*Fakultät für Physik, Ludwig-Maximilians-Universität München, München, Germany*
- ⁹⁹*Max-Planck-Institut für Physik (Werner-Heisenberg-Institut), München, Germany*
- ¹⁰⁰*Nagasaki Institute of Applied Science, Nagasaki, Japan*
- ¹⁰¹*Graduate School of Science and Kobayashi-Maskawa Institute, Nagoya University, Nagoya, Japan*
- ^{102a}*INFN Sezione di Napoli, Italy*
- ^{102b}*Dipartimento di Scienze Fisiche, Università di Napoli, Napoli, Italy*
- ¹⁰³*Department of Physics and Astronomy, University of New Mexico, Albuquerque, New Mexico, USA*
- ¹⁰⁴*Institute for Mathematics, Astrophysics and Particle Physics, Radboud University Nijmegen/Nikhef, Nijmegen, Netherlands*
- ¹⁰⁵*Nikhef National Institute for Subatomic Physics and University of Amsterdam, Amsterdam, Netherlands*
- ¹⁰⁶*Department of Physics, Northern Illinois University, DeKalb, Illinois, USA*
- ¹⁰⁷*Budker Institute of Nuclear Physics, SB RAS, Novosibirsk, Russia*
- ¹⁰⁸*Department of Physics, New York University, New York, New York, USA*
- ¹⁰⁹*Ohio State University, Columbus, Ohio, USA*
- ¹¹⁰*Faculty of Science, Okayama University, Okayama, Japan*
- ¹¹¹*Homer L. Dodge Department of Physics and Astronomy, University of Oklahoma, Norman, Oklahoma, USA*
- ¹¹²*Department of Physics, Oklahoma State University, Stillwater, Oklahoma, USA*
- ¹¹³*Palacký University, RCPTM, Olomouc, Czech Republic*
- ¹¹⁴*Center for High Energy Physics, University of Oregon, Eugene, Oregon, USA*
- ¹¹⁵*LAL, Université Paris-Sud and CNRS/IN2P3, Orsay, France*
- ¹¹⁶*Graduate School of Science, Osaka University, Osaka, Japan*
- ¹¹⁷*Department of Physics, University of Oslo, Oslo, Norway*
- ¹¹⁸*Department of Physics, Oxford University, Oxford, United Kingdom*
- ^{119a}*INFN Sezione di Pavia, Italy*
- ^{119b}*Dipartimento di Fisica, Università di Pavia, Pavia, Italy*
- ¹²⁰*Department of Physics, University of Pennsylvania, Philadelphia, Pennsylvania, USA*
- ¹²¹*Petersburg Nuclear Physics Institute, Gatchina, Russia*
- ^{122a}*INFN Sezione di Pisa, Italy*
- ^{122b}*Dipartimento di Fisica E. Fermi, Università di Pisa, Pisa, Italy*
- ¹²³*Department of Physics and Astronomy, University of Pittsburgh, Pittsburgh, Pennsylvania, USA*
- ^{124a}*Laboratorio de Instrumentacao e Fisica Experimental de Particulas-LIP, Lisboa, Portugal*
- ^{124b}*Departamento de Fisica Teorica y del Cosmos and CAFPE, Universidad de Granada, Granada, Spain*
- ¹²⁵*Institute of Physics, Academy of Sciences of the Czech Republic, Praha, Czech Republic*
- ¹²⁶*Faculty of Mathematics and Physics, Charles University in Prague, Praha, Czech Republic*
- ¹²⁷*Czech Technical University in Prague, Praha, Czech Republic*
- ¹²⁸*State Research Center Institute for High Energy Physics, Protvino, Russia*
- ¹²⁹*Particle Physics Department, Rutherford Appleton Laboratory, Didcot, United Kingdom*
- ¹³⁰*Physics Department, University of Regina, Regina, Saskatchewan, Canada*
- ¹³¹*Ritsumeikan University, Kusatsu, Shiga, Japan*
- ^{132a}*INFN Sezione di Roma I, Italy*
- ^{132b}*Dipartimento di Fisica, Università La Sapienza, Roma, Italy*
- ^{133a}*INFN Sezione di Roma Tor Vergata, Italy*
- ^{133b}*Dipartimento di Fisica, Università di Roma Tor Vergata, Roma, Italy*
- ^{134a}*INFN Sezione di Roma Tre, Italy*
- ^{134b}*Dipartimento di Fisica, Università Roma Tre, Roma, Italy*
- ^{135a}*Faculté des Sciences Ain Chock, Réseau Universitaire de Physique des Hautes Energies-Université Hassan II, Casablanca, Morocco*
- ^{135b}*Centre National de l'Energie des Sciences Techniques Nucleaires, Rabat, Morocco*
- ^{135c}*Faculté des Sciences Semlalia, Université Cadi Ayyad, LPHEA-Marrakech, Morocco*
- ^{135d}*Faculté des Sciences, Université Mohamed Premier and LPTPM, Oujda, Morocco*
- ^{135e}*Faculté des sciences, Université Mohammed V-Agdal, Rabat, Morocco*
- ¹³⁶*DSM/IRFU (Institut de Recherches sur les Lois Fondamentales de l'Univers), CEA Saclay (Commissariat à l'Energie Atomique), Gif-sur-Yvette, France*
- ¹³⁷*Santa Cruz Institute for Particle Physics, University of California Santa Cruz, Santa Cruz, California, USA*
- ¹³⁸*Department of Physics, University of Washington, Seattle, Washington, USA*
- ¹³⁹*Department of Physics and Astronomy, University of Sheffield, Sheffield, United Kingdom*
- ¹⁴⁰*Department of Physics, Shinshu University, Nagano, Japan*
- ¹⁴¹*Fachbereich Physik, Universität Siegen, Siegen, Germany*
- ¹⁴²*Department of Physics, Simon Fraser University, Burnaby, British Columbia, Canada*
- ¹⁴³*SLAC National Accelerator Laboratory, Stanford, California, USA*
- ^{144a}*Faculty of Mathematics, Physics & Informatics, Comenius University, Bratislava, Slovak Republic*

- ^{144b}*Department of Subnuclear Physics, Institute of Experimental Physics of the Slovak Academy of Sciences, Kosice, Slovak Republic*
- ^{145a}*Department of Physics, University of Johannesburg, Johannesburg, South Africa*
- ^{145b}*School of Physics, University of the Witwatersrand, Johannesburg, South Africa*
- ^{146a}*Department of Physics, Stockholm University, Sweden*
- ^{146b}*The Oskar Klein Centre, Stockholm, Sweden*
- ¹⁴⁷*Physics Department, Royal Institute of Technology, Stockholm, Sweden*
- ¹⁴⁸*Departments of Physics & Astronomy and Chemistry, Stony Brook University, Stony Brook, New York, USA*
- ¹⁴⁹*Department of Physics and Astronomy, University of Sussex, Brighton, United Kingdom*
- ¹⁵⁰*School of Physics, University of Sydney, Sydney, Australia*
- ¹⁵¹*Institute of Physics, Academia Sinica, Taipei, Taiwan*
- ¹⁵²*Department of Physics, Technion: Israel Institute of Technology, Haifa, Israel*
- ¹⁵³*Raymond and Beverly Sackler School of Physics and Astronomy, Tel Aviv University, Tel Aviv, Israel*
- ¹⁵⁴*Department of Physics, Aristotle University of Thessaloniki, Thessaloniki, Greece*
- ¹⁵⁵*International Center for Elementary Particle Physics and Department of Physics, The University of Tokyo, Tokyo, Japan*
- ¹⁵⁶*Graduate School of Science and Technology, Tokyo Metropolitan University, Tokyo, Japan*
- ¹⁵⁷*Department of Physics, Tokyo Institute of Technology, Tokyo, Japan*
- ¹⁵⁸*Department of Physics, University of Toronto, Toronto, Ontario, Canada*
- ^{159a}*TRIUMF, Vancouver, British Columbia, Canada*
- ^{159b}*Department of Physics and Astronomy, York University, Toronto, Ontario, Canada*
- ¹⁶⁰*Faculty of Pure and Applied Sciences, University of Tsukuba, Tsukuba, Japan*
- ¹⁶¹*Department of Physics and Astronomy, Tufts University, Medford Massachusetts, USA*
- ¹⁶²*Centro de Investigaciones, Universidad Antonio Narino, Bogota, Colombia*
- ¹⁶³*Department of Physics and Astronomy, University of California Irvine, Irvine, California, USA*
- ^{164a}*INFN Gruppo Collegato di Udine, Italy*
- ^{164b}*ICTP, Trieste, Italy*
- ^{164c}*Dipartimento di Chimica, Fisica e Ambiente, Università di Udine, Udine, Italy*
- ¹⁶⁵*Department of Physics, University of Illinois, Urbana, Illinois, USA*
- ¹⁶⁶*Department of Physics and Astronomy, University of Uppsala, Uppsala, Sweden*
- ¹⁶⁷*Instituto de Física Corpuscular (IFIC) and Departamento de Física Atómica, Molecular y Nuclear and Departamento de Ingeniería Electrónica and Instituto de Microelectrónica de Barcelona (IMB-CNM), University of Valencia and CSIC, Valencia, Spain*
- ¹⁶⁸*Department of Physics, University of British Columbia, Vancouver, British Columbia, Canada*
- ¹⁶⁹*Department of Physics and Astronomy, University of Victoria, Victoria, British Columbia, Canada*
- ¹⁷⁰*Department of Physics, University of Warwick, Coventry, United Kingdom*
- ¹⁷¹*Waseda University, Tokyo, Japan*
- ¹⁷²*Department of Particle Physics, The Weizmann Institute of Science, Rehovot, Israel*
- ¹⁷³*Department of Physics, University of Wisconsin, Madison, Wisconsin, USA*
- ¹⁷⁴*Fakultät für Physik und Astronomie, Julius-Maximilians-Universität, Würzburg, Germany*
- ¹⁷⁵*Fachbereich C Physik, Bergische Universität Wuppertal, Wuppertal, Germany*
- ¹⁷⁶*Department of Physics, Yale University, New Haven, Connecticut, USA*
- ¹⁷⁷*Yerevan Physics Institute, Yerevan, Armenia*
- ¹⁷⁸*Centre de Calcul de l'Institut National de Physique Nucléaire et de Physique des Particules (IN2P3), Villeurbanne, France*

^aDeceased.

^bAlso at Department of Physics, King's College London, London, United Kingdom.

^cAlso at Laboratório de Instrumentação e Física Experimental de Partículas - LIP, Lisboa, Portugal.

^dAlso at Faculdade de Ciências and CFNUL, Universidade de Lisboa, Lisboa, Portugal.

^eAlso at Particle Physics Department, Rutherford Appleton Laboratory, Didcot, United Kingdom.

^fAlso at Department of Physics, University of Johannesburg, Johannesburg, South Africa.

^gAlso at TRIUMF, Vancouver, British Columbia, Canada.

^hAlso at Department of Physics, California State University, Fresno CA, USA.

ⁱAlso at Novosibirsk State University, Novosibirsk, Russia.

^jAlso at Department of Physics, University of Coimbra, Coimbra, Portugal.

^kAlso at Department of Physics, UASLP, San Luis Potosi, Mexico.

^lAlso at Università di Napoli Parthenope, Napoli, Italy.

^mAlso at Institute of Particle Physics (IPP), Canada.

ⁿAlso at Department of Physics, Middle East Technical University, Ankara, Turkey.

^oAlso at Louisiana Tech University, Ruston, LA, USA.

^pAlso at Dep Física and CEFITEC of Faculdade de Ciências e Tecnologia, Universidade Nova de Lisboa, Caparica, Portugal.

- ^qAlso at Department of Physics and Astronomy, University College London, London, United Kingdom.
- ^rAlso at Department of Physics, University of Cape Town, Cape Town, South Africa.
- ^sAlso at Institute of Physics, Azerbaijan Academy of Sciences, Baku, Azerbaijan.
- ^tAlso at Institut für Experimentalphysik, Universität Hamburg, Hamburg, Germany.
- ^uAlso at Manhattan College, New York, NY, USA.
- ^vAlso at CPPM, Aix-Marseille Université and CNRS/IN2P3, Marseille, France.
- ^wAlso at School of Physics and Engineering, Sun Yat-sen University, Guanzhou, China.
- ^xAlso at Academia Sinica Grid Computing, Institute of Physics, Academia Sinica, Taipei, Taiwan.
- ^yAlso at School of Physics, Shandong University, Shandong, China.
- ^zAlso at Dipartimento di Fisica, Università La Sapienza, Roma, Italy.
- ^{aa}Also at DSM/IRFU (Institut de Recherches sur les Lois Fondamentales de l'Univers), CEA Saclay (Commissariat à l'Energie Atomique), Gif-sur-Yvette, France.
- ^{bb}Also at Section de Physique, Université de Genève, Geneva, Switzerland.
- ^{cc}Also at Departamento de Fisica, Universidade de Minho, Braga, Portugal.
- ^{dd}Also at Department of Physics, The University of Texas at Austin, Austin, TX, USA.
- ^{ee}Also at Department of Physics and Astronomy, University of South Carolina, Columbia, SC, USA.
- ^{ff}Also at Institute for Particle and Nuclear Physics, Wigner Research Centre for Physics, Budapest, Hungary.
- ^{gg}Also at California Institute of Technology, Pasadena, CA, USA.
- ^{hh}Also at Institute of Physics, Jagiellonian University, Krakow, Poland.
- ⁱⁱAlso at LAL, Université Paris-Sud and CNRS/IN2P3, Orsay, France.
- ^{jj}Also at Nevis Laboratory, Columbia University, Irvington, NY, USA.
- ^{kk}Also at Department of Physics and Astronomy, University of Sheffield, Sheffield, United Kingdom.
- ^{ll}Also at Department of Physics, Oxford University, Oxford, United Kingdom.
- ^{mm}Also at Department of Physics, The University of Michigan, Ann Arbor, MI, USA.
- ⁿⁿAlso at Discipline of Physics, University of KwaZulu-Natal, Durban, South Africa.